Response to reviewer 1 of "Budget of the total nitrogen in the Yucatan Shelf: driving mechanisms through a physical-biogeochemical coupled model"

S. Estrada-Allis on behalf of all co-authors.

August 2019

We would like to thank the reviewer for the comments to the paper and the suggestions for improving it. Following are our responses (in blue) to all comments. The modifications to the original manuscript can be found in the attached document named Tracking-changes.pdf, where new text is marked in blue and removed text in red.

Overview:
The authors present an analysis of the total nitrogen budget on the Yucatan shelf as influenced by physical transports, mixing, river inputs, and biogeochemical processes. A coupled physical biogeochemical model was used to quantify the processes driving nitrogen source and sink terms. On the eastern boundary of the Yucatan shelf, the Yucatan Current is the dominant flux. Bottom Ekman transport towards the shelf is also important in this area. On the western and northwestern boundary, coastal trapped waves drive exchanges with the open Gulf of Mexico. A westward current on the inner shelf results in N exports at the western boundary of the inner shelf. The results of this work are interesting because the Yucatan shelf has been poorly studied and because the geographic setting provides an interesting interplay of different physical processes that are overlaid on one another.

1 General Comment

Unfortunately, I cannot recommend publication of the manuscript at this time for three reasons. First, I found the validation of the physical model insufficient. If there are any measurements of ocean currents for the Yucatan shelf, these should be presented and discussed to evaluate the accuracy of the modeled physical transports. If there are no data for currents, which may be likely especially outside the Yucatan current, the model could be validated by presenting comparisons of modeled versus observed salinity data. Second, I find that the manuscript lacks a discussion of how model bias in physical and biogeochemical state variables may influence results and there is no presentation of uncertainty estimates for the calculated budget source and sink terms, which makes it impossible to compare magnitudes of these terms. Third, the sink and source values were not presented as normalized to a unit area (e.g. m2) and thus the results from this study cannot be compared to results from previous N budget work in the Gulf of Mexico or elsewhere.

The issues raised by the reviewer in this first general comment have been addressed in the following way:

We have extended the Yucatan shelf (YS) model validation by comparing the model current velocity with observations reported in the literature (Sheinbaum et al., 2002; Athié et al., 2015; Sheinbaum et al., 2016). The model velocity structure, mean and standard deviation are in good agreement with these observations (see appendix A, subsection A4 and new Figure A9). A qualitative comparison is carried out for salinity with observations reported in Enriquez et al. (2013), see Figure 1 included here for comparison with Figure 9 in Enriquez et al. (2013).

We have added a point-by-point comparison of the salinity from the GOMEX IV cruise (see P9 L11-15, and new Figure 5) and a comparison of the mean chlorophyll vertical profiles observed for three different years in the YS (see new appendix A, subsection A2 and new Figure A6) with successful results. In order to prove that the model is able to reproduce the seasonality of the upwelling, the bottom shelf temperature is also shown as well as the seasonality of the upwelling marked by isotherm 22.5 ^{o}C (see P8 L28-32, new Figure 3) for comparison with Merino (1997). Moreover, the model sea level anomaly over the YS is compared with satellite altimetry data and the model's current velocity with the Global Current product (see new appendix A, subsection A3 and new Figure A7). We hope that all these new comparisons between model and observations are enough to convince the reviewers that the model results on the YS shelf are reliable and capture the main features of the observed variability. Note that the size and number of figures in the new version of this paper has increased considerably. Those for validation are included in appendix A which may be shortened or added instead as supporting information rather than an appendix if necessary.

Regarding the bias of the model, we have added appendix B named "Model statistics". In general, the model tends to overestimate the NO3 and temperature, mainly at the surface. A possible consequence of this is that the total nitrogen (TN) budget over the shelf may be overestimated by the model although differences are less than 2% (see new appendix B). It is important to mention a couple of extra things about this: firstly, the bias is reduced in the upwelling area, which is one of the main objectives of this study and is the region where most of the TN is entering the shelf. Secondly, despite a possible NO3 overestimation, the main nitrogen flux pathways remain unchanged.

Regarding the issue of budget units there are only a few published papers that address quantification of net biogeochemical budgets of the shelves of the Gulf of Mexico. A recent example Zhang et al. (2019) (see their figures 14 and 16) show the sources and sinks of TN for part of the Gulf of Mexico in Gmol N

yr^{-1}. Xue et al. (2013), (their figure 13), report the TN budget for the shelves of the Gulf of Mexico (except for the YS) in mol N. In other regions also, (Fennel et al. (2006), (their Figure 8)), the sources and sinks of N are expressed in mmol N yr^{-1}, similar to our Figure 9. None of these papers express the net budgets in units per unit area m^2. We understand the the concern of the reviewer regarding this issue, but prefer to express our results in the units used by other relevant works in the region to ease comparison. We certainly agree that in doing so, the results depend on the size of each region or shelf but believe they provide useful information to the overall GoM TN budget. For all these reasons we have kept the net budget units as in the original manuscript. Note that in our Table 1, the budget is expressed in molN yr^{-1}, same as in Table 2 of Xue et al. (2013) who compute budgets in the other GoM shelves using a similar model but different set-up. We are convinced this allows a better comparison of different model results in the region. We can easily compute budgets per unit area or length (fluxes) but would not be able to compare them with results available in the literature.

2 Specifics Comments

1. Abstract, L11: Is there a reason for choosing the 250 m isobath as the shelf boundary?
The reason for choosing the 250 m is explained in P4 L16-20 of the previous manuscript and remains in the new one: 200-250 m is the mean depth of the shelf break of the Yucatan peninsula (e.g., Ruiz-Castillo et al., 2016), please see Figure 1 as well. We also pointed out that the YS can be separated into two compartments based on quite different values of the mean kinetic energy (see Figure 1b and c).

Page 1
2. The first paragraph of the Introduction needs to be rewritten. References should be updated with recent relevant work on shelf carbon and nitrogen budgets. The last sentence in this paragraph incorrectly lists acidification and eutrophication as socio-economic activities. These processes may result from socio-economic activities but are not activities in themselves. Likewise, the processes listed as part of the climate system are not ones that would immediately come to mind. Please rewrite.
Following the reviewer's comment the first paragraph of the Introduction has been rewritten and the most recent work about nitrogen budget is also referenced. Please, check section 1 of the Introduction in the new version

Page 2,
3. L3: Probably should cite Walsh et al. 1989 here
Citation has been placed in P2 L20.
4. L12-13: It would be good to provide more detail about these controversies to help the reader understand the motivation for this study.

The introduction section has been modified to make it clearer and easier to understand our motivations which are now at the end of the section, after a short explanation of the controversies regarding the dynamics that control the YS variability(section 1 of Introduction).

5. L26: Show the Yucatan Current in Figure 1.

A better description of the Yucatan Current is included in the new manuscript (P3 L10-13). A yellow line has been added in Figure 1a to show a zonal transect of the Yucatan Current.

Page 3,

6. L23: Change "was ran" to "was run"

Thanks, this has been corrected in the new manuscript (P5 L2).

Page 4,

7. L12: Suggest deleting the first sentence and starting the paragraph with something like "The XIXIMI cruises provided profiles of nutrients and "

Thanks, this has been corrected in the new manuscript (P5 L26-27).

8. L22: Does the SDet equate to dissolved organic nitrogen (DON) in the model? In the real world, the components of total nitrogen are DIN, DON, and PON (or PN since there's some adsorbed inorganic nitrogen on particles). Dissolved organic nitrogen is often equal to or greater than dissolved inorganic nitrogen in the coastal ocean and in coastal rivers. If the SDet does not equate to DON, then your TN definition is incorrect. If SDet does equate to DON, then the assumption of setting PON in rivers equal to 0.1 mmol N m-3 (see comment 11 below) is incorrect.

Here we want to clarify two important things. The first is that the YS does not have rivers. The freshwater sources or more specific the Submarine Groundwater Discharges (SGD) come from a complex cave system called "cenotes", lagoons and other sources. The second is that the Fennel model does not have DON as a state variable, hence cannot be equated with SDetN. The model variables are described in the old manuscript in P4 subsection 2.2. For a more detailed description of the model refer to Fasham et al. (1990); Fennel et al. (2006, 2011). For freshwater sources, the particulated Nitrogen fluxes are assumed to enter as the pool of SDet (Fennel et al., 2011) and, together with the freshwater DON, is set with a small and constant value of 0.1 N m^{-3}, see answer to comment 11 below for more details. The definition of TN is the combination of DIN and PON, with DIN the sum of NO3 and NH4, and PON the sum of Phy, Zoo and the two detritus pools. This definition is the one used in Xue et al. (2013), which until now, is the only study that quantifies a long-term budget of TN for the whole GoM.

Biogeochemical models are approximations to reality and make several assumptions and simplifications depending on their complexity. The above mentioned published papers use empirical values and ad-hoc approximations that have shown merit in reproducing the main features of the biogeochemistry of the GoM. Our model parameters are in tune with those cited papers and are modified only if observations are available or local conditions suggest they should be "tuned" within reasonable values to better reproduce the few available observations.

9. L26 and equation (2): This equation is only for the water-column. The total nitrogen budget also includes the loss to denitrification and to burial in the sediments. Please clarify.

We agree with your comment. Thanks. This has been corrected in the new manuscript (P6 L11-13).

Page 5,

10. L16-20: More details are required about how the freshwater inputs were calculated. Since the freshwater inputs are unknown, it would be justified to include a time-series figure of these inputs, perhaps in the appendix.

Thank you for the suggestion. A time-series for the most important river systems and freshwater sources (Mississippi/Atchafalaya, Usumacinta-Grijalva, and freshwater sources of the Yucatan Shelf) are included in a new appendix C.

11. L23: Setting the PON to this small value is not justified. I suspect that PON must include DON, else the definition of TN used in this study is incorrect. DON concentrations are generally >> 0.1 mmol N m-3.

This question is related to previous comment 8. As we explained, DON is not included in the Fennel model as state variable. PON is taken as the sum of Phy, Zoo and the detritus pools, which together to DIN (NO3 and NH4), are the definition of TN as in Xue et al. (2013). PON were initialized with a small constant value of 0.1 mmol N^{-3}. This a numerical approach that works well due to the fact that the physical-biogeochemical coupled model evolves with time until it reaches a distribution representative of the model dynamics in accordance with observations. As we also mentioned, it is used in all the cited literature. In order to get this adjustment to reasonable values the analysis and budgets presented in the paper are carried out after a 30 year model spin-up. In fact, Fennel et al. (2006) argues that the adjustment timescales for near surface biogeochemical variables are on the order of days to weeks. Therefore the model "forgets" these initial values relatively quickly and produces realistic values based on its internal dynamics. Again, it is just a numerical technique used to produce more realistic results after model spin-up.

12. L26: Provide dates for the November cruise.

The dates for November cruise are now included in the new manuscript (P7 L17).

13. Section 3.1 seems like it should be in the appendix with the other basin wide modeling results. These results aren't really germane to the analysis except as boundary conditions to the shelf.

Following your comment, section 3.1. is now included in appendix A which deals with model validation. Figures are now renamed as Figure A4, A5 and A6.

Page 6,

14. L20: Why is there no model comparison with salinity data? This should be included to provide confidence the model is accurately representing physical transports.

We have added Figure 5 and description of the salinity comparison with GOMEX IV observations in P9 L11-15. Moreover, a T-S diagram is qualitatively compared (here, Figure 1) with observations shown in Enriquez et al. (2013) (see the first General comments section)

Page 7,

15. L3-9: Poorly worded paragraph. The explanation of why the model results cannot be compared with other results is incorrect. The results from this study should be compared to other studies to put the overall budget for the Yucatan shelf into some context in comparison to other more well-studied shelves in the Gulf such as the West Florida and Louisiana shelves. I recommend normalizing your budget fluxes to area so that they are comparable to other flux estimates.

We addressed this issue in our reply to the first general comment. Text has been changed accordingly. We do believe that even if integrated budgets were given normalized by area, one should be aware that dynamics are very different on each shelf so having similar or different values per unit area may not help interpretation of what causes those similarities or differences, which was the intention of the last phrase referred to by the reviewer in the comment above. Again, Zhang et al. (2019) and Xue et al. (2013) do not report net budgets per unit area and therefore our Table 1 can be directly compared to their results. We stress again that we could easily compute budgets by unit area but that would not help comparison with results from other shelves available in the literature

16. L15: The trend is mentioned here but there's no explanation. Is it real? What is driving the trend? What source/sink terms have changed? The model is deterministic so there's no reason not to get to the bottom of this, especially since the trend suggests that the N budget is not at steady state.

The explanation of the trend is in P7 L15-22 of the old manuscript. It is not an artifact of the model since chlorophyll from satellite products exhibits the same positive trend over nine years. Having said that, finding the cause or causes of this trend is not trivial. Neither the biogeochemical input data nor the freshwater inputs have this trend. The trend may be related to physical processes, for example the variability/strength of the Yucatan Current, as suggested by the study of **?**. However, many observational uncertainties remain. The main goal of this study is the description of the general budget of the Yucatan Shelf. The observations have such a trend and the model is able to reproduce it, so we are confident of our results. Finding out what is or are the mechanisms behind such trend is certainly a very interesting problem, but is out of the scope of the present study and further research is needed in order to get to the bottom of this. This is now better explained in P10 L26-31 of the revised manuscript.

17. L19: I'm not sure what you mean by "a very efficient biological cycle". Please be more specific.

This is related to the efficiency of the inner shelf in that sources and sinks of DIN are in balance with PON, i.e., almost all the NO3 is consumed by phytoplankton or remineralized and in balance with the particulate organic nitrogen. This sentence has been clarified in P10 L31-32.

18. L16-17: This logic doesn't make sense to me. Earlier in the ms it was

stated that the chlorophyll time series were used in an inverse analysis to prescribe freshwater and N inputs (also see comment 10). Thus, the TN trend and the chlorophyll trend may not really be independent. Please address whether these are completely independent variables.
We sincerely regret the use of the wording "inverse method" in the original manuscript. It has unfortunately caused a lot of unnecessary confusion. Chlorophyll was not used to determine fresh water or nutrient fluxes. All we did was to compile as much data as possible including literature references regarding fresh water and nutrient data to build a climatology of fresh water and nutrient fluxes to force the model at the southern GoM boundary. Again, no chlorophyll data were used for this. Whilst in the northern GoM there are long time series of nutrient, salinity, temperature and volume transports for most of the rivers, at the southern GoM boundary data are very sparse and scarce. We used some data from near coast stations to infer nutrient fluxes (e.g. near coast stations of the GOMEX IV cruise). We have added the appendix C to explain this in more detail including figures and have changed the wording to avoid confusion. Therefore the trend in model TN is not caused by the trend in observed chlorophyll data.

Page 8,
19. L22: Please report the rates of denitrification (mmol N m-2 d-1 or something similar) obtained from the model.
The rates of denitrification obtained from the model are given in mmolN m-2 d-1 and included in Table 1 in the revised manuscript. The rates of denitrification are averaged for the nine simulated years and reported in P11 L14-15.
20. L24: Fennel et al. (2006) was a study of the Mid-Atlantic and did not address GoM shelves.
This has been corrected in the new manuscript, reference now is to (Xue et al., 2013) instead. Thank you (see P12 L14).

Page 9,
21. L29-: This paragraph should be deleted. The last sentence makes it clear that the present analysis cannot address these phenomena. According to the reviewer suggestion (see also response to comment regarding the coherence plot of Reviewer 2), we have modified the analysis of the CTWs of sesction 4.1. Now, the wavelet power spectrum analysis is performed to show the climatology (daily averages from the 9 year results) of SLA, TN fluxes and along-shelf wind-stress (new Fig. 12) and concentrate on seasonal variations or higher frequency. Although we do not show now the year to year variability in the wavelet spectrum, we could not avoid mentioning the coincidence between the years of highly energetic events and the occurrence of relevant climatic signals (El Niño). The paragraph was modified mentioning this coincidence but recognizing that longer time-series are needed to investigate such variability.

Page 10,
22. L30: Insert "to" after "due" Thank you, this has been corrected in the new

manuscript.
23. L31: Change “show” to “shows” Thank you, this has been corrected in the new version of the manuscript.

Page 11,
24. L13: Is “2015” a typo? Yes, thank you, is a typo and has been corrected in the new version P16 L28.
25. L28: Delete “the” before “unique” Thank you, this has been corrected in the new manuscript P17 L19.
26. Prior to Concluding Remarks there needs to be a discussion of the uncertainties in your budget analysis. How does model bias for N concentrations affect your budget? What is the error (standard deviation of the mean) of each term in the mean budget? Without including this, there is no way to make meaningful judgements about the magnitude of the budget terms.
Thank you, the impact of the model uncertainties has been added to the revised version of the manuscript in appendix B.

Page 12,
27. L1-2: Figure 15 shows the physical system but not the biogeochemical system. Table 1: Normalizing the fluxes to a unit area would be more meaningful since the flux estimates presented are driven by the length of the boundaries and the area of the inner and outer shelf.
Figure 15 shows the physical processes that affect/modulate the biogeochemical system in the YS. Figure 9 shows the biogeochemical system. As we explained before, units in Table 1 are according to other similar studies (Xue et al. (2013) or Zhang et al. (2019) to ease comparison. As in the references, numbers represent net (integrated) values/contributions for the YS. Perhaps we should add here that the goal of the paper is to understand the main processes controlling the YS TN budget. The units used allow comparison with published results but detailed comparison of our results with other GoM shelves is a subject to be addressed in the future
29. Figure 1: These maps use degrees-minutes whereas other maps use decimal degrees. Be consistent. On Figure 1, the grey contours are difficult to see in panel (a). In panel (b), the vectors are too small to be seen in my copy.
Following the reviewer suggestion, the maps with decimal degrees have been modified to degrees-minutes. The grey contours of Figure 1 are now in black and we have increased the line width to improve the visualization. The vectors of panel b of Figure 1 have been changed to black. It is not straightforward to use larger vector sizes to improve the figure since the Yucatan Current is much more intense than the surrounding currents over the shelf larger vectors in panel b will distort the figure making it impossible to visualize. We have done our best to improve the figure hoping it is easier to see
30. Figure 2: It is hard to see the dashed boxes in my copy. Note the isobaths again in this figure caption so the reader knows what these lines are.
We have increased the width of the dashed boxes and we note the three isobaths in Figure 2.

31. Figure 3: Should be in appendix with basin-wide results.
Figure 3 is now Figure A4 of appendix A in the revised version.
32. Figure 4: Should be in appendix. In panel (a), the shadow and dashed line are difficult to differentiate. In panel (b), report the slope of the linear fit.
Figure 4, both panel (a) and (b), has been modified according to your suggestion and it is now Figure A5 of appendix A in the revised version.
33. Figures 5, 6, 7: Report model evaluation statistics such as bias and RMSE. The bias in temperature, NO3, and chlorophyll is generally positive with model results being greater than observations. How does this affect the TN budget calculated with the model?
additional statistical metrics (bias, RMSE) are now included in the revised version (section 3.1, P8 and 9). We consider that given the focus of this study, a critical area that needs to be evaluated is the upwelling region. More attention is paid to its validation with observations in the new manuscript as we explained before in answering your general comments and comment 14. The model may overestimate or underestimate some values but we believe it captures the basic mechanisms determining the balances
34. Figure 8: For panels a, c, and e report the p-values for the trend lines. The legends are confusing. Perhaps rename them to Inner Shelf TN, Inner Shelf DIN, Inner Shelf PON, etc.
The p-values are now added and the legends have been changed accordingly, thank you (Figure 8).
35. Figure 9: There are differences in values and significant digits presented here and Table 1. Double check these values and make corrections. Also some numerical values for fluxes are difficult to read. A simple 2-D map may make a better figure. Plus, the upside down (S-N) orientation is odd for the 3-D figure.
Thank you for the suggestion, the values of Table 1 and Figure 9 are now expressed in mmolN yr^{-1} in order to be comparable with the budgets for the GoM shown in Fennel et al. (2006) and Xue et al. (2013). Numerical values of Table 1 are now bigger. Figure 9 has been rotated to a N-S diagram. Numbers are higher and isobaths are highlighted.
36. Figure 10: Font is too small for gray depths. Latitude is shown in decimal degrees here. “Isobtahs” is misspelled in the caption.
Thank you, Figure 10 has been modified accordingly in the new manuscript.
37. Figure 11: I can’t see the red dot for the station at Lat = 18.3 and Long = -88.1.
The dots are now bigger in panel a, and the panel b is in degree instead of decimal latitude and longitude map.
38. Figure 12: Is this figure necessary? It seems to just show a correlation between currents and SLA that could likely be seen with a simple correlation analysis. What is the unit cpd-1 in the y-axis labels?
Thank you for the suggestion. As explained in comment 21, we have modified section 4.1. Now Fig. 12, along with new Fig. 13, show that the high-frequency variability of the TN fluxes at the western YS border are modulated by surface Ekman transport and propagation of CTWs. We wanted to capture these variations in time but following your comments we concentrate on seasonal and

higher frequency variations. That is the reason why we use the "climatology"of the wavelet spectrum and coherence analysis (as suggested also by reviewer 2). Capturing this time changes can not be obtained from a simple correlation analysis. Our analysis allows us to capture the increased variability during winter at the western YS border.

39. Figure 13: Difficult to see isobaths in panel (a). In panels b, c, and d, change the blue lines to black to match the y-axis label or change the y-axis label to blue.

Isobaths in panel (a) are now thicker and in black. In panels b, c and d, each color lines match with the y-axis label.

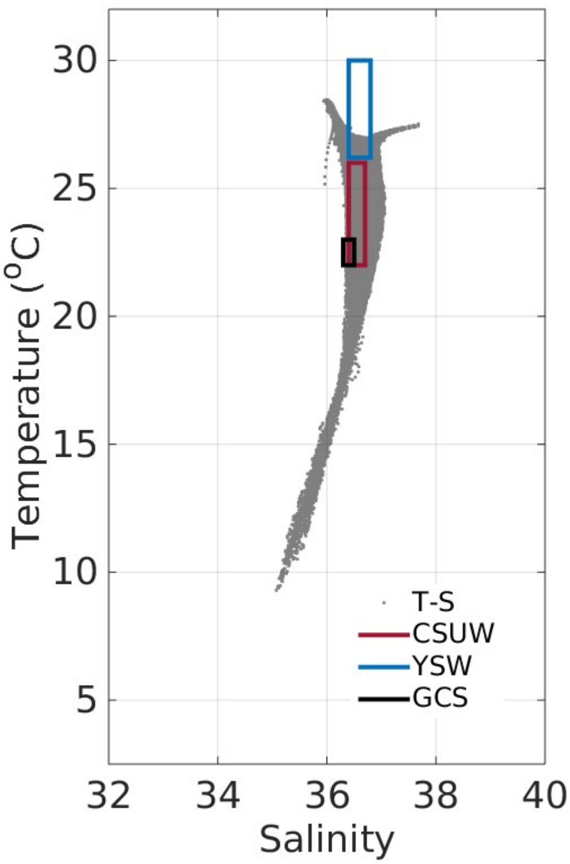

Figure 1: Spatially and temporally averaged over nine simulated years T-S diagram for the whole YS. Color boxes denote the three main water masses found on the shelf: the Caribbean Subtropical Underwater (CSUW), the high salinity, warm and surface Yucatan Sea Water (YSW) and Gulf Common Water (GCS). For more information refer to Enriquez et al. (2013).

References

Athié, G., J. Sheinbaum, R. Leben, J. Ochoa, M. R. Shannon, and J. Candela, 2015: Interannual variability in the yucatan channel flow. *Geophys. Res. Lett.*, **42**, 1496–1503, doi:10.1002/2014GL062674.

Enriquez, C., I. Mariño Tapia, G. Jeronimo, and L. Capurro-Filograsso, 2013: Thermohaline processes in a tropical coastal zone. *Continental Shelf Research*, **69**, 101–109, doi:10.1016/j.csr.2013.08.018.

Fasham, M. J. R., H. W. Ducklow, and S. M. McKelvie, 1990: A nitrogen based model of plankton dynamics in the oceanic mixed layer. *Jorunal of Marine Resesearch*, **48**, 591 – 639.

Fennel, K., R. Hetland, Y. Feng, and S. DiMarco, 2011: A coupled physical-biological model of the northern gulf of mexico shelf: Model description, validation and analysis of phytoplankton variability. *Biogeosciences*, **8**, 1881–1899.

Fennel, K., J. Wilkin, J. Levin, J. Moisan, J. O'Reilly, and D. Haidvogel, 2006: Nitrogen cycling in the middle atlantic bight: results from a three-dimensional model and implications for the north atlantic nitrogen budget. *Global Biogeochemical Cycles*, **20**, doi:10.1029/2005GB002456.

Merino, M., 1997: Upwelling on the yucatan shelf: hydrographic evidence. *Journal of marine systems*, **13**, 101–121.

Ruiz-Castillo, E., J. Gomez-Valdes, J. Sheinbaum, and R. Rioja-Nieto, 2016: Wind-driven coastal upwelling and westward circulation in the yucatan shelf. *Continental Shelf Research*, **118**, 63–76, doi:10.1016/j.csr.2016.02.010.

Sheinbaum, J., G. Athié, J. Candela, J. Ochoa, and R.-A. A., 2016: Structure and variability of the yucatan and loop currentsalong the slope and shelf break of the yucatan channel andcampeche bank. *Dynamics of Atmospheres and Oceans*, **76**, 217–239, doi:10.1016/j.dynatmoce.2016.08.001.

Sheinbaum, J., J. Candela, A. Badan, and J. Ochoa, 2002: Flow structure and transport in the yucatan channel. *Geophys. Res. Lett.*, **29 (1–6)**.

Xue, Z., R. He, K. Fennel, W.-J. Cai, S. Lohrenz, and C. Hopkinson, 2013: Modeling ocean circulation and biogeochemical variability in the gulf of mexico. *Biogeosciences*, **10**, 7219–7234, doi:10.5194/bg-10-7219-2013.

Zhang, S., C. A. Stock, E. N. Curchitser, and R. Dussin, 2019: A numerical model analysis of the mean and seasonal nitrogen budget on the northeast u.s. shelf. *Journal of Geophysical Research: Oceans*, **124**, doi:10.1029/2018JC014308, URL https://agupubs.onlinelibrary.wiley.com/doi/abs/10.1029/2018JC014308, https://agupubs.onlinelibrary.wiley.com/doi/pdf/10.1029/2018JC014308.

Response to reviewer 2 of: *"Budget of the total nitrogen in the Yucatan Shelf: driving mechanisms through a physical-biogeochemical coupled model"*

S. Estrada-Allis on behalf of all co-authors.

August 2019

We thank the reviewer for the comments to our paper and for providing valuable suggestions to improve it. Our responses to each one of them follow (in blue). Modifications to the manuscript can be found in the attached document Tracking-changes.pdf, where new text is marked in blue and removed text in red.

1 General Comments

This work presents an estimation of the Total Nitrogen (TN) budget in the Yucatan Shelf (YS). The estimate is obtained using a coupled physical-biochemical model (ROMS), validated by some in-situ and satellite observations. The model solution is available for 9 year (2002-2010) while the in-situ observations used to validate the solution within the YS are available for Nov 2015. Physical processes that are relevant in explaining the estimated TN budget are identified and described. The main input of N is at the eastern boundary through the interaction of the western boundary current with the shelf break, presumably mainly due to Ekman transport at the bottom boundary layer. The imported N is then advected westward by the wind driven-circulation along the shelf. Most the N that enters the inner shelf (depths shallower than 50 m) is consumed by phytoplankton, and part of the N that enters the outer shelf (depths 50-250 m) is exported to the deep ocean in the west and northwest parts of the YS. This export of N is modulated by Coastally Trapped Waves with a typical period of 10 days.

I think this manuscript addresses a relevant scientific question within the scope of BG, and the modeling results suggest a very interesting case for the relevance of likely physical processes controlling or modulating the import and export of N in and out of the YS. However, I think some revisions are needed in terms of validating the model, justifying the model physics or at least acknowledging the limitations and implications for the estimated budget, and the analysis and overall presentation of the work done. Below I outline some suggested revisions that might guide the authors when improving the manuscript.

Thanks for your comment. We have extended the Yucatan shelf (YS) validation by comparing the structure and velocity values with observations found in the literature (Sheinbaum et al., 2002; Athié et al., 2015; Sheinbaum et al., 2016). The velocity and its standard deviation are in a good agreement with the observed mean values reported in the literature (see P10 L22 and new appendix A4, Figure A9). A qualitatively comparison is made in terms of salinity with the observations reported in Enriquez et al. (2013), see Figure A6 in the appendix A of the revised manuscript and compared to Figure 9 from Enriquez et al. (2013).

We have added a point-by-point comparison of the salinity from the GOMEX IV cruise (see P9 L11-15) and a comparison of the mean chlorophyll vertical profiles observed during three different years in the YS (see new appendix A2, Figure A6) with successful results. In order to prove that the model reproduces the seasonality of the upwelling, the bottom shelf temperature is also shown and the seasonality of the upwelling isotherm of 22.5 ^{o}C (see P8 L27-31, Figure 3). Moreover, the model sea level anomaly over the YS is compared with altimetry data from satellite and the model current velocity with the Global Current product (see new appendix A3, Figure A7). Most of the content related to model validation is contained in section 3 and appendix A of the revised version. We hope that all these new model-data comparisons convince the reviewers of the capability of the model to reproduce main features of the observed variability in the region. Note that the size and number of figures in the new version of this paper has increased considerably. Those for validation are included in appendix A which may be shortened or added as supporting information instead of an appendix if necessary.

2 Specific Comments

2.1 Model Validation

While this study focuses on the YS and its vicinity, most of the convincing validation presented is for the whole Gulf of Mexico (GoM). There is a need to validate and characterize the background state in the YS in order to add credibility to the results. While I understand there is a scarcity of *in situ* observations in the YS, some vertical sections of temperature and salinity have been reported previously (e. g., Enriquez et al., 2013). There are also lots of *in situ* observations in the western boundary current (e.g., Sheinbaum et al., 2002, 2016) that could be used to convince the reader that the model physics is reliable. Specially those closer to the 250 m isobath if available. There is no need to do an exhaustive analysis of such observational data-sets, but to show a congruence between model and observed mean background state.

In agreement with the reviewer we have extended the model YS validation, see our previous response to the general comment and all section 3 and appendix

A of the revised version.

The *in situ* biochemical observations were taken in Nov 2015, while the model solution is available until 2012. Ideally one would have a solution contemporaneous with the observations but if that is not possible then the approach presented is the best next choice: compare the mean and standard deviation for Nov with the observations. But then one wonders is the agreement with observations will hold for other months given that the authors present long-term means for the budgets. The authors seem to suggest that seasonality is weak, but I think that needs to be shown. For instance, does the inner shelf remains well mixed throughout the year as it seems to be the case in Nov?, or does some stratification develops during summer and if so, how that affects the budget?.

The reviewer is right and our goal is just to show that the model is capable to reproduce basic statistics from available observations (mean profiles and standard deviations). To extend our validation of basic statistics (see also comment above for the T-S profiles), we have added a comparison between chlorophyll profiles from other years (August 2016 and July 2018) temporally and spatially averaged for the whole YS (see appendix A2 and Figure A6). The mean and standard deviation profiles of chlorophyll and salinity are presented to show the degree of variability within the shelf. Unfortunately, nutrient and particulate organic nitrogen observations are scarce.

Horizontal and vertical sections of the bottom shelf temperature are also added to the new manuscript to show that the model is capable of representing the seasonal variability (P8 L27-31, Figure 3). In Figures 3c and d one can see that the isotherm of 22.5 ^{o}C, which represents the upwelling waters at Cape Catoche outcrops to the shelf during spring. Whereas during autumn months, the isotherm is not able to reach the shelf in agreement with observations reported in (Merino, 1997) and consistent with the strengthening/weakening of the upwelling of nutrients and chlorophyll during those seasons. The stratification of the shelf is a complex issue that depends on the proximity of oceanic waters with the coast and freshwater sources. However, it is a very interesting question that merits a more comprehensive study using higher horizontal resolution than the one used presently.

Similarly, more analysis can be done using satellite products to validate the circulation in the YS. This is specially important to compensate for the scarcity of *in situ* observations. How does the observed Sea Level Anomaly correlates with that of the model in the YS? The authors could for instance compare the annual cycles of the aviso SLA and the model (without Mean Dynamic Topography) to convince the readers that the background model physics on the shelf is reliable. Is the pressure gradient across the shelf break well resolved by the model? A similar comparison could be done with scatterometer winds. The use of OSCAR currents, while very low resolution, might be possible given the wide YS. SST is not a robust validation set since the authors are using bulk fluxes at the surface and the CFSR model (I assume) is forced by satellite SST. Therefore the model is implicitly nudged to observed SST via the 2 m air temperature.

Following the reviewer suggestion, we improved the model validation by comparing Sea Level Anomaly from AVISO and the model (see new APPENDIX A, and Figure A7). However, one should be careful when using the AVISO product in shallow areas and close to the shore. Instead of OSCAR, we use GlobalCurrent products (http://www.globcurrent.org) to evaluate the shelf model velocity. This choice is based on the fact that this product includes both Ekman and geostrophic velocities, with Ekman being an important contribution to the circulation on the shelf, Those comparisons suggest pressure gradient across the shelf break is properly resolved. Validation of the CFSR reanalysis winds in the GoM has been carried by other authors (e.g Chawla et al 2013, https://doi.org/10.1016/j.ocemod.2012.07.005). Thank you for your comment regarding the SSTs for validation, this is taken into consideration for the basin-scale model validation.

2.2 Model Physics

One the main findings reported in the manuscript is that the input of N in the southeast part of the shelf comes from Ekman transport at the bottom boundary layer. The vertical stretching used was developed to study the surface vorticity balance and while this might be a wise choice for the whole GoM, it is not the best for the YS NT budget given the relevance of the bottom boundary layer. This limitation needs to be further analyzed and acknowledged in the manuscript. The authors could for instance estimate the bottom boundary layer thickness (a common estimate is thickness 0.4*frictionalvelocity/Corilisparamater, where frictional velocity is estimated from the bottom stress). How this thickness compares to the thickness the the first model sigma layer for the 250 m isobath?. That is, how well is the bottom boundary layer resolved?. If it is not very well resolved I still think the bulk characteristics of the budget will hold (i.e., the main sources and sinks and the TN pathways), but this limitation needs to be acknowledged.

We agree with the reviewer. The chosen vertical stretching (Azevedo Correia de Souza et al., 2015) was developed to provide higher resolution near the surface. In fact, in most areas of the study region important fluxes are concentrated near the surface (e.g. Figure 10, previous manuscript). In shallow areas there is high resolution (because of the use of sigma-s coordinates) but one may expect some issues on the slopes close to the shelf but deep. Certainly, we agree that the bottom Ekman layer needs to be as well represented as possible, particularly if we think bottom Ekman layer transports may be important for the dynamics. We estimated the size of the bottom Ekman layer using standard formulas based on bottom stress and friction velocity for homogeneous and stratified fluids (Cushman-Roisin and Beckers, 2011). Analysis (not shown), indicates the bottom Ekman layer width is on average between 10-30 m whereas the model bottom layer width is about 20 m. Since we estimate bottom Ekman layer transports using the vertical size of the near-bottom cells, our estimates could be somewhat biased. We acknowledge this in the new version of the manuscript (P16 L32-35).

2.3 Technical Corrections

Abstract:
L4: I think it should be "Coastal-Trapped Waves" or "Coastally Trapped Waves"

Thank you, this has been corrected as "Coastal-Trapped Waves" in the revised version.

L8: Define DIN or spell it out.

The DIN term is spelled out in the Abstract in the revised version.

Introduction:
L6: Processes

Thank you, this has been corrected in the revised version (see P2 L23)

Section 2.1: L23: run

Thank you, this has been corrected in the revised version (see P5 L2)

L25: In what sense it is "consistent with the observational data"?

To be time-consistent, i.e., in the sense that the model and observations match in the same time range, as far as possible (P5 L3).

L27: Is the boundary condition daily means? Monthly? What is done with the tides?

The boundary conditions are daily averaged. The tides are hourly and added as a separate spectral forcing at the boundaries. This is clarified in the revised version (see P5 L7)

L30: Mention that the surface fluxes are computed using the bulk formulae for the marine boundary layer and provide a reference.

We mentioned this in the revised version, thank you (see P5 L312)

Section 2.2
Formula (2) is confusing. While the model is in sigma levels the vertical integration is in depth (I hope so!) where the ?dz? is the corresponding sigma layer thickness. The formula also uses summation indexes (x1:xn an y1:yn) as limits for integrals, which is very confusing. One option could be just to do a single integral over area elements dA. Also this expression is equated with the same abbreviation used for expression (1). Maybe use an overbar??

Indeed, the model is in sigma levels and the vertical integration is in depth from layer thicknesses. We agree that formula (2) is confusing. To make the text more readable we decided to remove this equation and is only described in the text of the revised manuscript (see P6 L11-13)

L19: How the unknown groundwater sources were "inversely estimated"? How many? Where? What are their fluxes?

We regret the use of the wording "inversely estimated" which has caused a lot of unnecessary confusion. All we did was to use all possible available information that we were aware of regarding fresh water and nutrient fluxes (temperature and salinity too) at the Mexican GoM coast. We also used near coastal nutrient measurements. Based on that limited information we computed a monthly climatology to force the model. It is important to mention that no chlorophyll data were used for this (see reply to comment 18 of reviewer 1). We have added a new appendix C to present examples of the monthly climatology of Mexican rivers (Usumacinta and Grijalva) and freshwater sources ("cenotes" and lagoons in the YS) used in this study and compared with the Mississippi and Atchafalaya river system for which we have more information. We have rephrased the description of the freshwater sources on P7 L11-14, and added appendix C for details in the revised version.

Section 3.1 is good enough but more work is needed in section 3.2 (regional validation) as suggested above.

Thank you for this suggestion. More validation is presented in the new version of the manuscript (see response to the general comments above, new section 3 and appendix A).

P7,L3: "Below 55 m the modeled and "?

This paragraph has been changed.

P7,L4: "since there is no data assimilation". This sentence doesn't make much sense since you are not comparing contemporaneous values.

Thank you, this sentence has been erased in the revised version (see P10 L7).

P7,L4: "and ARE in"

This paragraph has been changed.

P7,L5: "To the best of our knowledge this is the first modeling study focusing on the nitrate budget of the YS."

This paragraph has been changed.

P7,L16: Usually the word "trend" is used for time, so I'll suggest erasing "along time".

Thank you, this has been corrected in (see P10 L26).

P7,L17: How Fig 8e compares to the model equivalent Chl? Does that also show the trend? Given the very large std in the Chl I can't help wonder how big are the error bars for the trend.

The model Chl compares well with the satellite Chl, as shown in Figure 1. This figure is added to Figure 8c in the revised version. The model also exhibits a positive trend. The large std of the Chl is probably related to the strong variability given by upwelling episodes over the shelf. Even in the presence of this high variability a trend in both observations and model (just for the simulation period) can be inferred although with large confidence intervals indeed, as shown in the next figure for the linear fit of the time series averaged over the YS of satellite Chl measurements and corresponding model Chl values. The dotted lines show the linear fit to the series and the thinner dotted lines the 95% confidence interval of the fits. Overall satellite Chl averaged over the YS and over the period of time between 2002-2010 is 0.38 $\pm$0.09 mgChl m^{-3} with corresponding values for the model being a mean of 0.36 $\pm$0.13 mgChl m^{-3} for the same area and time period.

P7,L21: "associated with the seasonal cycle AND INTERANNUAL variability". The trend is presumably related to the interannual part. It could be good to compare that with the physics of the model such as the western boundary

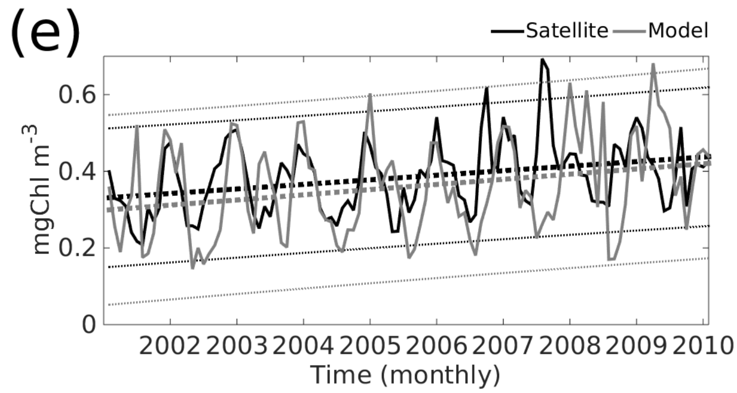

Figure 1: Time series of satellite surface Chl (mgChl m^{-3}) (thick gray line) and model (thick black line), averaged for the period of years between 2002-2010 and over the YS area. Thick dashed lines are the fitted trends for each temporal series, and thin dashed lines are the corresponding 95% confidence interval. Equations for the linear fits are Chl_{trend} = 0.0010 month + 0.28 for satellite, and Chl_{trend} = 0.0011 month + 0.30 for the model chlorophyll trend.

current strength, across-shelf pressure gradient, etc.

We agree with the reviewer. Determining the origins of this trend is an interesting problem that requires further research. Based on the study of (Varela et al., 2018) we tried to establish a link between the trend and dynamic indices for example, the strength of the Yucatan Current. This index (Yucatan Current strength) has no clear seasonality in the model (Figure 2 first panel), and depicts a large std higher than the mean. No significant correlation was found with the positive trend of nitrogen or chlorophyll (Figure 2 second panel). We also investigated the closeness of the Yucatan Current core to the shelf but that was also uncorrelated with the chlorophyll trend (Figure 2 third panel). The same happens with changes in the cross-shelf sea level anomaly. Therefore the question needs to be addressed in future work. This is now mentioned in P10 L28-31 of the revised version.

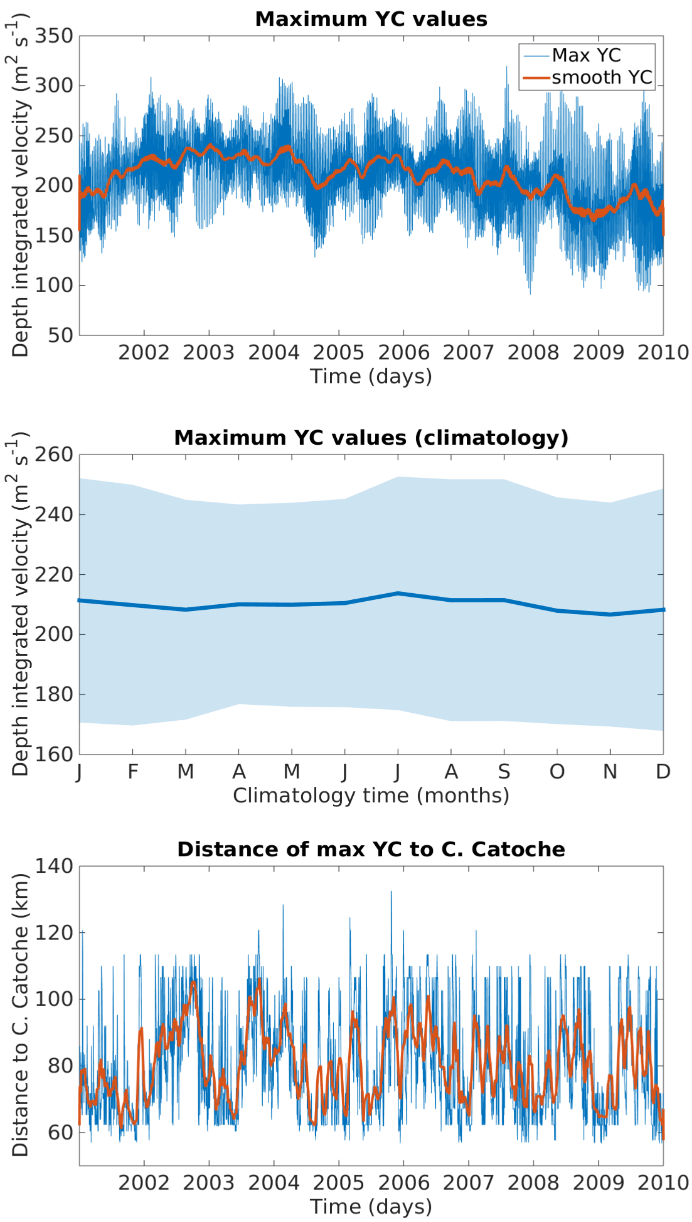

Figure 2: Temporal series of: Yucatan Current (YC) strength in the first panel and its climatology with the standard deviation in shaded in the second panel and the closeness of the YC with the Yucatan Shelf at Cape Catoche in the third panel.

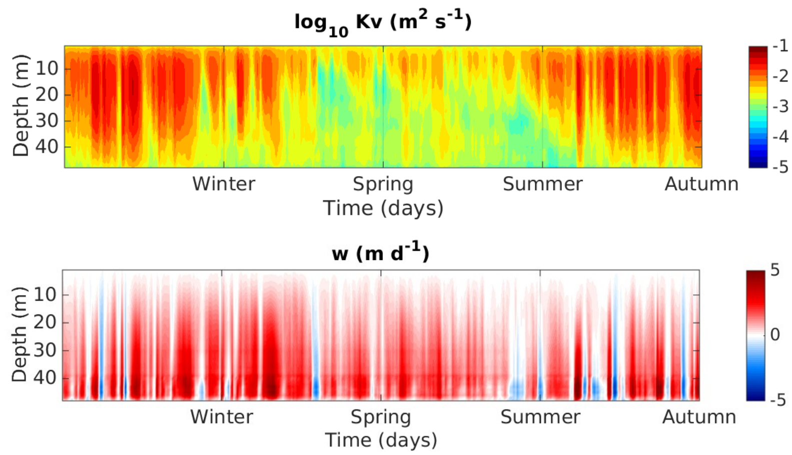

Figure 3: Hovmoller diagrams (time-depth) for the inner shelf and year 2009. Upper panel shows the vertical diffusion coefficient in logarithmic scale (Kv, m^2 s^{-1}). Lower panel shows the vertical velocity (w, m d^{-1}).

P7,L31: "inner shelf"

Thank you, this has been corrected (see P10 L22).

P8,L2-4: Is this the situation all year round? Is it well mixed all year?

This is an interesting question. The inner-shelf is not uniformly mixed all year but presents a seasonal cycle with increased vertical mixing during winter and a decrease in summer. The main idea we want to express here is that on shallow waters, DIN and PON concentrations are in balance, due to, on the one hand, vertical mixing that is more efficient in a small volume of water, i.e., wind-driven mixing and convective processes can easily reach the shelf bottom. On the other hand, vertical shear generated by the bottom friction can also break the stratification and carry nutrients into the euphotic layer. This seems to occur during winter (Figure 3 upper panel). For summer months, when the convective mixing is weak, nutrients probably do not upwell to the euphotic zone by vertical mixing but due to intense upward vertical velocities (Figure 3 lower panel). The causes of this almost uniform pattern in the vertical velocity can be due to topographic, Ekman, or other ageostrophic effects. It is, in fact, another interesting question that will be addressed in an ongoing study with a higher submesoscale eddy-resolving model configuration. The sentence has been modified in P11 L19-24 of the revised manuscript.

P8,L11: Please indicate all the geographical locations mentioned in the text in Fig 1a (Campeche Basin, YS/Campeche Bank, Campeche shelf, etc.).

The geographical location of Campeche Sea, Deep Gulf of Mexico and Caribbean sea are now indicated in Figure 1a. Yucatan peninsula is indicated in Fig. 1b, and Inner and Outer YS are indicated in Fig.1c. Moreover, we have deleted Campeche Bank to avoid confusion with Yucatan shelf.

P9,L6-7: Please rephrase.

The paragraph has been changed completely.

P9,L16 onwards. Maybe include a coherence plot of cross-shelf velocity vs SLA and wind stress?

Thank you for the suggestion. We have modified section 4.1 that now focuses on seasonal or higher frequency variations using coherence between cross-shelf TN fluxes vs SLA, as well as along-shelf wind-stress. Relevant conclusions arise from this analysis. The coherence between the TN fluxes and the SLA are meaningful, better indicating relations between variables and connection with CTWs. We noticed that the along-shelf wind is also responsible for the high-frequency variability of the TN flux through Ekman transports. Fig. 12 was modified accordingly to show the high-frequency variability and a daily climatology of the wavelet spectra allows to identify an intensification of the variability during winter, likely related with the "Nortes" winds. Moreover, new Fig. 13 shows the coherence and phase between the different time series (see all section 4.1).

P10,L1: EASTERN!

This has been corrected thank you. (see P15 L13).

P10,L7: "Another". Revise the whole sentence.

The sentence has been rephrased.

P10,L30: "due to"

This has been corrected, thank you.

P10,L31:shows or showed?

shows.

P11,L1: erase "produce bottom"

The sentence has been rephrased, thank you (see P16 L13).

P11,L3: "A similar mechanism has been found for the southern" (Shaeffer et al., 2014)?

The sentence has been rephrased, thank you (see P16 L24).

P11,L13: revise the value of rho 0

This has been modified by 1025 kg m^{-3}. Thank you. (see P16 L28).

P11,L14: "We found that" The formulation used for the bottom Ekman transport implies westward flow for a northward flowing western boundary current, so was that really a finding?

The sentence has been rephrased, thank you (see P16 L29-30).

P11,L17: How Fig 14c shows that "the Ekman transport is responsible for 65 % of the TN that is entering the shelf."?

The sentence has been rephrased, as the reviewer noted the Figure 14c (now Figure 15) does not show the percentage (see P17 L5).

P11,L24: Rephrase. Maybe "The high-resolution modeling work of (Jouanno et al., 2018) suggest that the bathymetric notch could be responsible for as a much as 50 % of the upwelling."

The sentence has been rephrased, thank you (see P19 L9-21).

P11,L28: change "but is not the unique" by "but is not the only process at work."

The sentence has been changed, thank you (see P17 L20-21).

P12,L17: This is not shown at all. How do we know it is the case? All figures and figure captions need to be carefully revised.

The sentence has been deleted. All the figures and captions have been revised in the new version of the manuscript.

Figure 8: Is it possible to combine (a)+(b) and (c)+(d)? And maybe include the model equivalent of (e)?

We have combined panels (a+b) and (c+d) of Figure 8. The model equivalent is now included in the revised version (see previous Figure 1) above.

Figure 10: Plot the sections using actual depths instead of sigma levels.

We have plotted the sections of Figure 10 using actual depths.

Figure 11: Is this signal visible in the aviso analysis? The signal is strong enough but the temporal variability might be "too fast" for the altimeter constellation to catch it.

The signal and temporal variability shown by the model output is in agreement with the observational study of Dubranna et al. (2011) and the modelling study of Jouanno et al. (2016). Not so clear from AVISO because it is too close to the coast. Thank you for your suggestion.

References

Athié, G., J. Sheinbaum, R. Leben, J. Ochoa, M. R. Shannon, and J. Candela, 2015: Interannual variability in the yucatan channel flow. *Geophys. Res. Lett.*, **42**, 1496–1503, doi:10.1002/2014GL062674.

Azevedo Correia de Souza, J., B. Powell, A. C. Castillo-Trujillo, and P. Flament, 2015: The vorticity balance of the ocean surface in hawaii from a regional reanalysis. *Journal of Physical Oceanography*, **45 (2)**, 424–440, doi:10.1175/JPO-D-14-0074.1, URL https://doi.org/10.1175/JPO-D-14-0074.1, https://doi.org/10.1175/JPO-D-14-0074.1.

Cushman-Roisin, B., and J. Beckers, 2011: *Introduction to geophysical fluid dynamics : physical and numerical aspects*, Vol. 101. 2nd ed., International Geophysical Series.

Dubranna, J., P. Pérez-Brunius, M. López, and J. Candela, 2011: Circulation over the continental shelf of the western and southwestern gulf of mexico. *Journal of Geophysical Research*, **116 (C08009)**, doi:10.1029/2011JC007007.

Enriquez, C., I. Mariño Tapia, G. Jeronimo, and L. Capurro-Filograsso, 2013: Thermohaline processes in a tropical coastal zone. *Continental Shelf Research*, **69**, 101–109, doi:10.1016/j.csr.2013.08.018.

Jouanno, J., K. Ochoa, E. Pallàs-Sanz, J. Sheinbaum, F. Andrade, J. Candela, and J. Molines, 2016: Loop current frontal eddies: Formation along the campeche bank and impact of coastally trapped waves. *Journal of Physical Oceanography*, **46 (11)**, 3339–3363, doi:10.1175/JPO-D-16-0052.1.

Jouanno, J., E. Pallàs-Sanz, and J. Sheinbaum, 2018: Variability and dynamics of the yucatan upwelling: High-resolution simulations. *Journal of Geophysical Research: Oceans*, **123**, doi:10.1002/2017JC013535.

Merino, M., 1997: Upwelling on the yucatan shelf: hydrographic evidence. *Journal of marine systems*, **13**, 101–121.

Sheinbaum, J., G. Athié, J. Candela, J. Ochoa, and R.-A. A., 2016: Structure and variability of the yucatan and loop currentsalong the slope and shelf break of the yucatan channel andcampeche bank. *Dynamics of Atmospheres and Oceans*, **76**, 217–239, doi:10.1016/j.dynatmoce.2016.08.001.

Sheinbaum, J., J. Candela, A. Badan, and J. Ochoa, 2002: Flow structure and transport in the yucatan channel. *Geophys. Res. Lett.*, **29 (1–6)**.

Varela, R., X. Costoya, C. E. iquez, F. Santos, and M. Gomez-Gesteira, 2018: Differences in coastal and oceanic sst trends north of yucatan peninsula. *Journal of Marine Systems*, **182**, 46–55, doi:10.1016/j.jmarsys.2018.03.006.

Budget of the total nitrogen in the Yucatan Shelf: driving mechanisms through a physical-biogeochemical coupled model

Sheila N. Estrada-Allis[1], Joao M. Azevedo Correia de Souza[2], Julio Sheinbaum[1], Cecilia Enríquez Ortiz[4], Ismael Mariño Tapia[3], and Jorge A. Herrera-Silveira[3]

[1]Physical Oceanography Department, CICESE, Ensenada, Baja California, Mexico
[2]MetOcean Solutions / MetService. Raglan. New Zealand.
[3]Departamento Recursos del Mar, CINVESTAV, Merida, Yucatan, Mexico.
[4]ENES-Merida, Facultad de Ciencias, Campus Yucatan, UNAM, Mexico.

Correspondence: Sheila N. Estrada-Allis (sheila@cicese.mx)

Abstract. Continental shelves are the most productive areas in the seas with strongest implications for global Total Nitrogen (TN) cycling. The Yucatan shelf is the largest shelf in the Gulf of Mexico (GoM), however, its general TN budget has not been quantified. This is largely due to the lack of significant spatio-temporal *in situ* measurements and the complexity of the shelf dynamics, including ~~the Yucatan Current,~~ coastal upwelling, ~~Coastal Trapped~~ Coastal-Trapped Waves (CTWs) and influence of the Yucatan Current (YC) via bottom Ekman transport ~~. Through a nine years output of a coupled physical-biogeochemical model of the GoM~~and dynamic uplift. In this paper, the TN budget in the Yucatan shelf is quantified using a nine-year output of a coupled physical-biogeochemical model of the GoM. Results indicate that the main entrance of inorganic nitrogen is through its southern and eastern margins. The TN is then advected to the ~~oligotrophic deep GoM and to the deep Campeche bay. The analysis also shows~~ deep oligotrophic Bay of Campeche and central GoM. They also show that the inner shelf (bounded by the 50 m isobath) is ~~efficient~~ "efficient" in terms of TN, since all the ~~DIN imported into the~~ Dissolved Inorganic Nitrogen (DIN) imported into this shelf is consumed by the phytoplankton. ~~Rivers~~ Submarine groundwater discharges contribute 20 % of the TN, while denitrification removes up to 53 % of TN that enters into the inner shelf. The high-frequency variability of the TN fluxes ~~are modulated by the Yucatan Current in the south and by~~ in the southern margin is modulated by fluxes from the YC due to bottom Ekman transport ~~produced by this current~~ enhanced when the YC leans against the shelf-break (250 m isobath) ~~in the east~~on the eastern margin. This current-topography interaction can help to maintain the upwelling of Cape Catoche, uplifting nutrient-rich water into the euphotic layer. The export of TN at both western and northwestern margins is modulated by CTWs with a mean period of about 10 days in agreement with recent observational and modelling studies.

1 Introduction

Continental shelves are the most productive areas in the ocean, widely recognized to play a critical role in the global cycling of nitrogen and carbon ~~(e.g., Fennel, 2010; Liu et al., 2010). The importance of continental shelves also lies in its~~ (e.g., Fennel, 2010; Liu et al., 2010) with direct implications for human activities, such as fisheries, tourism, and ~~resources.~~

~~Their interaction with anthropogenic pollution sources is hence expected to have significant consequences not only in~~ marine resources (Zhang et al., 2019).

The importance of nitrogen budgets in shelves has motivated numerous observational and modelling studies of different shelves in the world (e.g., Fennel et al., 2006; Xue et al., 2013; Ding et al., 2019; Zhang et al., 2019). Their importance lies in that nutrient supply fuels primary productivity which in turn impacts the socio-economical ~~activities, e.g. , overfishing,~~ and recreational activities in those regions. Furthermore, the nitrogen shelf exchanges with the deep ocean influences the carbon cycle (Huthnance, 1995; Enriquez et al., 2010), and it is strongly correlated with other shelf processes such as: acidification, eutrophication~~(Enriquez et al., 2010), but also in the climate system, e.g.,~~ red tides, hypoxia/anoxia zones, pCO2 and sediment denitrification ~~(Fennel et al., 2006; Seitzinger et al., 2006)~~(Fennel et al., 2006; Seitzinger et al., 2006; Enriquez et al., 2010).

In the GoM, (Figure 1a), with a horizontal extension of almost 250 km, the Yucatan Shelf (YS) (Figure 1b and c) is one of the largest shelves in the world. The Yucatan state in Mexico occupies the 12th place in volume catches and the 6th place in production value of fisheries in the country. The fishery production is increasing every year with an enhancement of 72% from the year 2008 to 2017 (Anuario de Pesca 2017, 2017). It has 340 km of littoral extension, representing 3.1% of Mexico's littoral zone.

Nutrient fluxes are intrinsically related with the productivity and nitrogen cycling of the shelves. However, sources and sinks of nutrients are highly uncertain and difficult to quantify. This is partly due to the large spatial and temporal variability associated with the cross-shelf and along-shelf regional nutrient budgets and the difficulty to measure them. Biogeochemical coupled modeling systems are a useful tool to quantify the shelf-open ocean nutrient exchange, taking into account the different spatial and temporal scales ~~implicated~~ involved in the biogeochemical cycle ~~(Fennel et al., 2006; Hermann et al., 2009; Xue et al., 2013; Damien et al., 2018)~~(Walsh et al., 1989; Fennel et al., 2006) (Hermann et al., 2009; Xue et al., 2013; Damien et al., 2018; Zhang et al., 2019).

The physical mechanisms that drive and modulate the cross-shelf transport of nutrients and biogenic material are also poorly known. Shelves are rich dynamical areas in which several ~~process~~ processes can coexist at different spatio-temporal scales. Ekman divergence, CTWs, current interactions with the shelf break, mesoscale structures, vertical mixing and topographic interactions, among others, are recurrent processes that may uplift nutrient-rich waters from the deep ocean into the photic zone in the shelves (e.g., Cochrane, 1966; Merino, 1997; Roughan and Middleton, 2002, 2004; Hermann et al., 2009; Shaeffer et al., 2014; Jouanno et al., 2018).

~~In this study, we use a coupled physical-biogeochemical model to study the nitrogen budget in the Yucatan Shelf (YS), which is the largest continental shelf in the Gulf of Mexico (GoM, Figure 1). The biological cycling of the YS is one the most poorly known processes in the GoM and controversies remain regarding its physical dynamics besides the long-term undersampling of biogeochemical variables (Zavala-Hidalgo et al., 2014; Damien et al., 2018), and the presence of underground freshwater discharges with unknown fluxes. The main objectives of this study include: (i) the quantification of the Total Nitrogen (TN) budget within the inner and outer YS; (ii) examine the sources and sinks of nitrogen in the continental shelf and (iii) analyze the physical mechanisms that modulate the cross-shelf TN transport.~~

1.1 ~~The study area: Yucatan shelf~~

~~With a horizontal extension of almost 250 km, the YS or Campeche Bank (Figure 1b and c) is one of the largest shelves in the world. The wind pattern over the YS is mainly influenced by the trade winds (easterly winds) throughout the year, with sporadic northeasterly wind events caused by cold fronts with relatively short duration (Gutierrez-de Velasco and Winant, 1996; Enriquez et al., 2013). These easterly winds drive a westward circulation over the shelf (Enriquez et al., 2010; Ruiz-Castillo et al., 2016).~~

~~The~~ In this regard, the YS is a ~~highly dynamic region~~ complex system due to the coexistence of different physical processes. ~~Merino (1997)~~ One of the first studies in the area is Merino (1997) who reported the uplift of nutrient-rich Caribbean waters from 220-250 m deep, reaching the YS at the “notch area” (small ~~black~~ yellow box in Figure 1)~~. This happens~~ , likely due to the interaction of the Yucatan Current (YC) with the YS. The mainly zonal Caribbean currents turn towards the GoM when reaching the Yucatan Peninsula forming the strong western boundary YC that flows through the Yucatan Channel located between the eastern slope of the YS and Northwestern Cuba (see yellow line in Figure 1a). Once inside the GoM the YC becomes the Loop Current (LC) (Candela et al., 2002) which interacts with the slope of the YS on its eastern side (Cochrane, 1966; Merino, 1997; Ochoa et al., 2001; Sheinbaum et al., 2002) ~~which favors~~ favoring the outcrop of deep nutrient-rich waters to shallower layers over the shelf. However, the mechanisms responsible of ~~the upwelling remains~~ this upwelling remain unclear.

The ~~alongshore westward winds~~ wind pattern over the YS is characterized by the trade Winds (easterly winds) throughout the year, with recurrent northerly wind events during autumn and winter caused by cold atmospheric fronts with relatively short duration (Gutierrez-de Velasco and Winant, 1996; Enriquez et al., 2013). The easterly winds drive a westward circulation over the inner-shelf (Enriquez et al., 2010; Ruiz-Castillo et al., 2016). They are also responsible for ~~upwelling events~~ the upwelling along the zonal Yucatan coast due to divergent Ekman transport ~~at Cape Catoche~~ (Figure 2). The upwelling is ~~suggested to be~~ present year-round along the north and northeast coast of the YS, with intensifications ~~during spring and~~ from late spring to autumn (Zavala-Hidalgo et al., 2006). ~~This pattern is corroborated by the model as shown in Figure 2. However, there are controversies regarding the seasonality of the upwelling~~Besides the wind-induced upwelling near the coast there is also upwelling produced by the interaction of the YC with the eastern YS which is considered the principal mechanism that brings deep nutrient-rich waters over the YS. Observational studies ~~show that the upwelled waters usually cannot reach the photic layer (Merino, 1997; Enriquez et al., 2013). Therefore, it is expected that the variability of the upwelling can be influenced by the dynamics of the Yucatan Current (Sheinbaum et al., 2002) and by the wind-driven Ekman transport (Enriquez et al., 2010; Reyes-Mendoza et al., 2016). Dynamical processes that may also be important for the upwellinginclude the extension and the intensity of the Loop Current (Bunge et al., 2002; Jouanno et al., 2018),~~ suggest high intrusions of upwelled waters during spring and summer which are suppressed during autumn-winter (Merino, 1997; Enriquez et al., 2013). This seasonal variability is not easy to explain since the YC near the YS does not show such clear seasonal signal and is dominated by higher frequency mesoscale variations (Sheinbaum et al., 2016), so several mechanisms have been proposed to understand it. For example, (Reyes-Mendoza et al., 2016) show how northerly winds can suppress the upwelling. These cold front northerly winds are active during autumn-winter and could explain in part the seasonality of the cold water intrusions.

But other mechanisms appear to be important too: CTWs (Jouanno et al., 2016), ~~and the~~ topographic features and bottom Ekman transport (Cochrane, 1968; Jouanno et al., 2018), extension and intensity of the Loop current (Sheinbaum et al., 2016) and encroachment and separation of the YC and LC from the shelf (Jouanno et al., 2018; Varela et al., 2018). External (off-shelf) sea level conditions may also generate pressure gradients that oppose the upwelling and explain its seasonality (Zavala-Hidalgo et al., 2006).

Regarding the freshwater inflow, a significant amount of sources have been identified in the YS related to ~~groundwater inflows~~ Submarine Groundwater Discharges (SGD) due to the karstic geological formation of Yucatan ~~peninsula~~ Peninsula (Pope et al., 1191; Gallardo and Marui, 2006), coastal lagoons (Herrera-Silveira et al., 2004), and ~~sinkholes~~springs (Valle-Levinson et al., 2011). Due to the complexity of ~~processes~~ mechanisms and scarcity of observations, the total discharge of ~~freshwater~~ SGD into the YS is not well known.

~~Owing to the spatial and temporal scarcity of biogeochemical observations, the budget and pathways of nitrogen to the GoM shelves has been poorly quantified. This is specially truth for the southern part of GoM. Coupled models demonstrated to be an efficient tool~~ Coupled hydrodynamic-biogeochemical models can be used to establish the ~~routes of the TN (Fennel et al., 2006). In this sense Xue et al. (2013)proposed a~~ TN routes in the marine environment (Fennel et al., 2006). Xue et al. (2013), proposed the first model for ~~the TN dynamics for~~ TN dynamics in the GoM shelves ~~, excluding however~~ but excluding the YS. ~~From our~~ To the best of the authors' knowledge, there are no studies describing the nutrient flux pathways in the ~~widest Yucatan shelf. Therefore,~~ YS, so the present work represents the first ~~quantitative analysis aiming~~ attempt of a quantitative analysis to understand the biogeochemical cycles and their modulation by physical process at one of the most important socio-economical areas of the southern ~~Gulf of Mexico.~~ GoM.

We use a coupled physical-biogeochemical model of the whole GoM to study the nitrogen budget in the YS. The biogeochemical cycles of the YS are some the most poorly known processes in the GoM and controversies remain regarding its physical dynamics besides the long-term undersampling of biogeochemical variables (Zavala-Hidalgo et al., 2014; Damien et al., 2018), as well as the presence of SGD with unknown fluxes. The main objectives of this study include: (i) quantification of the Total Nitrogen (TN) budget within the inner and outer YS; (ii) investigation of the sources and sinks of nitrogen in the continental shelf and (iii) analysis of the physical mechanisms that modulate the cross-shelf TN transport

2 Model set-up and observational data

2.1 Physical model

The physical model is a GoM configuration of the Regional Ocean Modeling System (ROMS) which is a hydrostatic primitive equations model that uses orthogonal curvilinear coordinates in the horizontal and terrain following (*sigma*) coordinates in the vertical (Haidvogel and Beckmann, 1999). A full description of the model numerics can be found in Shchepetkin and McWilliams (2005) and Shchepetkin and McWilliams (2009). Horizontal grid resolution is $\sim$ 5 km, with 36 modified *sigma* layers in the vertical. We used a new vertical stretching option (Azevedo Correia de Souza et al., 2015) that allows higher resolution near the surface. The numerical domain, which covers the whole GoM, is shown in the bathymetry map in Figure 1a. The model was ~~ran~~ run for 20 years (1993 to 2012), from which we ~~used~~ use 9 years (2002 to 2010) in the present analysis in order to be ~~consistent with the observational~~ time-consistent with observational satellite data.

The bathymetry is provided by a combination of the "General Bathymetric Chart of the Oceans" (GEBCO) database (http://www.gebco.net/) with data collected during several cruises in the GoM. The initial and open boundary conditions for temperature, salinity and velocity come from the GLORYS2V3 reanalysis ~~(Ferry et al., 2012).~~ which contains daily averaged fields(Ferry et al., 2012). The model is also forced with hourly tides obtained from the Oregon State University TOPEX/Poseidon Global Inverse Solution (TPXO) (Egbert and Erofeeva, 2002). Hourly atmospheric forcing comes from the "Climate Forecast System Reanalysis" (CFSR) (Dee et al., 2014). These include cloud cover, 10 m winds, sea level atmospheric pressure, incident short and ~~longwave~~ long wave radiation, latent and sensible heat fluxes, and air temperature and humidity at 2 m. These variables are provided at ≈38 km horizontal resolution and are used to estimate surface heat fluxes in the model using bulk formulae (Fairall et al., 2003). The model uses a recursive three-dimensional MPDATA advection scheme for tracers, a third-order upwind advection scheme for momentum and a turbulence closure scheme for vertical mixing from Mellor and Yamada (1982).

2.2 Biogeochemical model

The biogeochemical model is described in Fennel et al. (2006), and is based on the Fasham et al. (1990) model which takes Nitrogen based nutrients as limiting factor. The model is solved for seven state variables, namely: Nitrate (NO_3), Amonium (NH_4), Phytoplankton (Phy), Zooplankton (Zoo), Chlorophyll (Chl), and two pools of detritus~~,~~: Large Detritus ($LDet$) and Small Detritus ($SDet$). Details of the model algorithm and coupling to ROMS can be found in Fennel et al. (2006).

Initial and boundary conditions for the biogeochemical variables were obtained from an annual climatology of NO_3, NH_4 and Chl. The climatology was calculated using all available profiles with the highest quality control from the World Ocean Database (Boyer et al., 2013), and profiles obtained from the XIXIMI cruises ~~executed by the CICESEgroup~~carried out by CICESE. The DIVA optimal interpolation (Troupin et al., 2012) scheme was used to ~~combine~~ interpolate the individual profiles in the climatology ~~using~~ to the model grid. DIVA takes into account the coast line geometry, sub-basins and advection to reduce errors due to artifacts in the interpolation.

~~However, it is well known that the available data density in the GoM is skewed towards the north.~~ The XIXIMI cruises ~~reduce this bias providing~~ provided profiles of nutrients and chlorophyll in the southern GoM which helps to reduce the bias between the northern and southern part of the GoM. The cruises encompass the region between 12°N and 26°N and -85°W and -97°W, and were ~~executed~~ carried out within the scope of the “Consorcio de Investigación del Golfo de México” (CIGoM) project (Gulf of Mexico Research Consortium project in English).

Close inspection of the shelf dynamics through maps of the temporally averaged velocity field U=($\overline{u}$,$\overline{v}$) (Figure 1b), where the overline denotes the temporal mean, and Mean Kinetic Energy MKE=0.5$(\overline{u}^2+\overline{v}^2)$ (Figure 1c) ~~allow~~ allows to delimit the shelf into two areas. The first is the inner shelf, delimited by the 50 m isobath where the strongest YS velocities develop

(Figure 1b) and where most of the MKE is enclosed (Figure 1c). The second area is the outer shelf between the 50 m and the 250 m isobaths, with the latter isobath representing the shelf break.

The TN examined in this study is taken as the sum of the Dissolved Inorganic Nitrogen (DIN) and the Particulate Organic Nitrogen (PON), with DIN = NO_3 + NH_4, and PON = $Phy + Zoo + SDet + LDet$, (Xue et al., 2013). The cross-shelf nitrogen fluxes are calculated as:

$$Q_{50m,250m} = \int_{-50,-250}^{\eta} \mathbf{u}_{cross}\ N_{z}\ dz \tag{1}$$

where $\mathbf{u}_{cross}$ is the velocity component normal to the 50 m or 250 m isobaths, η is the model sea level ~~anomaly and N_z~~ and N can be any component of the TN. Accordingly, the total budget is obtained as ~~:~~

$$\int_{\sigma_n}^{\eta}\int_{y_n}^{y_1}\int_{x_n}^{x_1} (N_z)\ dx\ dy\ d\sigma = Q_{50m,250m}$$

~~where x, y and σ indicate longitude, latitude and sigma (terrain-following) layer, with n the number of horizontal grid points or vertical model layers~~the integral over the area of the shelf and over the depth of the water column for both the inner and outer shelves. The budget also includes the loss to denitrification and to burial in the sediments, which are taken into account for the quantification of the TN budget as sinks of Nitrogen.

The initial concentration of the biogeochemical variables (NH_4, Phy, Zoo, Chl, and pools of detritus) is set to a small and positive value following Fennel et al. (2006, 2011); Xue et al. (2013). As mentioned in these references, the model quickly (days to weeks) adjusts internally to proper variable values. The biological model parameters used in this study are those shown in Table 1 of Fennel et al. (2006), except for the vertical sinking rates which were reduced about 10%, to fit the depth of the Deep Chlorophyll Maximum (DCM) observed with the APEX profiling floats (see Figure A4).

2.3 Freshwater sources

Two riverine systems account for 80% of the freshwater discharge into the GoM, the Mississippi/Atchafalaya system with 18,000 m^3s^{-1}, and Usumacinta/Grijalva system with 4500 m^3s^{-1} (Dunn, 1996; Yáñez Arancibia and Day, 2004; Kemp et al., 2016) ~~. Riverine~~ (see appendix C). Freshwater contributions to water volume, salinity, temperature and DIN concentration are included as grid-cell sources into the model. Apart from the two main systems, a total of 81 freshwater sources are included, taking ~~account for~~ into account freshwater discharges in the Florida, Texas and Yucatan shelves from years 1978 to 2015. For the US rivers the daily data were obtained from the U.S. Geological Survey (USGS) (https://www.usgs.gov/) and the Gulf of Mexico Coastal Ocean Observing System (GCOOS) (https://products.gcoos.org/). ~~Monthly climatological values were calculated for the Mexican rivers, using temporally scattered information found in the literature (Rojas-Galaviz et al., 1992; Milliman and Syvitski, 1992; Poot-Delgado et al., 2015; Conan et al., 2016) and a data collection~~

~~effort within Mexican institutions by Dr. Jorge Zavala-Hidalgo (*personal communication*). Therefore the US rivers present inter-annual variability but it is absent in the Mexican rivers.~~

Although the YS has no rivers, freshwater inputs play a key role impacting the local ecosystem (Herrera-Silveira et al., 2002). These inputs come from ~~underwater groundwater sources~~ SGD linked to the "cenotes" ~~(caves) system~~ ring (sink holes) system inland. The freshwater flux, temperature, salinity, and nutrient concentrations for these sources are not usually known. ~~For modeling purposes, these are inversely estimated by adjusting the model results to the few temperature and salinity *in situ* data available and to chlorophyll satellite images.~~

~~The nitrogen concentration for freshwater sources is essentially DIN. For most of the northern rivers (e.g., Mississippi and Atchafalaya), PON is also considered (Fennel et al., 2011; Xue et al., 2013). For the remaining freshwater sources the PON contribution is set as a constant small value of 0.1 mmolN m^{-3}.~~

~~We also use hydrographic and biogeochemical observational stations taken during~~ Monthly climatological values were calculated for the Mexican rivers and SGD systems, using temporally scattered information found in the literature (e.g., Rojas-Galaviz et al., 1992; Milliman and Syvitski, 1992; Poot-Delgado et al., 2015; Conan et al., 2016) and a data collection effort within Mexican institutions led by Dr. Jorge Zavala-Hidalgo (*personal communication*) and from the GOMEX IV cruise ~~in the study area~~of CINVESTAV (Centro de Investigación y Estudios Avanzados at Merida Yucatan) within the CIGOM project. During this cruise a total of 71 profiles of NO_3, potential temperature, salinity and chlorophyll were collected at standard depths ~~in~~ during 2-20 November 2015. The localization of the profiles are shown in Figure 2.

3 ~~Model results evaluation~~

2.1 ~~Basin model evaluation for the GoM~~

~~The lack of spatio-temporal biological data sets to validate biogeochemical models in the GoM is a well known problem (Walsh et al., 1989; Damien et al., 2018). The most abundant dataset is the satellite derived surface chlorophyll concentration. These observations give us a general overview of the chlorophyll temporal and spatial distribution patterns at basin scales. Monthly mean time series (1998-2010) of chlorophyll-a concentration from Aqua-MODIS and SeaWiFS 9 km and 4 km (when available) satellite products are used for model evaluation. The temporal series averaged for the whole deep GoM (i.e., excluding high productive coastal areas with less than -1000 m depth) show a good agreement between the coupled model and the observations. The model tends to overestimate the *Chl* in winter and underestimation in summer (Figure A5). Despite some exceptional years~~ Therefore the US rivers present inter-annual variability but it is absent in the Mexican freshwater sources (see appendix C for more details).

The nitrogen concentration for freshwater sources is essentially DIN. For most of the northern rivers (e.g., ~~1999), the modeled chlorophyll concentration values fall in the range exhibited by the satellite products. Mean satellital *Chl* is 0.1448 ± 0.04 mgChl m^{-3} in contrast with mean modelling *Chl* of 0.1433 ± 0.09 mgChl~~ Mississippi and Atchafalaya), PON is also considered (Fennel et al., 2011; Xue et al., 2013). For the remaining freshwater sources the PON contribution is set as a constant small value of 0.1 mmolN m^{-3}.

~~Observations of the chlorophyll vertical structure are available from eight APEX profiling floats with 537 profiles of Chl from 0 to 2000 m every ten days within the GoM (BOEM project) (Figure A4). A more detailed description of this database is provided by Hamilton et al. (2017), and the Chl data calibration by Pasqueron de Fommervault et al. (2017). The resulting profiles give valuable information to evaluate biogeochemical models through the water column, in contrast to the surface only information from satellite measurements (Pasqueron de Fommervault et al., 2017; Damien et al., 2018). The comparison shows that the model~~

3 Model evaluation for the YS

The model dynamics and its biogeochemistry are validated to guarantee the hindcast simulation is able to reproduce ~~the depth of the DCM measured by the floats. The DCM seasonal cycle is also well represented by the model. It is interesting to note the high dispersion in the data, revealing the large Chl variability found in the deep GoM.~~

~~The basin-scale physical validation of the model is presented in appendix A. The main features of the GoM variability are well represented by the model, specially the Loop Current which is a dominant player in the dynamics of the GoM. Climatology maps of~~ basic features of the observations in the GoM, particularly in the YS. Model statistics including biases of physical and biological variables are computed to have some feel of their impact on the estimation of the TN budget over this shelf. Since this a basin-scale coupled model, a general evaluation of the results and their statistics is carried out considering sea surface temperature~~(SST) are also shown. The model is able to reproduce the seasonal cycles of both SST and~~ , mixed layer depth~~.~~ , mean kinetic energy, surface chlorophyll and deep chlorophyll maximum over the whole Gulf of Mexico with emphasis on the YS. The results are presented in A.

3.1 ~~Regional model evaluation for the YS~~

~~The upwelling~~

3.1 YS *In situ* data comparison

Recall that upwelling into the YS is more intense during ~~Spring~~ spring-summer and weaker in ~~Autumn as indicated in recent observational studies (Ruiz-Castillo et al., 2016)~~autumn-winter (Ruiz-Castillo et al., 2016; Merino, 1997). While the model presents upwelling during all the simulated months, this seasonal behavior is ~~well~~ represented in the ~~climatologies obtained from the simulation results~~ model climatologies shown in Figure 2. The ~~same~~ figure also shows the position of ~~the~~ oceanographic stations occupied during the GOMEX IV oceanographic cruise, and the delimitation of three areas of particular interest: the inner shelf, the outer shelf, and the upwelling region at Cape Catoche. The climatology of the YS bottom temperature (Figure 3) shows that cold waters enter into the shelf during spring in agreement with the enhancement of chlorophyll concentrations (Figure 2b). The zonal vertical cross-sections show that the isotherm 22.5 °C, which traces the upwelled water (Cochrane, 1968; Merino, 1997), outcrops into the shelf during spring (Figure 3c). However, this is not the case for autumn (Figure 3d), and the upwelling is weaker (Figure 2d).

A point-by-point comparison between the model results and the *in situ* observations is shown using only data for November months from 2002 to 2010 in the model, for compatibility with the observation dates (Figures 4, 5, 6 and 7). Since the hindcast simulates different years we only expect to reproduce basic features of these observations. The range of temperatures at different depths shown by the model agrees well with those observed during the GOMEX IV (Figure 4). The mean ~~observed temperature value~~ temperature of the observations is 25.5 ±2.9 °C, while the model ~~exhibits a mean temperature of~~ mean temperature is 24.3 ±3.7 °C. ~~These differences 0.3 - 1.5°C are considered acceptable considering there is no dataassimilation in the model~~The bias of -1.3 °C is deemed acceptable considering the model mean is a 9 year mean whereas the mean from observations is from just one month and a different year. A critical area to be evaluated is the upwelling region (see dashed box in Figure 2a), the bias there is -1.1 °C with a root mean square error of 1.68 °C. This means that the model tends to be slightly colder than the observations even inside upwelling waters.

The model mean salinity is 36.5 ±0.2 which matches the 36.5 ±0.2 from observations (Figure 5). Whereas in the surface the model salinity is in relatively good agreement with observations (Figure 5a), differences become more important at deeper layers (Figures 5b and 5c). The root-mean-square error of model salinity (0.23) is low as well as the bias (-0.04) which tends to underestimate the salinity observations. These low differences are also found in the bias for the upwelling area, although here the model overestimates the salinity by 0.21. The model is able to represent main characteristics of the Caribbean Subtropical Underwater coming from the Caribbean Sea (Merino, 1997) and the Gulf Common Water from the GoM (e.g., Enriquez et al., 2013) within the YS. The warm and high salinity Yucatan Sea Water at the surface described in Enriquez et al. (2013) is present in the model too, although temperatures do not exceed 31°(not shown) as in observations.

For Chl, the model results fall within the range obtained from the fluorometer observations for the inner-shelf, outer-shelf and upwelling areas (Figure 7). The mean observed Chl (0.52 ±0.58 mgChl m^{-3}) is slightly larger than the model results (0.44 ±0.42 mgChl m^{-3}) but within the one standard deviation range, with a bias of -0.08 mgChl m^{-3} and a root mean square error of 1.16 mgChl m^{-3}. Notice that there is agreement in Chl concentration between model and observations in the three layers between 150 m depth and the surface (Figures 7a, b and c). In the upwelling area the model has lower concentrations than observations with a bias of -0.39 mgChl m^{-3} and a root mean square error of 1.39 mgChl m^{-3}, although the bias is relatively low, it needs to be taken into consideration for the total Nitrogen budget. Additionally, a comparison with observed mean chlorophyll vertical profiles over the YS is presented in appendix B. Profiles have similar structure but model tends to underestimate the DCM.

To evaluate the temporal behavior of the model Chl, time series of the surface chlorophyll averaged over the shelf are compared to similar time series from satellite surface chlorophyll from MODIS (see Figure 8c, and Appendix A for a description of the satellite product) for the hindcast period. Mean values of satellite surface Chl are 0.38 ±0.09 mgChl m^{-3} and 0.36 ±0.13 mgChl m^{-3} in the model. Besides reproducing temporal mean and variability of the surface chlorophyll, the model is able to reproduce a positive trend present in the nine years of satellite data. No trend is present in any of the biogeochemical forcings of the model and determining which physical mechanisms produce it requires further investigation (see below).

The simulated nutrient concentration depicts similar order of magnitude values (~~3.1~~ 3.12 ± ~~4.8~~ 4.57 mmolN m^{-3}) as the observed profiles (~~3.7~~ 3.67 ± ~~5.2~~ 5.24 mmolN m^{-3}) (Figure 6). Surface nutrient concentrations are underestimated by a 1.7

(mmolN m^{-3}) compared to observed profiles (Figure 6a). At subsurface depths (25 - 55 m), the model tends to underestimate the NO_3 concentrations~~,~~; however, in the upwelling area, model NO_3 concentrations are closer to the observed values with a bias of -0.71 m^{-3} and larger standard deviations for both model (4.09 $\pm$ 5.0 m^{-3}) and observations (4.81 $\pm$ 6.33 m^{-3}) (Figure 6b). The temporal variability of the modeled NO_3 is larger than the observed NO_3 at the surface and bottom as shown by the largest standard deviation in Figure 6b.

Below 55 m ~~, both~~ the modeled and observed NO_3 are in good agreement in both, the outer shelf and the upwelling area (Figure 6c). Again, these model results are deemed consistent with observations ~~(since there is no data assimilation) and~~ and are in the range of other values reported in the literature (Merino, 1997). ~~Since our knowledge, this is the first modeled study focus on the nitrate budget of the YS. Thereby, a direct comparison of the nitrate concentrations with other modeled results near the study area, e.g., Fennel et al. (2006) and Xue et al. (2013), is not straightforward because of~~ Comparison of similar budgets from other shelves in the GoM can be made (e.g., Xue et al., 2013) though clear interpretation of similarities and differences between them may be difficult given the differences in ~~the dynamics and the nitrate sources between the different shelves of the GoM~~dynamics and nitrate sources and sinks controlling the budgets on each shelf. One could easily compute budgets per unit area or length for a more sensible comparison among different shelves but in the literature only total budgets are available (see table 2 in Xue et al. (2013)).

~~For Chl~~In addition, the model ~~results fall within the range obtained from the fluorometer observations for the inner-, outer-shelf and upwelling area (Figure 7). The mean observed Chl (0.52 $\pm$0.6 mgChl m^{-3}) is slightly larger than the model results (0.44 $\pm$0.6 mgChl m^{-3}) but within the one standard deviation range, with mean differences between 0.1 - 0.4mgChl m^{-3}. Notice that there is agreement in Chl concentration between model and observations in the three layers between 150 m depth and the surface (Figures 7a, b and c)~~sea level elevation and surface ocean currents are compared against altimeter products in appendix A. In this appendix, the YC variability and transport in the model are compared with data from three moorings located on the slope close to the eastern YS rim described in Sheinbaum et al. (2016).

4 Total Nitrogen budget and cross-shelf transports in the YS

~~The spatial averages of TN~~ Time series of spatially averaged TN over th YS suggest a positive trend over the nine simulated years. ~~This is observed for~~ The trend is seen in both the inner and the outer ~~shelf~~ shelves (Figures 8~~a-d). The positive trend along time is also observed for temporal series of satellite chlorophyll, spatially averaged for the Yucatan Peninsula~~ a and b). This, perhaps, could be expected given the positive trend in both model and satellite surface Chl mentioned before (Figure 8~~e), indicating that the modelled trend is not an artifact of the coupled model .~~ c). Varela et al. (2018) report a cooling trend of the inner YS and suggest may be associated with an eastward shift of the YC. We searched for possible connections between the trends in chlorophyll and TN and indices measuring the position and strength of the YC in the model but found no correlation. This is an interesting problem currently under investigation to be reported elsewhere.

In the inner shelf there are similar total integrated values of DIN and PON (Figure 8~~b), whereas~~ a). This indicates the presence of a very efficient biogeochemical cycle in the inner shelf (see explanation below). By contrast, in the outer shelf, DIN values are larger than PON (Figure 8~~d) . This is related to a very efficient biological cycle in terms of TN in the inner shelf, and to the fact that~~ b) probably because the integration in the outer shelf includes a large volume below the euphotic zone. The temporal series of the integrated TN show a combination of low frequency variability associated with the seasonal cycle ~~and a high-frequency signal (periods lower than 30 days)~~as well as interannual variability, but longer period integrations are required to properly investigate the latter.

To understand the high TN variability in the ~~YS-TN temporal series and to elucidate the contributions from different sources, the~~ YS quantification of the cross-shelf fluxes becomes necessary. Their impact on the TN budget and the physical mechanisms modulating such fluxes are investigated next.

~~The cross-shelf~~ Cross-shelf fluxes are quantified for the two compartments, the inner and outer shelves (Figure 1b), and for all ~~of~~ the boundaries of each compartment. ~~An~~ A schematic view of the main incoming and outgoing pathways of cross-shelf TN fluxes is shown in Figure 9. The yearly averages of the spatially integrated cross-shelf fluxes are shown in Table 1.

For the inner shelf, both PON and DIN are imported through its northern and eastern boundaries and exported through the west and south borders. ~~The inner~~ Inner shelf acts as a source of PON for the Campeche ~~basin~~ Bay at the southwest margin. The major source of TN for the inner shelf is from the outer shelf ~~through~~ via the Cape Catoche upwelling~~region~~, representing 80% ~~. Freshwater sources contribute a~~ of the total while freshwater sources contribute with 20%. Although ~~this~~ the latter is a relatively ~~high~~ large source of nitrogen, its relevance seems to be confined to the NW part of the inner-shelf. In general, there is ~~a~~ compensation between the DIN and PON concentrations in the inner-shelf (Figure 8~~b) . This is attributed~~ a) due to an efficient biogeochemical cycle ~~, where~~ whereby almost all the DIN imported into the shelf is consumed by the phytoplankton and thus converted into PON. ~~This efficiency relies in the shallow water column~~ The efficiency relies on the shallowness of the inner shelf (50 m depth)~~, meaning that~~ . If strong mixing conditions were present, organic matter would be distributed throughout the water column. This is enhanced during winter, when vertical wind-driven mixing and convective processes are strong enough to reach the sea bottom. Additionally, vertical shear likely generated by bottom friction can lead to instabilities and vertical mixing able to break the stratification and carry nutrients to the euphotic zone. During summer months, vertical mixing is weaker (not shown). Turns out vertical velocities in the inner shelf ~~is completely in the photic zone and under a strong mixing regime that redistributes the organic matter trough the water column~~in the model are quite intense and upward throughout the year ($\sim$ 5 m day^{-1}) carrying nutrients to the euphotic layer. The cause of these vertical velocities is under investigation using a higher resolution model configuration.

By contrast, in the outer shelf, the largest inputs of PON and DIN are advected through its southeastern corner. The eastern boundary is a source of DIN but a sink of PON for the outer shelf. Therefore, the budget reveals that the PON exported to the inner shelf is produced in the outer shelf and not advected from Caribbean waters. ~~The remaining TN flows escapes from the YS towards the deep GoM and the Campeche bay across the northern and western boundaries respectively.~~

The contribution of TN from the inner shelf to the outer shelf represents only 1.5% of the total inputs.

Over the outer shelf the fluxes of nutrients and organic matter are driven by a westward wind driven circulation (Ruiz-Castillo et al., 2016) ~~to be~~ and exported to the deep GoM ~~through the north and to the Campeche basin through the west border~~and the Campeche Bay through the north and west borders respectively. This represents a source of DIN, Phy and Zoo to ~~the Campeche and the deep GoM, which are by definition oligotrophic areas~~these oligotrophic regions.

In that regard, the model reveals a quasi-permanent thin filament of Chl that is advected from the northwest corner of the outer shelf to the west of the Campeche ~~bay~~ Bay (Figure 10a). A vertical section of the cross shelf fluxes along the 250 m isobath in the western YS (TN, Figure 10b) shows that while the export of organic matter to the open sea is concentrated in the surface layers (Figure 10d), the bottom layer presents a net DIN export (Figure 10c). The climatological average over nine years of simulated Chl show that this filament is intensified during winter times (not shown), although it is present during the whole ~~simulated~~ simulation period. Sanvicente-Añorve et al. (2014) studied the larval dispersal for coral reef ecosystems in the southern GoM. They show that the northwestern corner of the outer YS acts as a sink region for larvae. Similar to other coral reef systems, they attributed the sink to the influence of the circulation patterns that lead to a unidirectional dispersion pattern during the whole year. Our model results support this idea providing nutrient dispersion patterns in the region over longer time periods.

Denitrification is a form of anaerobic microbial respiration in which nitrate and nitrite are finally reduced to dinitrogen. It represents a major sink for bioavailable nitrogen. The spatio-temporal average rate of denitrification for the YS is of 1.11 ± 0.13 mmolN m^{-2} d^{-1}. Our results suggest that denitrification removes up to the 53% of the TN ~~into~~ in the inner shelf, a significant percentage that agrees with estimates ~~for~~ from other shelves in the GoM ~~(Fennel et al., 2006)~~(Xue et al., 2013). On the other hand, denitrification in the outer shelf only removes 9% of the TN. Our results also indicate ~~that~~ the denitrification rate tends to increase with time for both inner and outer shelves (not shown), similar to TN concentration (Figures 8a and ~~c~~b). This is expected since denitrification is a reduction process, hence an ~~increases in the~~ increase in nitrate concentration means more available DIN to be reduced to dinitrogen.

4.1 Physical modulation of cross-shelf TN flux by CTWs

Many physical process coexist at different spatio-temporal scales in the YS that modulate the cross-shelf transport of nutrients and organic matter. We suggest that at least two process are responsible for such modulation: ~~the CTWs and the~~ CTWs and interaction of the ~~Yucatan Current with the~~ YC with the eastern shelf break.

CTWs can be generated by wind forcing over irregular bottom topography along the coast ~~. These perturbations propagate with the shelf on their right in the northern hemisphere,~~ and have been the subject of ~~research~~ investigation for a long time (e.g., Clarke, 1977). ~~The~~ In the GoM, CTWs are forced by alongshore winds and then travel anti-clockwise with the coast on its right until they reach the western portion of the Yucatan Peninsula (Dubranna et al., 2011; Jouanno et al., 2016).

CTWs have a signature in ~~the sea level ,~~ sea level that is well captured in relatively high resolution models such as the one used in the present study (~ 5 km). ~~These waves have been reported as being responsible for the modulation of upwelling systems such as the Australian coastal upwelling (Shaeffer et al., 2014). Few modelling and observational studies (Kolodziejczyk et al., 2011; Dubranna et al., 2011; Jouanno et al., 2016)~~ Few observational and modelling studies (Dubranna et al., 2011; Jouanno et al., 2016) describe the characteristics of CTWs in the GoM. Jouanno et al. (2018), in their modelling study, suggest that CTWs may influence the Yucatan upwelling pulses. In this study, the presence of CTWs is corroborated and its effect ~~modulating the~~ on the modulation of cross-shelf nutrient fluxes at the west margin of the YS is exposed.

The ~~CTWs are remotely forced by alongshore winds, and occasionally in the Florida shelf (Dubranna et al., 2011; Jouanno et al., 2016), although are not necessarily ubiquitous of the northern part of the GoM. These waves then travel anti-clockwise with the coast on its right until they reach the western portion of the Yucatan peninsula. Observational and modelling studies pointed out that these waves cannot propagate beyond the Campeche shelf (Kolodziejczyk et al., 2011). The mechanism behind the vanishing of CTWs at the Campeche shelf may be related to a competition between the planetary β effect and the topography effect (Venegas-Vega, 2017). At the southern GoM the planetary effect induces the wave propagation and eddies to the west, while the topographic local effect induces a wave propagation towards the east. As a result, the propagation is inhibited at these places. The same pattern is present~~ presence of CTWs in the model simulations ~~, as evidenced by the hovmoller~~ is evidenced in the hovmöller diagram along the 50 m isobath shown in Figure 11. ~~In agreement with previous observational and modelling studies of CTWs in the GoM (Dubranna et al., 2011; Jouanno et al., 2016), we find phase speeds~~ Phase speeds are in the range of [2 - 4] m s^{-1} ~~(Figure 11b)~~in agreement observations (Dubranna et al., 2011) and other models (Jouanno et al., 2016).

~~The multi-taper spectral analysis of Figure 12 (left hand figures) shows that the spectral shape and the range between 10 and 13 days of significant period peaks, are in close agreement between SLA and~~

The western boundary cross-shelf ~~velocity time series (Figures 12a and b). Although similar peak periods between 7 and 12 days are found for the~~ TN in the inner shelf, exhibits high-frequency variability, in agreement with temporal series of wind-stress ~~time series~~ and SLA (Figure 12~~c), the resemblance with the cross-shelf velocity is not so evident as for the SLA. Moreover, analysis~~). The daily climatology of the wavelet power ~~spectra of~~ spectrum of each temporal series in the right-hand side of Figure 12, show that both the along-shelf wind stress and changes in the SLA may be linked with the cross-shelf ~~velocity (Figure 12, right hand figures), sea level anomaly (Figure 12b) and the wind-stress (Figure 12c), shows that characteristic periods of the cross-shelf velocity in the 50 m isobath are well correlated with characteristic mean periods shown by the sea level anomaly temporal series (r^2=0.41). By contrast, these periods are not correlated with the mean periods exhibited by the local wind-stress (r^2=0.16). This shows that the ocean perturbations are remotely generated, with small influence from the local wind variability . The characteristic periods of each wavelet power spectrum are shown in Figure 12d. These periods are computed from the spectral wavelet analysis, by connecting periods of maximum power energy per day. The correlation coefficients found are statistically significant with p-values that greatly exceed the 95% confidence level. The mean and standard deviation of each time-series shown in Figure 12d are displayed in the wavelet power spectra. Notice that a mean period of 10.4 days for the cross-shelf velocity wavelet spectrum matches the mean period found for the SLAs~~TN variability in the inner shelf. The three variables show maximum energy during winter times when CTWs are expected to be more intense, and the wind increases its magnitude due to the pass of the "Nortes" (cold front winds).

~~The~~ It is worth mentioning that the wavelet power spectrum ~~analysis also provides a new view of the inter-annual variability of the nutrient flux. There are specific years in which the power increases. See for instance the years~~ for the whole 2002-2010 period (not shown) depicts an interesting intensification of cross-shelf flow (and nutrient fluxes) during 2003,2004,2009 and

2010 ~~in Figure 12a and b. These time intervals are consistent with years in which a El Niño Modoki or pseudo El Niño events are reported (Ashok et al., 2007; Ashok and Yamagata, 2009). For instance, Conan et al. (2016) suggest that El Niño Modoki 2009-2010 event influenced the biogeochemical cycling of phyto and bacterio-plankton communities in Términos Lagoon (South of GoM, in~~ which coincides with Niño-Modoki events (Ashok et al., 2007; Ashok and Yamagata, 2009). This is an issue that deserves further investigation.

To further examine the relationship between these physical and biogeochemical variables, a cross-correlation spectral analysis is shown in Figure 13 for the time series of Figure 12. The variability of along-shelf wind-stress and cross-shelf TN fluxes shows significant coherence in the 8-10 day period band at nearly zero phase lag (Figure 13. Coherence between cross-shelf TN fluxes and SLA is also coherent in the same band (peaks at 8 and 8.4 days) but 180 degrees out of phase. This is consistent with offshore Ekman transport produced by along-shelf northerly winds triggering nutrient and organic matter fluxes across the western boundary of the ~~Campeche shelf). They found that in this period the export of organic matter to the GoM was weak, making the Lagoon function as an nitrogen sink. This particular type of El Niño, is produced when the sea surface temperature warms in the central Pacific (rather than in the western Pacific as the classic El Niño) and is surrounded by colder waters to the east and west. As a result wet conditions are produced in the central Pacific. There are evidences suggesting that El Niño Modoki can lead to an increase in the activity of tropical cyclones (Larson et al., 2012). Notice however that the year 2005, widely recognized to be the most intense hurricane season of the GoM, is not marked in the El Niño Modoki index and in the wavelet analysis presented here. Hence, our analysis is not enough to draw any conclusion and further modeling and sampling effort research is needed.~~ YS and negative sea level anomalies at the coast.

4.2 ~~Influence of the Yucatan Current in the coastal upwelling~~

~~Other physical mechanisms act to modulate~~ Propagation of CTWs is evident in the Hovmöller diagram of Figure 11 and most certainly modulates the cross-shelf ~~transport on the YS eastern and southeastern borders, specially affecting the DIN. The main import of TN to the YS is through the south, which can be related to advection by instabilities or encroachment of the intense Yucatan Current. This current flows from the Caribbean sea through the Yucatan channel to finally become the Loop Current.Similarly, the export of TN to the deep GoM through the YS northern margin can be related to advection by the Yucatan Current and mesoscale structures.~~ TN transport. The coherent 8-10 day period band (and at other higher frequencies, e.g 5-6 day period) is in agreement with those reported in the literature for CTWs in the GoM (e.g., Jouanno et al., 2016). Since the coherence analysis is carried out using time-series of spatially averaged quantities (from 20°30’ N to almost 22°N, approximately 100 km), that probably masks this modulation.

~~However, this process can’t be responsible for the second most important import of TN to the shelf at the eastern boundary. Here, other factors such as wind-induced upwelling at Cape Catoche and the interaction between the topography and the Yucatan Current can drive a TN flux to the YS (Jouanno et al., 2018). Previous observational studies found that the upwelling at Cape Catoche is~~

4.2 Influence of the Yucatan Current in the coastal upwelling

Observational studies suggest that favorable-upwelling winds at the northern Yucatan coast are present all year ~~(Ruiz-Castillo et al., 2016; Pérez-Santos et al., 2010), being more intense during spring time (Zavala-Hidalgo et al., 2006). The reason for this seasonality is not correlated with the Trade winds, since these are present throughout the year~~round (Ruiz-Castillo et al., 2016; Pérez-Santos et al., 2010). Cold SSTs on the YS vary seasonally and are particularly characterized by a cold water band on the inner YS very close to the coast that appears in spring and continues until the beginning of autumn (Ruiz-Castillo et al., 2016; Zavala-Hidalgo et al., 2006). Pérez-Santos et al. (2010), ~~through~~ using ten years of sea surface wind data from ~~the QuikSCATsatellite, found that the~~ QuikSCAT, show that Ekman transport is the main contributor to the upwelling over the north YS (93 %), ~~whereas the~~ with Ekman pumping only ~~contributes the~~ contributing 7%. ~~Therefore, the wind stress curl through classic Ekman pumping theory can not be the main driving mechanism of the upwelling.~~

This upwelling regime requires a supply of cold, rich-nutrient deeper waters from the open ocean to maintain the observed biological productivity on the YS.

The ~~interaction~~ main import of TN to the YS is through the southeast and eastern YS boundaries through processes related to the dynamics of the Yucatan ~~current with the shelf break has been proposed as a mechanism to uplift deep waters into the shelf, feeding the upwelling process (Merino, 1997; Enriquez et al., 2013; Jouanno et al., 2018).~~ and Loop currents and their interaction with YS shelf-break such as intensification, separation and/or encroachment from the coast, bottom boundary layer transport, advection, instabilities, eddies and topographic features. See (Roughan and Middleton, 2002), for a discussion of upwelling mechanisms on the East Australian Current that appear to be relevant here too as several local studies indicate (Cochrane, 1966; Merino, 1997; Zavala-Hidalgo et al., 2006; Enriquez et al., 2010, 2013; Enriquez and Mariño Tapia, 2014) (Carrillo et al., 2016; Jouanno et al., 2016, 2018).

On the other hand, the export of TN to the deep GoM through the YS northern margin can also be related to advection by the YC and associated mesoscale structures (Roughan and Middleton, 2002; Carrillo et al., 2016; Enriquez and Mariño Tapia, 2014).

Correlation analysis between the ~~Yucatan Current and the~~ strength of the cross-shelf flow from the YC and TN, PON and DIN fluxes at the eastern margin, all vertically integrated, show high values at ~~interannual~~ seasonal time scales (Figure 14). The time series are filtered by a 30 day moving average window to remove high frequency variability. The square of the correlation coefficients (r^2) for TN, DIN, and PON against the vertically integrated YC are indicated on top of the Figure 14. The results show that TN fluxes are well correlated with the strength of the current.

To investigate the possible role of the position and trajectory of the ~~Yucatan Current~~ YC and its closeness to the YS ~~has been also proposed as an upwelling mechanism (Enriquez et al., 2010, 2013; Jouanno et al., 2018). When the Yucatan Current is closest to the Yucatan Peninsula, an increase in the sea surface height can be produced, favoring that Caribbean waters enters into the shelf. We have computed~~ in the upwelling (Enriquez et al., 2010, 2013; Jouanno et al., 2018) we computed an index measuring the closeness of the ~~Yucatan Current core to the~~ YC core to Cape Catoche and ~~Notch areas~~the Notch areas in the model, which are ~~the~~ two places where ~~nutrients can be upwelled (not shown)(Jouanno et al., 2018). Our results~~

~~pointed out that there is not a seasonality in the closeness of the current that explains the intensity of~~ water tends to upwell (Merino, 1997; Jouanno et al., 2018). The index depicts no seasonality that could be directly connected to strong(weak) upwelling during spring(autumn). This is an indication that seasonality of the ~~upwelling during Spring or its weakness during Autumn. However, we found an smaller but significant correlation with the sea surface height, supporting the reasoning of a dynamical upwelling due water accumulation in the coast. This analysis also show that the slope of the isotherm 22.5 °C, which traces the upwelled water (Cochrane, 1968; Merino, 1997), is slightly more steepness when the current core is close to the shelf.~~ inflow of rich nutrient water into the YS is probably influenced more by other processes as discussed in Reyes-Mendoza et al. (2016), such as cold front winds that can stop the upwelling or other non-local perturbations.

~~This study suggests that, at~~

One of the important mechanisms suggested since Cochrane (1966) to be responsible for the YS eastern boundary ~~,~~ upwelling and the nutrient flux towards the coast ~~can be driven by the Ekman bottom layer transport from the~~ is bottom Ekman layer transport produced by interaction of the ~~Yucatan Current with the~~ YC with the upper slope and shelf break. The stress exerted by the intense along-shore velocity of the ~~Yucatan Current at the sharp shelf break produce a bottom~~ YC on the topography generates an Ekman spiral at the bottom ~~. Similar to a surface Ekman spiral in the Northern Hemisphere, a northward along-shelf flow will generate~~ boundary layer and a net depth integrated transport to the left ~~in the bottom boundary layer,~~ i.e., a cross-shelf transport towards the shelf ~~. Similar mechanism has been for the southeastern Australian shelf Shaeffer et al. (2014). Using glider observations , the authors found that the~~ in the boundary layer. For example, Shaeffer et al. (2014) using glider observations find that bottom Ekman transport can explain up to the 71% of the bottom cross-shelf transport variability ~~. It is worth noting that Sheinbaum et al. (2016), throughout three years of mooring measurements, show that the mean current near 1000 m oriented along the eastern edge of the YS flows towards the Caribbean sea, i.e., southwards. A southward flow at the eastern part of the YS will generates a coastal downwelling by an eastward Ekman transport. Notwithstanding, they also found that near surface, between 60 and 500 m, the mean current direction is northwest and its magnitude is stronger than the deepest southwards current.~~ on the southeastern Australian shelf produced by the East Australian Current.

~~Until now this process has not been fully tested. The present study provides a first~~ Here we present modeling evidence that ~~a bottom Ekman mechanism can~~ bottom Ekman layer transport could be the precursor ~~for~~ of the upwelling in Cape Catoche. The Bottom Ekman Transport (U_{bE}, m^2 s^{-1}) can be taken as $U_{bE} = -\tau_{by}/(\rho_o f)$, where τ_{by} is the bottom stress computed by $\tau_{by} = \rho_o C d v_b \sqrt{u_b^2 + v_b^2}$, with $Cd = 1x10^{-3}$ the drag coefficient, u_b and v_b are the bottom velocities at the 250 m isobath, f the Coriolis frequency and $\rho_o =$ ~~2015~~ 1025 kg m^{-3} the reference potential density of the sea water. ~~We found that~~ The analysis shows that the time-mean U_{bE} is ~~positive towards the shelf , and it is largely~~ toward the shelf (defined positive here), and is well correlated with the bottom cross-shelf water transport ($r^2 = 0.71$, $ci = 95\%$) ~~flowing towards the shelf~~ calculated directly (Figure 15a). The Ekman transport is calculated from the theoretical formula (i.e. stress divided by the coriolis frequency) whereas the direct transport is calculated using the bottom velocities and integrating on the last grid cell. We should mention here that the bottom grid cell at this depth has a vertical size of ∼20 m. Using standard formulas to estimate the width of the Ekman layer (e.g., Cushman-Roisin and Beckers, 2011; Perlin et al., 2007) from bottom velocities or stresses and stratification we obtain values ∼ 10-30 m, therefore the layer is not really resolved by the model grid. The correlation is also large ~~along~~

over time ($r^2 = 0.78$, $ci = 95\%$) as shown in Figure 15b. ~~The comparison between the~~ Figure 15c shows that the vertically integrated TN transport averaged over nine simulated years and over latitude is towards the coast at 250 m depth, that is, at the bottom-most model layer which is considered here as the bottom Ekman layer.

Comparison between bottom layer Ekman transport and the time mean vertically integrated TN transport across the eastern 250 m isobath ~~(Figure 15c) show that the~~ indicates that bottom Ekman transport is responsible for 65 % of the TN that is entering the shelf. The ~~remaining flux in upper layers seems must be related to recirculation of the Yucatan Current by baroclinic meandersand small-scale structures whose role on the upwelling process needs to be further investigated.~~

~~Despite being an important mechanism acting to uplift nutrient-rich waters to the shelf helping the Cape Catoche upwelling~~mechanisms that explain the remaining flux need to be further investigated and are probably related to meanders, eddies, topographic features and other processes. Moreover, bottom Ekman transport ~~is not~~ can be arrested by stratification and may not be dominant everywhere along the YS east coast as has been documented in other western boundary upwelling regions (e.g., Roughan and Middleton, 2002, 2004). Our goal here was only to estimate the size of the ~~only possible mechanism. Other processes, such as the interaction of the Loop Current with the notch could develop intense vertical velocities thus enhancing the upwelling (Jouanno et al., 2018), encroachment of the current jet and mesoscale structures effects (Roughan and Middleton, 2002, 2004). Regarding current-topography interactions, Jouanno et al. (2018), by running a high-resolution model of the GoM, found that removing the notch from the bathymetry, the upwelling could be reduced in a 50% .~~

~~Here, we suggest that the upwelling of Cape Catoche is maintained by the combined effect of physical processes of topographic nature, in which the Ekman bottom transport has an important role, but is not the unique. Other processes, such as, current encroachment and eddy induced upwelling can have also important roles that must be analyzed in future research~~TN fluxes related to the bottom Ekman layer to determine its relative importance.

5 Concluding remarks

We present the results of a nine year simulation from a physical-biogeochemical coupled model for the GoM, focusing on the YS. The TN budget, main nutrient transport pathways and their modulation by physical process over the Yucatan shelf are evaluated. Our work provides a first general view of the shelf physical-biogeochemical coupled system, schematized in Figure 16.

The results indicate that TN, especially DIN, enters the outer-shelf through the southern and eastern margins. The TN is then driven by a westward shelf current and is exported to the deep GoM and Campeche ~~Sea~~ Bay through the northern and western boundaries, respectively. In the inner-shelf, the biogeochemical nitrogen-based cycle seems to be ~~effective~~ very efficient for NO_3 remineralization/consumption by the phytoplankton converting the DIN to PON. The freshwater sources represent an important contribution of about 20% to the DIN concentration, although it is restricted to the northwest of the Yucatan peninsula. ~~The denitrification~~ Denitrification represents the main sink of nutrients for the inner shelf, removing more than the 50% of the nitrogen. ~~Despite~~ Although the inner shelf contributes to the TN ~~to~~ at the west boundary of the outer

~~shelf~~YS, this contribution is less than 2%, indicating low connectivity from the inner to the outer Yucatan shelf. ~~On contrary~~In fact, the outer shelf ~~acts as~~ is the main nitrogen ~~supply to~~ supplier of the inner shelf, mainly of PON which comes from the eastern margin. ~~Moreover~~Further more, a quasi-constant filament in the west outer shelf border ~~represent~~ represents an important source of both organic and inorganic nitrogen for the oligotrophic Campeche ~~sea~~Bay.

~~While the surface Ekman layer~~ Surface Ekman layer dynamics at the western and northwestern ~~outer shelf borders transport~~ shelf borders play an important role in the transport of nutrient and organic matter to the Campeche Bay and the deep central GoM~~, this process is not able to explain~~ . Part of the high-frequency variability of the TN ~~cross-shelf fluxes. The results presented here show that such nitrogen fluxes are modulated by CTWs generated in the northern part of the GoM. These CTWs present mean periodsof 10 days and phase speeds between 2 and 4 (m s^{-1}). The strength of this modulation can be reinforced depending on the wind conditions influenced by strong storms and hurricanes.~~ fluxes at the western YS boundary are correlated and in phase with the along-shelf wind-stress modulating the variability of TN across the western shelf of Yucatan in the 5-10 period band. These high-frequency TN fluxes are also correlated with changes in SLA at similar periods, which are also typical of CTWs found in the GoM. Coherence is 180 degrees out of phase and consistent with negative SLA resulting from offshore transport. This exchanges are enhanced during winter due to cold frontal atmospheric systems “Nortes”.

The advection by the ~~Yucatan Current~~ YC dominates the nutrient concentration import to the ~~shelf~~ YS through the southeast border. This advection, together with the influence of mesoscale structures control the export of nutrients to the deep GoM at the northern margin. A different process modulates the flux of nutrients at the eastern YS margin. ~~Wind driven upwelling at Cape Catoche and the Yucatan Current~~ The YC flowing parallel to the slope ~~play~~ plays an important role in the intrusion of DIN into the shelf. Initial estimates carried out here suggest that~~the~~ , in the model, bottom Ekman layer transport explains the deep TN flux through the eastern YS boundary~~since there~~ . There is a positive mean transport (into the shelf) over the nine simulated years along the the eastern shelf break ~~. This indicates that the~~ so friction generated between the ~~Yucatan Current~~ YC and the shelf break can produce ~~a bottom Ekman spiral~~ bottom Ekman transports with a net transport towards the shelf. ~~Bottom Ekman transport can be arrested by stratification and may not be dominant everywhere along the YS east coast as has been documented in other western boundary upwelling regions (e.g., Roughan and Middleton, 2002, 2004)~~

In summary, the upwelling of Cape Catoche in the model is maintained by interaction between the YC and the topography, in which the bottom Ekman transport plays an important role, but is not the only process at work. External forcings and mechanisms appear to control its seasonality (winds, CTWs). Current separation/ encroachment, eddy and topographically induced upwelling can have important roles too that must be analyzed in future research.

Data availability. Data from the model simulation used in this study are available upon request to the corresponding author

Appendix A: Model evaluation

A1 Basin scale model evaluation

This study is focused ~~in~~ on the Yucatan shelf region, whose hydrodynamics and biogeochemical outputs ~~are previously validated . However, a~~ were previously validated before the analysis. Such general evaluation of the physical model ensures that the main dynamics of the whole GoM is correctly represented ~~. Thereby, the physical model is also evaluated in terms of their hydrography and general dynamics. Temporal averaged maps of~~ and is presented here. Time mean eddy kinetic energy (EKE, m^2 s^{-2}) ~~obtained from AVISO sea surface height are~~ map computed from AVISO geostrophic velocities (http://www.marine.copernicus.eu) is used to compare it with the EKE ~~computed by~~ from the model (Figures A1a and b) for 17 years (1995-2012). The model is able to capture the main features of the eddy field exhibited by the altimeter product ~~. The~~ as well as the main structure of the Loop Current~~is well represented by the model~~. In particular~~mean and variability of~~ , the mean and standard deviation of the eddy kinetic energy field ~~is~~ are reasonably captured by the model. ~~A recognized feature is the~~ The model produces hook-like pattern of EKE in the western part of the GoM, between 24 and 28 °N~~(Gough et al., 2019), and~~ , that is more evident in the standard deviation of ~~the EKE model~~ model EKE (Figures A1c and d). This pattern is ~~verified in both simulations and observations and~~ not so clear in the AVISO maps but has been identified using lagrangian data (e.g., Gough et al., 2019). It is associated with ~~a strong anticyclonic~~ the GoM western boundary current that isolates the western continental shelf from the open ocean~~GoM. On the other hand, the enhancement of the EKE magnitude in ROMS~~. EKE is higher in the model, particularly at the Yucatan channel and Florida ~~strait, is~~ Straits, probably due to the higher resolution of the model (∼5 km) ~~respect~~ compared to the altimeter product (∼28 km).

Seasonal climatologies of the sea surface temperature (SST) are also compared with ~~satellital product of~~ the Aqua-MODIS ~~atmosphere~~ satellite products (http://modis-atmos.gsfc.nasa.gov) (Figure A2). The model SST shows a good agreement with ~~both the interannual and~~ seasonal cycles exhibited by the satellite data. The overall bias for the deep GoM SST (depths $>$ 1000 m) is in the range [-0.21, +0.21] °C. Larger differences are found near the coast. The model tends to underestimate the coastal SST during winter and ~~spring times, while~~ overestimates it during summer~~and autumn, respect to the satellital data~~. Nevertheless, these differences are less than 0.5 °C, and ~~its average is in~~ on average differences are on the order of 0.05 °C with ~~an~~ a standard deviation of 0.4 °C. ~~One of the reasons for this discrepancy lies in that satellite-derived provided~~ The relatively good agreement between model and data is perhaps not very surprising considering that observed air temperatures are provided to the model to compute heat fluxes using bulk formulae. At the same time, no flux correction is applied in the ~~temperature relative only to a few microns of the sea surface, which is in fact named as the skin layer temperature (McKiver et al., 2016). Other reason can be also due to the representation of rivers, specially in the southern part of the GoM, where there exist a lack of temporal observations of the main freshwater sources. The river runoff can modify the surface thermal stratification inducing differences between the skin SST and the observed SST below 0.5 m approximately (Donlon et al., 2002).~~ model so it is important to confirm that there is no drift in the simulation.

In order to evaluate the mixed layer depth, a total of 2629 ARGO floats profiles, ~~availables in the time~~ available in the period between 1995-2012, are compared with the mixed layer depth given by the model in the deep GoM. This is an important quantity in terms of biogeochemical behavior ~~,~~ since the Gulf is an ~~oligrotrophic~~ oligotrophic region in which ~~primary production is controlled by~~ the vertical advection of nutrients controls primary production to the photic layer (Fennel et al., 2006; Xue et al., 2013; Damien et al., 2018). The biogeochemical cycles are partly controlled by the difference between the deep and dark nutrient-rich waters and the upper ocean layer where the availability of light promotes the growth of phytoplankton and hence zooplankton. Figure A3 shows that the model ~~is able to~~ can reproduce the seasonal cycle of the mixed layer in the GoM, with deepening during winter and shallowing during summer seasons (Damien et al., 2018; Portela et al., 2018). The model ~~also shows~~ depicts shallower mixed layer depths during summer ~~, and deepens during winter times respect to the Argo floats~~and deeper during winter than the Argo observations. The higher variability of the observed data ~~are likely related with~~ is likely related to mesoscale structures and submesoscale process which can locally ~~deepening~~deepen/~~shallowing the depth of~~ shallow the mixed layer (e.g., Boccaletti et al., 2007; Fox-Kemper et al., 2008; Levy et al., 2012) not fully represented by the model. Despite the differences found, the bias between observations and model mixed layer depths are on the order of 1.4 m.

The lack of spatio-temporal biological data sets to validate biogeochemical models in the GoM is a well-known problem (Walsh et al., 1989; Damien et al., 2018). Only satellite-derived surface chlorophyll concentration is available with enough spatial and temporal cover but only at the surface. These observations give us a general overview of the chlorophyll temporal and spatial distribution patterns at basin scales. Monthly mean time series (2002-2010) of chlorophyll-a concentration from Aqua-MODIS and SeaWiFS 9 km and 4 km (when available) satellite products are used for a basin-scale model evaluation. The temporal series averaged for the whole deep GoM (i.e., excluding high productive coastal areas with less than -1000 m depth) show a good agreement between the coupled model and the observations. The model tends to overestimate the Chl in winter and underestimate it in summer (Figure A5). Despite some exceptional years (e.g., 1999), the modeled chlorophyll concentration values fall in the range exhibited by the satellite products. Mean satellite Chl is 0.1448 $\pm$ 0.04 mgChl m^{-3} in contrast with mean modelling Chl values of 0.1433 $\pm$ 0.09 mgChl m^{-3}. ~~Moreover, physical processes developed below the~~

Observations of the vertical chlorophyll structure are available from eight APEX profiling floats with 537 profiles of Chl from 0 to 2000 m every ten days within the GoM (Pasqueron de Fommervault et al., 2017) (Figure A4). A more detailed description of this database is provided by Hamilton et al. (2017), and the Chl data calibration is explained in Pasqueron de Fommervault et al. (2017). The resulting profiles give valuable information to evaluate biogeochemical models through the water column, in contrast to the surface only information from satellite measurements (Pasqueron de Fommervault et al., 2017; Damien et al., 2018). The comparison shows that the model is able to reproduce the depth of the DCM measured by the floats. The DCM seasonal cycle is also well represented by the model. It is interesting to note the high dispersion in the data, revealing the large Chl variability found in the deep GoM.

A2 Regional chlorophyll model evaluation

In addition to the comparison of the surface chlorophyll temporal series with satellite products (Figure 8c), $in\ situ$ spatially averaged vertical profiles of chlorophyll from three GOMEX cruises carried out during November 2015, August 2016 and July 2018 are also compared with the model chlorophyll profiles averaged for all the July, August and November from 2002 to 2010. The observed profiles superimposed in blue, are shown in Figure A6. The result shows that the model is also able to reproduce the large variability of the observed data. Highest values of chlorophyll from model profiles are found at the surface layers, between 5 ~~km of horizontal resolution are barely permitted by this model configuration. Despite the differences found , the bias between observations~~ and ~~model mixed layer depths are in the order of 1.4 m~~ 15 m depth. Values higher than 6 mgChl m^{-3} represent only the 0.64% of the total simulated points, while for observations, the percentage is about 0.06% and are also located at the surface between 10 and 35 m depth.

A3 Regional altimetry and ocean currents comparison

The variance of the Absolute Dynamic Topography (ADT) from AVISO, which is the sea surface height above the geoid obtained as the sum of the sea level anomaly and the mean dynamic topography, is compared with the variance of the sea level of the model output (Figure A7). Observed and model ssh variance have good resemblance. There are slight differences in the northern coast of the YS. Remember, however, that the accuracy of the altimeter observations is reduced in shallow areas (Vignudelli et al., 2011).

The variability and magnitude of the current over the shelf is also compared against the GlobCurrent product (www.globcurrent.org) (Rio et al., 2014). Since the current velocity over the YS is a westward wind-driven flow (Ruiz-Castillo et al., 2016), a comparison with only the geostrophic velocity contribution might not represent the whole state of the velocity field. In this regard, the GlobCurrent product is the result of combining geostrophic altimeter velocity with the addition of the wind-forced Ekman velocity contribution under ocean mixed layer model assumptions. The results are shown in Figure A8. The model correctly represents the mean surface current magnitude and direction over the shelf, highest differences are found close to the Yucatan coast (Figure A8a and b). The variability ellipses (Figure A8c) show that the current variability over nine years from the model agree with those from observations. Near the northern Yucatan coast, values are lower in both model and data. However, the model ellipses are zonally oriented in contrast to the meridional orientation of the ellipses from the satellite product. The other important difference is found at the west coast of the YS, where the model exhibits a southwestward oriented ellipses whereas the satellite shows a westward orientation. This might influence the direction of the TN fluxes at the west YS boundary, a subject which is further addressed in appendix B. Similarly, as the previous comparison with the AVISO product, significant differences are found near-coast but there are probably significant errors in the data Vignudelli et al. (2011). In contrast, the YC is well represented by the model in terms of its spatio-temporal variability, although its magnitude is overestimated, which again is probably an effect of better model spatial resolution.

A4 Yucatan Current evaluation

The CICESE-CANEK mooring sections monitoring the flow in the region duiring 2009-2011 is shown in Figure 1a (yellow zonal line). The current velocity normal to the three mooring transects shown in Figure 8 of Sheinbaum et al. (2016) during years 2009 to 2011 is used for validation. They observe that the YC (YUC transect) was located between the surface and 800 m depth, which agrees with our model results shown in Figure A9a. The core of the YC is located over the West Yucatan slope, and its mean of 1.18 m s^{-1} is in a very good agreement with observations (Sheinbaum et al., 2002, 2016). The model also shows that the highest standard deviation is at the surface on the western side of the channel with a value of 0.3 m s^{-1} (Figure

A9d), in contrast with the 0.4 m s^{-1} found by Sheinbaum et al. (2016). They argue that this variability is due to changes in the current position and the counter-flow. At deeper layers (below 900 m), the model shows that the current flows towards the GoM at the center of the section. On both, the western and eastern side of the section, the model is able to reproduce the southward flow as shown in Sheinbaum et al. (2016).

For sections PE and PN (Figure A9b and c), the model exhibits mean velocities of 0.24 $\pm$ 0.24 m s^{-1} and 0.36 $\pm$0.29 m s^{-1}, these values are lower than reported by Sheinbaum et al. (2016) of 0.6 $\pm$ 0.7 m s^{-1} and 0.4 $\pm$0.6 m s^{-1} (Figures A9e and f). One should consider that the model has high variability. Moreover, these sections may or may not be influenced by the core of the Loop Current. Sheinbaum et al. (2016) estimate a reduction of about 30-50% in the maxima of the mean when the Loop Current core is not passing over the sections moorings. The southward flow over the slope of section PE below 1000 m is well represented by the model (Figure A9b), as well as the flow across the whole PN section (Figure A9c).

Appendix B: Model uncertainties

The bias of the model with respect to observations described in section 3 and appendix A are analyzed in order to analyze the uncertainties that the quantification of the TN budget can have due to them

As pointed out in appendix A, the model tends to overestimate/underestimate Chl/SST in winter and underestimate/overestimate Chl/SST in summer. This bias would produce upwelling of Cape Catoche more intense during spring than in summer, and those upwelling waters are still visible during winter (Figures 2). The filtered seasonal time series of the Ekman bottom transport, shown in Figure 15b (black line), show the same pattern. The time series indicates that water from the Caribbean Sea entering into the YS through bottom Ekman transport increases during spring towards the summer, decreasing during autumn and increasing again during winter. This is in agreement with Figure 3.

Regarding the water column comparisons, the model underestimates NO_3 concentration. Although the nutrient concentration will affect directly the cross-shelf DIN fluxes, the PON and hence the TN will also be indirectly underestimated. However, this underestimation is present for the whole YS, which indicates two things; firstly that the TN budget will in general be lower than predicted here, and secondly, that the main pathways of the TN fluxes will remain unchanged. If we consider this bias, the mean NO_3 concentration could be reduced in 15%, as this nutrient represents the 12% of the total nitrogen, the TN budget could also be reduced in 1.8% compared to the values of Table 1.

With respect to the temperature for the entire water column, the model is 5% colder than the observed profiles over the whole shelf. The growth of the phytoplankton depends on the temperature through the maximum growth rate. This is in agreement with the negative bias of chlorophyll since this is affected by the phytoplankton concentration. The same is occurring with the surface comparisons of Chl and SST with satellite data. Hence, lower temperatures might cause a decrease in PON concentration. However, as the phytoplankton represent 15% of the TN, the impact of a slight temperature reduction is less than 0.04%. It is worth noting that all these biases are averaged for the whole shelf. In the particular area of Cape Catoche upwelling, which is one of the main focus of this study, the differences are found under the mean. Moreover, this area, together with the southern boundary, represent the main entrance of TN to the shelf.

The model shows that the YC transport, though in the range of the observed values, tends to be underestimated (Figure A9). A weakness of this current might cause a reduction in the bottom Ekman transport, which in turn would imply that the cross-shelf flux of TN, mainly PON, will be lower than theone presented here. On the other hand, the TN fluxes along the west coast can be biased toward the southwest instead of to the west as the satellite velocity product suggested (Figure A8). However, comparisons with altimeter products near the coast must be taken with care since the estimation errors are highest in coastal areas (Vignudelli et al., 2011).

The complexity of the biogeochemical cycles cannot be easily oversimplified, but our results show that even though underestimated, the main pathways of the TN fluxes across shelf are well represented by the model. This is the first step to conduct a more general observational study in the Mexican shelves, in order to evaluate the impact of the TN budget over different fields such as the socio-economical, the ecosystem and the climate system.

Appendix C: Freshwater sources inputs

As already described in subsection 2.3, freshwater, and nitrogen input from 81 major rivers and freshwater systems are included in the coupled model simulation. The Mississippi and Atchafalaya riverine systems are the largest fluvial source in the GoM (red and blue points in Figure A10a). Their nitrogen delivers tripled in the last decades and are meaningfully correlated with the coastal DIN concentration in the northern GoM (Xue et al., 2013). Nutrient and transport of this system generally peaked in spring-summer in agreement with the time series inputs shown in Figure A10b.

The Usumacinta-Grijalva rivers system (green points in Figure A10a) is the most important freshwater source in the southern GoM (Xue et al., 2013). The highest riverine discharge of this system, accompanied by an enhancement of nutrient concentration, occurs during winter and decreases during spring (Figure A10c). In contrast to the northern riverine sources, the data available for the southern freshwater sources of the GoM are scarce or undersampled. In order to obtain southern freshwater inputs, a time series is built based on the composite of temperature, salinity, volume transport and nutrient concentration at the location of the freshwater sources or near it. The information is obtained from values reported in the literature (Milliman and Syvitski, 1992; Herrera-Silveira et al., 2002, 2004; Yáñez Arancibia and Day, 2004) (Hudson et al., 2005; Herrera-Silveira and Morales-Ojeda, 2010; Poot-Delgado et al., 2015; Kemp et al., 2016; Conan et al., 2016) and from observational hydrographic stations near the Yucatan coast (subsection 2.3). In general, the information reported does not cover a large time series. Therefore, all the information is used to build a climatology which will serve as freshwater model input. An example of this climatological inputs is depicted in Figure A10c and d for the Usumacinta/Grijalva rivers and the Yucatan freshwater sources (magenta point in Figure A10a) (Yáñez Arancibia and Day, 2004; Poot-Delgado et al., 2015; Conan et al., 2016). The YS receive freshwater and nutrient inputs from spring and runoff from mangrove areas, lagoons, and cenotes. High nutrient concentrations are reported for YS lagoons (e.g., Dzilam Lagoon) (Herrera-Silveira and Morales-Ojeda, 2010).

As one can notice, the inter-annual variability is visible in northern riverine systems, while is absent in the southern freshwater sources due the lack of information. Moreover, it is essential to note that the small-scale variability in most of the GoM rivers structure is not fully resolved by the horizontal resolution of our model configuration.

Competing interests. The authors declare that they have no conflict of interest

Acknowledgements. This research is funded by the National Council of Science and Technology of Mexico - Mexican Ministry of Energy- Hydrocarbon Trust, project 201441. This is a contribution of the Gulf of Mexico Research Consortium (CIGoM). The authors would like to thank the NASA Goddard Space Flight Center, Ocean Ecology Laboratory, Ocean Biology Processing Group. Moderate-resolution Imaging Spectroradiometer (MODIS) Aqua Chlorophyll Data; 2014 Reprocessing. NASA OB.DAAC, Greenbelt, MD, USA. doi: 10.5067/AQUA/MODIS/ L3M/CHL/2014 and to the Sea-viewing Wide Field-of-view Sensor (SeaWiFS) Chlorophyll Data; doi: 10.5067/ORBVIEW-2/SEAWIFS/ L3M/CHL/2014. The Ssalto/Duacs altimeter products were produced and distributed by the Copernicus Marine and Environment Monitoring Service (CMEMS) (http://www.marine.copernicus.eu). We acknowledge the provision of supercomputing facilities by CICESE. The authors are grateful to Dr Victor Camacho-Ibar (UABC) and Dr Sharon Herzka (CICESE), who provided nutrient data measured during the XIXIMI-IV cruise (funded by INECC-SEMARNAT, FOINS-CONACYT, Mexico). The APEX floats dataset were produced in the framework of the ~~‘1000~~“Lagrangian Study of the Deep Circulation in the Gulf of ~~Mexico’1000~~Mexico”, funded by the Bureau of Ocean and Energy Management, USA. Argo data were collected and made freely available by the International Argo Program and the national programs that contribute to it. (http://www.argo.ucsd.edu, http://argo.jcommops.org). The Argo Program is part of the Global Ocean Observing System. Argo float data and metadata from Global Data Assembly Centre (Argo GDAC). SEANOE. http://doi.org/10.17882/42182.

References

Anuario de Pesca 2017: Anuario Estadístico de Acuacultura y Pesca Edición 2017 de la comisión nacional de acuacultura y pesca., 2017.

Ashok, K. and Yamagata, T.: The El Niño with a difference, Nature, 461, 481–, https://doi.org/10.1038/461481a, 2009.

Ashok, K., Behera, S. K., Rao, S. A., Weng, H., and Yamagata, T.: El Niño Modoki and its possible teleconnection, Journal of Geophysical Research, 112, https://doi.org/10.1029/2006JC003798, 2007.

Azevedo Correia de Souza, J., Powell, B., Castillo-Trujillo, A. C., and Flament, P.: The Vorticity Balance of the Ocean Surface in Hawaii from a Regional Reanalysis, Journal of Physical Oceanography, 45, 424–440, https://doi.org/10.1175/JPO-D-14-0074.1, https://doi.org/10.1175/JPO-D-14-0074.1, 2015.

Boccaletti, G., Ferrari, R., and Fox-Kemper, B.: Mixed Layer Instabilities and Restratification, Journal of Physical Oceanography, 37, 2228–2250, https://doi.org/10.1175/JPO3101.1, https://doi.org/10.1175/JPO3101.1, 2007.

Boyer, T., Antonov, J. I., Baranova, O. K., Coleman, C., Garcia, H. E., Grodsky, A., Johnson, D. R., Locarnini, R. A., Mishonov, A. V., O'Brien, T., Paver, C., Reagan, J., Seidov, D., Smolyar, I. V., and Zweng, M. M.: World Ocean Database 2013, NOAA Atlas NESDIS 72, S. Levitus, Ed., A. Mishonov, Technical Ed.; Silver Spring, MD, 209 pp., https://doi.org/10.7289/V5NZ85MT, 2013.

Bunge, L., Ochoa, J., Badan, A., Candela, J., and Sheinbaum, J.: Deep flows in the Yucatan Channel and their relation to changes in the Loop Current extension, Journal of Geophysical Research, 107, https://doi.org/10.1029/2001JC001256, 2002.

Candela, J., Sheinbaum, J., Ochoa, J., Badan, A., and Leben, R.: The potential vorticity flux through the Yucatan Channel and the Loop Current in the Gulf of Mexico,, Geophys. Res. Lett., 29, 2059, https://doi.org/10.1029/2002GL015587, 2002.

Carrillo, L., Johns, E., Smith, R., Lamkin, J., and Largier, J.: Pathways and hydrography in the Mesoamerican Barrier Reef System Part 2: Water masses and thermohaline structure, Continental Shelf Research, 120, 41 – 58, https://doi.org/https://doi.org/10.1016/j.csr.2016.03.014, http://www.sciencedirect.com/science/article/pii/S0278434316301145, 2016.

Clarke, A. J.: Observational and numerical evidence for wind-forced coastal trapped long waves, Journal of Physical Oceanography, 7, 231–247, https://doi.org/10.1175/1520-0485(1977)007<0231:OANEFW>2.0.CO;2, 1977.

Cochrane, J.: Currents and Waters of the Eastern Gulf of Mexico and Western Caribbean, of the Western Tropical Atlantic Ocean, and of the Eastern Tropical Pacific Ocean, Houston, Texas: TAMU, Technical report No. 68-8T, pp. 19–28., 1968.

Cochrane, J. D.: The Yucatan Current, upwelling off Northeastern Yucatan, and ccurrent and waters of Western Equatorial Atlantic., Oceanography of the Gulf of Mexico. *Progress Rep. TAMU Ref. No. 66-23T,* pp. 14-32, 1966.

Conan, P., Pujo-Pay, M., Agab, M., Calva-Benítez, L., Chifflet, S., Douillet, P., Dussud, C., Fichez, R., Grenz, C., Gutierrez-Mendieta, F., Origel-Moreno, M., Rodríguez-Blanco, R., Sauret, C., Severin, T., Tedetti, M., Torres-Alvarado, R., and J. F., G.: Biogeochemical cycling and phyto- and bacterio-plankton communities in a large and shallow tropical lagoon (Términos Lagoon, Mexico) under 2009-2010 El Niño Modoki drought conditions, Biogeosciences, 14, 959–975, https://doi.org/10.5194/bg-14-959-2017, 2016.

Cushman-Roisin, B. and Beckers, J.: Introduction to geophysical fluid dynamics : physical and numerical aspects, vol. 101, International Geophysical Series, 2nd edn., 2011.

Damien, P., Pasqueron de Fommervault, O., Sheinbaum, J., Jouanno, J., and Duteil, O.: Partitioning of the Gulf of Mexico based on the seasonal and interannual variability of chlorophyll concentration, Journal of Geophysical Research, 2018.

Dee, D. P., Balmaseda, M., Balsamo, G., Engelen, R., Simmons, A. J., and Thépaut, J.-N.: Toward a Consistent Reanalysis of the Climate System, Bulletin of the American Meteorological Society, 95(8), 1235–1248, https://doi.org/10.1175/BAMS-D-13-00043.1, 2014.

Ding, R., Huang, D., Xuan, J., Zhou, F., and Pohlmann, T.: Temporal and spatial variations of crossshelf nutrient exchange in the East China Sea, as estimated by satellite altimetry and in situ measurements. 124, 1331– 1356. https://doi.org/10.1029/2018JC014496, Journal of Geophysical Research: Oceans, 124, 1331– 1356, https://doi.org/10.1029/2018JC014496, 2019.

Donlon, C. J., Minnett, P. J., Gentemann, C., Nightingale, T. J., Barton, I. J., Ward, B., and Murray, M. J.: Toward improved validation of satellite sea surface skin temperature measurements for climate research, J. Climate, 15, 353–369, 2002.

Dubranna, J., Pérez-Brunius, P., López, M., and Candela, J.: Circulation over the continental shelf of the western and southwestern Gulf of Mexico, Journal of Geophysical Research, 116, https://doi.org/10.1029/2011JC007007, 2011.

Dunn, D. D. .: Trends in Nutrient Inflows to the Gulf of Mexico from Streams Draining the Conterminous United States 1972 - 1993, U.S. Geological Survey, Water-Resources Investigations Report 96-4113. Austin, Texas: U.S. Geological Survey. 60 pp., 1996.

Egbert, G. D. and Erofeeva, S. Y.: Efficient inverse modeling of barotropic ocean tides, J. Atmos. Ocean. Tech., 19, 183– 204, 2002.

Enriquez, C. and Mariño Tapia, I.: Mechanisms driving a coastal dynamic upwelling, in: Proceedings of the 17th Physics of Estuaries and Coastal Seas (PECS) Conference, Porto de Galinhas, Pernambuco, Brazil, PECS, 2014.

Enriquez, C., Mariño Tapia, I., and Herrera-Silveira, J.: Dispersion in the Yucatan coastal zone: Implications for red tide events, Continental Shelf Research, 30, 127–137, https://doi.org/10.1016/j.csr.2009.10.005, 2010.

Enriquez, C., Mariño Tapia, I., Jeronimo, G., and Capurro-Filograsso, L.: Thermohaline processes in a tropical coastal zone, Continental Shelf Research, 69, 101–109, https://doi.org/10.1016/j.csr.2013.08.018, 2013.

Fairall, C. W., Bradley, E. F., Hare, J. E., Grachev, A. A., and Edson, J. B.: Bulk Parameterization of AirSea Fluxes: Updates and Verification for the COARE Algorithm,, J. Climate, 16, 571–591, 2003.

Fasham, M. J. R., Ducklow, H. W., and McKelvie, S. M.: A nitrogen based model of plankton dynamics in the oceanic mixed layer, Jorunal of Marine Resesearch, 48, 591 – 639, 1990.

Fennel, K.: The role of continental shelves in nitrogen and carbon cycling: Northwestern North Atlantic case study, Ocean Sci., 6, 539–548, https://doi.org/10.5194/os-6-539-2010, 2010, 2010.

Fennel, K., Wilkin, J., Levin, J., Moisan, J., O'Reilly, J., and Haidvogel, D.: Nitrogen cycling in the Middle Atlantic Bight: results from a three-dimensional model and implications for the North Atlantic nitrogen budget, Global Biogeochemical Cycles, 20, https://doi.org/10.1029/2005GB002456, 2006.

Fennel, K., Hetland, R., Feng, Y., and DiMarco, S.: A coupled physical-biological model of the Northern Gulf of Mexico shelf: Model description, validation and analysis of phytoplankton variability, Biogeosciences, 8, 1881–1899, 2011.

Ferry, N., Parent, L., Garric, G., Drevillon, M., Desportes, C., Bricaud, C., and Hernandez, F.: Scientific Validation Report (ScVR) for reprocessed analysis and reanalysis, MyOcean Project Rep., WP04-GLO-MERCATOR, MYO-WP04-ScCV-rea-MERCATOR-V1.0, Toulouse, France., 2012.

Fox-Kemper, B., Ferrari, R., and Hallberg, R.: Parameterization of Mixed Layer Eddies. Part I: Theory and Diagnosis, Journal of Physical Oceanography, 38, 1145–1165, https://doi.org/10.1175/2007JPO3792.1, https://doi.org/10.1175/2007JPO3792.1, 2008.

Gallardo, A. and Marui, A.: Submarine groundwater discharge: an outlook of recent advances and current knowledge, Geo-Marine Letters, 26, 102–113, 2006.

Gough, M. K., Beron-Vera, F. J., Olascoaga, M. J., Sheinbaum, J., Jouanno, J., and Duran, R.: Persistent transport pathways in the northwestern Gulf of Mexico, J. Phys. Oceanogr., 49, 353–367, https://doi.org/10.1175/JPO-D-17-0207.1, 2019.

Gutierrez-de Velasco, G. and Winant, D.: Seasonal patterns of wind stress and stress curl over the Gulf of Mexico, J. Geophys. Res., 101, 18 127–18 140, 1996.

Haidvogel, D. B. and Beckmann, A.: Numerical Ocean Circulation Modeling, Imperial College Press, 1999.

Hamilton, P., Bower, A., Furey, H., Leben, R., and Pérez-Brunius, P.: Deep Circulation in the Gulf of Mexico: A Lagrangian Study., U.S. Dept. of the Interior, Bureau of Ocean Energy Management, Gulf of Mexico OCS Region, New Orleans, LA. OCS Study BOEM 2017-0xx. 285 pp., 2017.

Hermann, A., Hinckley, S., Dobbins, E. L., Haidvogel, D. B., Bond, N. A., Mordy, C., Kachel, N., and Stabeno, P. J.: Quantifying cross-shelf and vertical nutrient flux in the Coastal Gulf of Alaska with a spatially nested, coupled biophysical model, Deep Sea Research Part II: Topical Studies in Oceanography, 56, 2474 – 2486, https://doi.org/https://doi.org/10.1016/j.dsr2.2009.02.008, http://www.sciencedirect.com/science/article/pii/S0967064509000484, 2009.

Herrera-Silveira, J. and Morales-Ojeda, S.: Subtropical Karstic Coastal Lagoon Assessment, Southeast Mexico. In: Coastal Lagoons, Marine Science, https://doi.org/10.1201/EBK1420088304-c13., 2010.

Herrera-Silveira, J., Medina-Gomez, I., and Colli, R.: Trophic status based on nutrient concentration scales and primary producers community of tropical coastal lagoons iinfluenced by groundwater discharges, Hydrobiologia, 475, 91–98, 2002.

Herrera-Silveira, J., Comin, F., Aranda-Cicerol, N., Troccoli, L., and Capurro, L.: Coastal water quality assessment in the Yucatan peninsula: management Implications, Ocean and Coastal Mangement, 47, 625–639, 2004.

Hudson, P., Hendrickson, D., Benke, A., Varela-Romero, A., Rodiles-Hernández, R., and Minckley, W.: Rivers of Mexico, pp. 1030–1084, Rivers of North America, Elsevier Inc., Estados Unidos, https://doi.org/10.1016/B978-012088253-3/50026-2, 2005.

Huthnance, J.: Circulation, exchange and water masses at the ocean margin: the role of physical processes at the shelf edge., Progress In Oceanography, 35, 353–431, https://doi.org/10.1016/0079-6611(95)00012-6, 1995.

Jouanno, J., Ochoa, K., Pallàs-Sanz, E., Sheinbaum, J., Andrade, F., Candela, J., and Molines, J.: Loop Current Frontal Eddies: Formation along the Campeche Bank and Impact of Coastally Trapped Waves, Journal of Physical Oceanography, 46, 3339–3363, https://doi.org/10.1175/JPO-D-16-0052.1, 2016.

Jouanno, J., Pallàs-Sanz, E., and Sheinbaum, J.: Variability and Dynamics of the Yucatan Upwelling: High-Resolution Simulations, Journal of Geophysical Research: Oceans, 123, https://doi.org/10.1002/2017JC013535, 2018.

Kemp, G. P., Day, J. W., Yáñez-Arancibia, A., and Peyronnin, N. S.: Can Continental Shelf River Plumes in the Northern and Southern Gulf of Mexico Promote Ecological Resilience in a Time of Climate Change?, Water, 8, https://doi.org/10.3390/w8030083, http://www.mdpi.com/2073-4441/8/3/83, 2016.

Kolodziejczyk, N., Ochoa, J., Candela, J., and Sheinbaum, J.: Deep Currents in the Bay of Campeche, Journal of Physical Oceanography, 41, 1902–1920, https://doi.org/10.1175/2011JPO4526.1, 2011.

Larson, S., Lee, S., Wang, C., Chung, E., and Enfield, D.: Impacts of noncanonical El Nino patterns on Atlantic hurricane activity, Geophys. Res. Lett., 39, https://doi.org/10.1029/2012GL052595, 2012.

Levy, M., Iovino, D., Resplandy, L., Klein, P., Madec, G., Treguier, A.-M., Masson, S., and Takahashi, K.: Large-scale impacts of submesoscale dynamics on phytoplankton: Local and remote effects, Ocean Modelling, 43-44, 77 – 93, https://doi.org/10.1016/j.ocemod.2011.12.003, 2012.

Liu, K.-K., Atkinson, L., Quinones, R., and Talaue-McManus, L.: Carbon and Nutrient Fluxes in Continental Margins: A Global Synthesis., IGBP Book Series, Berlin., 2010.

McKiver, W. J., Sannino, G., Braga, F., and Bellafiore, D.: Investigation of model capability in capturing vertical hydrodynamic coastal processes: a case study in the north Adriatic Sea, Ocean Sci., 12, 51–69, https://doi.org/doi.org/10.5194/os-12-51-2016, 2016.

Mellor, G. and Yamada, T.: Development of a turbulence closure model for geophysical fluid problems, Rev. Geophys., 20, 851–875, 1982.

Merino, M.: Upwelling on the Yucatan shelf: hydrographic evidence, Journal of marine systems, 13, 101–121, 1997.

Milliman, J. and Syvitski, J.: Geomorphic/tectonic control of sediment discharge to the ocean: the importance of small mountainous rivers, Journal of Geology, 100, 525–544, 1992.

Ochoa, P., Sheinbaum, J., Badan, A., Candela, J., and Wilson, D.: Geostrophy via potential vorticity inversion in the Yucatan Channel, J. Mar. Res., 59, 725–747, 2001.

Pasqueron de Fommervault, O., D'Ortenzio, F., Mangin, A., Serra, R., Migon, C., Claustre, H., and Schmechtig, C.: Seasonal variability of nutrient concentrations in the Mediterranean Sea: Contribution of Bio-Argo floats., Journal of Geophysical Research: Oceans, 2015.

Pasqueron de Fommervault, O., Pérez-Brunius, P., Damien, P., and Sheinbaum-Pardo, J.: Temporal variability of chlorophyll distribution in the Gulf of Mexico: bio-optical data from profiling floats, Biogeosciences Discussions, 2017.

Pérez-Santos, I., Schneider, W., Sobarzo, M., Montoya-Sánchez, R., Valle-Levinson, A., and Garcés-Vargas, J.: Surface wind variability and its implications for the Yucatan basinCaribbean Sea dynamics, Journal of Geophysical Research, 115, https://doi.org/10.1029/2010JC006292, 2010.

Perlin, A., Moum, J. N., Klymak, J. M., Levine, M. D., Boyd, T., and Kosro, P. M.: Organization of stratification,turbulence, and veering in bottom Ekman layers, Journal of Geophysical Research, 112, https://doi.org/10.1029/2004JC002641, 2007.

Poot-Delgado, C. A., Okolodkov, Y. B., Aké-Castillo, J. A., and von Osten, J. R.: Annual cycle of phytoplankton with emphasis on potentially harmful species in oyster beds of Terminos Lagoon, southeastern Gulf of Mexico., Revista de Biología Marina y Oceanografía, 50, 465–477, https://doi.org/10.4067/S0718-19572015000400006., 2015.

Pope, K. O., Ocampo, A. C., and Duller, C. E.: Mexican site for K/T impact crater, Nature, 351, 105, 1191.

Portela, E., Tenreiro, M., Pallàs-Sanz, E., Meunier, T., Ruiz-Angulo, A., Sosa-Gutiérrez, R., and Cusí, S.: Hydrography of the central and western Gulf of Mexico. Journal of Geophysical, Journal of Geophysical Research, 123, 5134–5149, https://doi.org/10.1029/2018JC013813, 2018.

Reyes-Mendoza, O., Mariño Tapia, I., Herrera-Silveira, J., Ruiz-Martínez, G., Enriquez, C., and Largier, J. L.: The Effects of Wind on Upwelling off Cabo Catoche, Journal of Coastal Research, 32, 638 – 650, https://doi.org/10.2112/JCOASTRES-D-15-00043.1, 2016.

Rio, M.-H., Mulet, S., and Picot, N.: Beyond GOCE for the ocean circulation estimate: Synergetic use of altimetry, gravimetry, and in situ data provides new insight into geostrophic and Ekman currents, Geophys. Res. Lett., 41, 8918–8925, https://doi.org/10.1002/2014GL061773, 2014.

Rojas-Galaviz, J., Yaáñez Arancibia, A., Day, J., and Vera-Herrera, F.: Estuarine Primary Producers: Laguna de Terminos—a Study Case, In, U. Seeliger, ed., Coastal Plant Communities of Latin America. San Diego: Academic Press., 1992.

Roughan, M. and Middleton, J.: A comparison of observed upwelling mechanisms off the east coast of Australia, Continental Shelf Research, 22, 2551–2572, https://doi.org/10.1016/S0278-4343(02)00101-2, 2002.

Roughan, M. and Middleton, J.: On the East Australian Current: Variability, encroachment, and upwelling, Journal of Geophysical Research, 109, https://doi.org/10.1029/2003JC001833, 2004.

Ruiz-Castillo, E., Gomez-Valdes, J., Sheinbaum, J., and Rioja-Nieto, R.: Wind-driven coastal upwelling and westward circulation in the Yucatan shelf, Continental Shelf Research, 118, 63–76, https://doi.org/10.1016/j.csr.2016.02.010, 2016.

Sanvicente-Añorve, L., Zavala-Hidalgo, J., Allende-Arandía, M. E., and Hermoso-Salazar, M.: Connectivity patterns among coral reef systems in the southern Gulf of Mexico, Marine Ecology Progress Series, 498, 27–41, https://doi.org/10.3354/meps10631, 2014.

Seitzinger, S., Harrison, J. A., Böhlke, J. K., Bouwman, A. F., Lowrance, R., Peterson, B., Tobias, C., and Drecht, G. V.: Denitrification across landscapes and waterscapes: a synthesis., Ecological Applications, 16, 2064–2090, https://doi.org/10.1890/1051-0761(2006)016[2064:DALAWA]2.0.CO;2, 2006.

Shaeffer, A., Roughan, M., and Wood, J.: Observed bottom boundary layer transport and uplift on the continental shelf adjacent to a western boundary current, J. Geophys. Res. Oceans, 119, 4922–4939, https://doi.org/10.1002/2013JC009735, 2014.

Shchepetkin, A. F. and McWilliams, J. C.: The Regional Oceanic Modeling System (ROMS): a split-explicit, free-surface, topography-following-coordinate oceanic model, Ocean. Model., 9, 347–404, 2005.

Shchepetkin, A. F. and McWilliams, J. C.: Correction and commentary for "Ocean forecasting in terrain-following coordinates: Formulation and skill assessment of the regional ocean modeling system" by Haidvogel et al. J. Comp. Phys. 227, pp. 3595-3624, J. Comput. Phys., 228, 8985–9000, 2009.

Sheinbaum, J., Candela, J., Badan, A., and Ochoa, J.: Flow structure and transport in the Yucatan Channel, Geophys. Res. Lett., 29, 2002.

Sheinbaum, J., Athié, G., Candela, J., Ochoa, J., and A., R.-A.: Structure and variability of the Yucatan and loop currentsalong the slope and shelf break of the Yucatan channel andCampeche bank, Dynamics of Atmospheres and Oceans, 76, 217–239, https://doi.org/10.1016/j.dynatmoce.2016.08.001, 2016.

Troupin, C., Barth, A., Sirjacobs, D., Ouberdous, M., Brankart, J.-M., Brasseur, P., Rixen, M., Alvera Azcarate, A., Belounis, M., Capet, A., Lenartz, F., Toussaint, M.-E., and Beckers, J.-M.: Generation of analysis and consistent error elds using the Data Interpolating Variational Analysis (Diva), Ocean Modelling, 52-53, 90–101, https://doi.org/10.1016/j.ocemod.2012.05.002, 2012.

Valle-Levinson, A., Mariño Tapia, I., Enriquez, C., and Waterhouse, A.: Tidal variability of salinity and velocity field related to intense point sources submarine groundwater discharges into the coastal ocean., Limnology and Oceanography, 56, 1213–1224, https://doi.org/10.4319/lo.2011.56.4.1213, 2011.

Varela, R., Costoya, X., iquez, C. E., Santos, F., and Gomez-Gesteira, M.: Differences in coastal and oceanic SST trends north of Yucatan Peninsula, Journal of Marine Systems, 182, 46–55, https://doi.org/10.1016/j.jmarsys.2018.03.006, 2018.

Venegas-Vega, F.: Wind-driven circulation in a closed basin with variable topography, Master's thesis, Centro de Investigación Científica y de Educación Superior de Ensenada, Baja California, Mexico, 2017.

Vignudelli, S., Kostianoy, A. G., Cipollini, P., and Benveniste, J.: Coastal Altimetry, Berlin, Heidelberg, https://doi.org/10.1007/978-3-642-12796-0, 2011.

Walsh, J. J., Dieterle, D. A., Meyers, M. B., and Müller-Karger, F. E.: Nitrogen exchange at the continental margin: A numerical study of the Gulf of Mexico, Prog. Oceanogr., 23, 245–301, 1989.

Xue, Z., He, R., Fennel, K., Cai, W.-J., Lohrenz, S., and Hopkinson, C.: Modeling ocean circulation and biogeochemical variability in the Gulf of Mexico, Biogeosciences, 10, 7219–7234, https://doi.org/10.5194/bg-10-7219-2013, 2013.

Yáñez Arancibia, A. and Day, J.: The Gulf of Mexico: Towards an integration of coastal management with large marine ecosystem management, Ocean Coast. Manag., 47, 537–563, 2004.

Zavala-Hidalgo, J., Gallegos-García, A., Martinez-López, B., Morey, S., and O'Brien, J. J.: Seasonal upwelling on the western and southern shelves of the Gulf of Mexico, Ocean Dynamics, 56, 333–338, 2006.

Zavala-Hidalgo, J., R., R.-C., A., M.-J., Morey, S. L., and Martínez-López, B.: The response of the Gulf of Mexico to wind and heat flux forcing: What has been learned in recent years?, Atmósfera, 27, 317 – 334, https://doi.org/10.1016/S0187-6236(14)71119-1, http://www.sciencedirect.com/science/article/pii/S0187623614711191, 2014.

Zhang, S., Stock, C. A., Curchitser, E. N., and Dussin, R.: A Numerical Model Analysis of the Mean and Seasonal Nitrogen Budget on the Northeast U.S. Shelf, Journal of Geophysical Research: Oceans, 124, https://doi.org/10.1029/2018JC014308, https://agupubs.onlinelibrary.wiley.com/doi/abs/10.1029/2018JC014308, 2019.

Table 1. Nutrient budget in molN yr^{-1} for the inner (50 m isobath) and outer (250 m isobath) of the Yucatan shelf, computed at each boundary (N, W, E and S) by using projected cross-shelf velocities. The flux of nutrients is integrated through the water column and temporally averaged. Years from 2002 to 2010 are used to compute the budget. Positive values means source of nutrients, whereas negative values represent sinks of TN as denitrification is always a nitrogen removal process.

~~Boundary PON DIN TN Fresh water/Inner[a] Inner-shelf budget (x10^{10} molN yr^{-1})N 0.34 1.63 1.97 0.76 W -0.72 -0.02 -0.73 0.72 E 2.35 1.68 4.32 0 S -2.29 -0.05 -2.34 0 Denitrification -3.34 Trend[b] -0.64 Outer-shelf budget (x10^{10} molN yr^{-1}) N -11.46 -7.42 -18.88 -1.97 W -1.85 -9.87 -11.72 0.72 E -0.28 7.65 7.36 -4.03 S 11.17 27.74 38.92 0 Denitrification -3.34 Trend[b] -0.66~~

Boundary	PON	DIN	TN	Fresh water/Inner[c]
Inner-shelf budget (x10^{10} molN yr^{-1})				
N	0.34	1.63	1.97	0.76
W	-0.72	-0.02	-0.73	0.72
E	2.35	1.68	4.32	0
S	-2.29	-0.05	-2.34	0
Denitrification	-3.34			
Trend[d]	-0.64			
Outer-shelf budget (x10^{10} molN yr^{-1})				
N	-11.46	-7.42	-18.88	-1.97
W	-1.85	-9.87	-11.72	0.72
E	-0.28	7.65	7.36	-4.03
S	11.17	27.74	38.92	0
Denitrification	-3.34			
Trend[b]	-0.66			

[a] ~~Fresh water sources are considered only for the inner-shelf. Inner can be taken as a source or sink of nitrogen only for the outer-shelf.~~

[b] ~~The positive trend of total nitrogen observed in the temporal series during nine years is also taken into consideration to close the budget.~~

[c] Fresh water sources are considered only for the inner-shelf. Inner can be taken as a source or sink of nitrogen only for the outer-shelf.

[d] The positive trend of total nitrogen observed in the temporal series during nine years is also taken into consideration to close the budget.

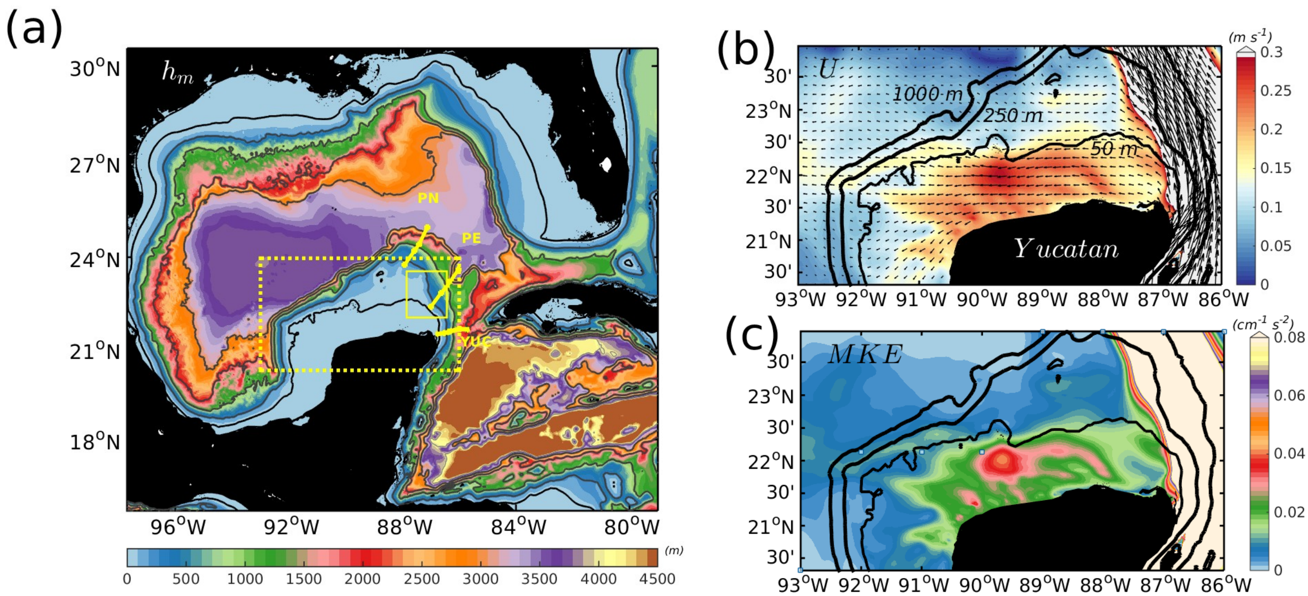

Figure 1. Bathymetry (h_m, m) of the whole model domain. Isobaths: 50, 250, 1000, 2000, 3000 and 4000 m are also shown in gray contours. The ~~black~~ yellow dashed box delimits the study area of the Yucatan shelf, where (b) is the surface temporally averaged velocity field (U, m s^{-1}) with magnitude in color and vectors representing the direction; and (c) is the surface Mean Kinetic Energy (MKE, cm^2 s^{-2}) computed for the year 2010. The smallest ~~black~~ yellow box in (a) shows the “notch” area and the three yellow lines are the moorings locations for transects YUC, PN and PE. The seas of the Deep Gulf of Mexico, Campeche and Caribbean are also shown in (a). The inner and outer Yucatan Shelf is denoted in (c).

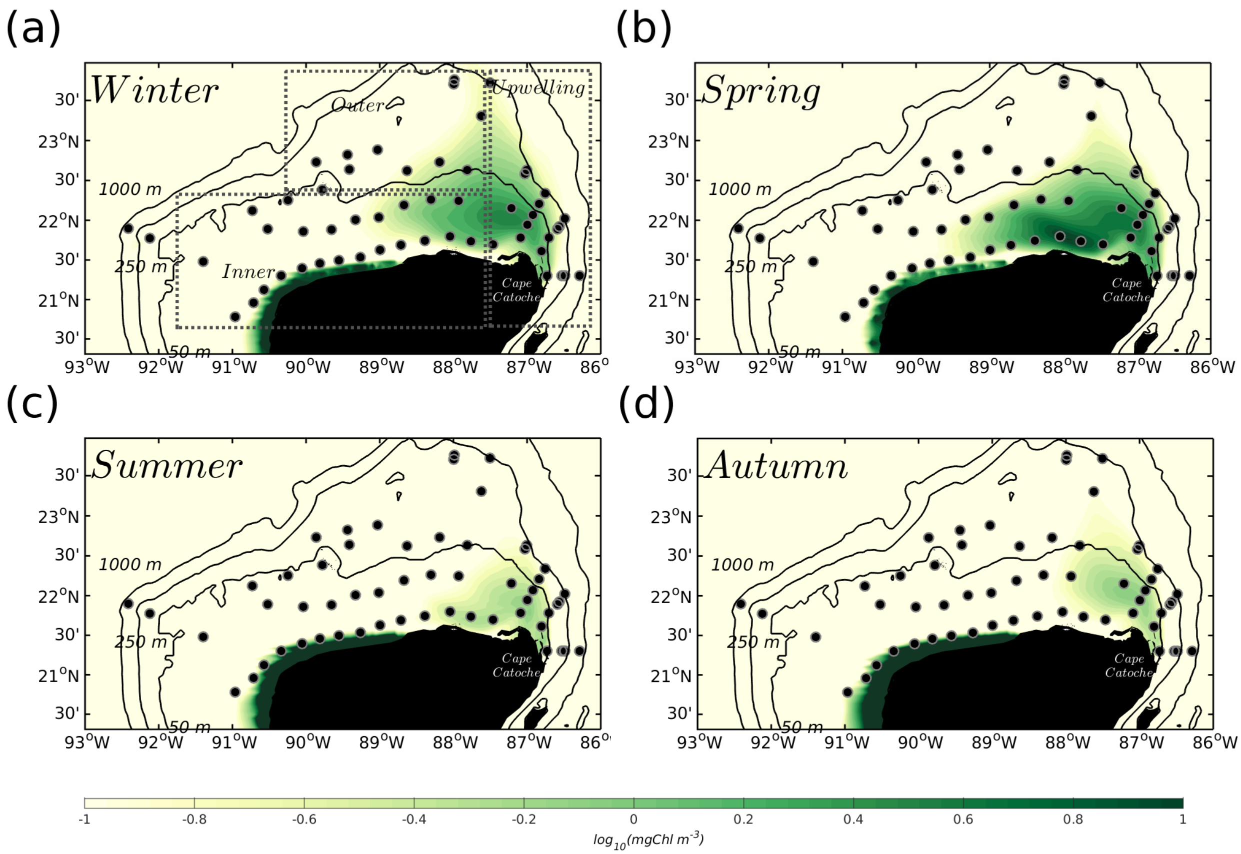

Figure 2. Seasonal climatology of surface chlorophyll (mgChl m^{-3}) given by the biogeochemical coupled model for: (a) Winter (Jan, Feb, Mar); (b) Spring (Apr, May, Jun); (c) Summer (Jul, Aug, Sep) and (d) Autumn (Oct, Nov, Dec), for the period between 2002 and 2010. Dashed boxes in (a) denote the three areas in which the validation with observations (black dots) was carried out, i.e., inner shelf, outer shelf and the upwelling region close to Cape Catoche.

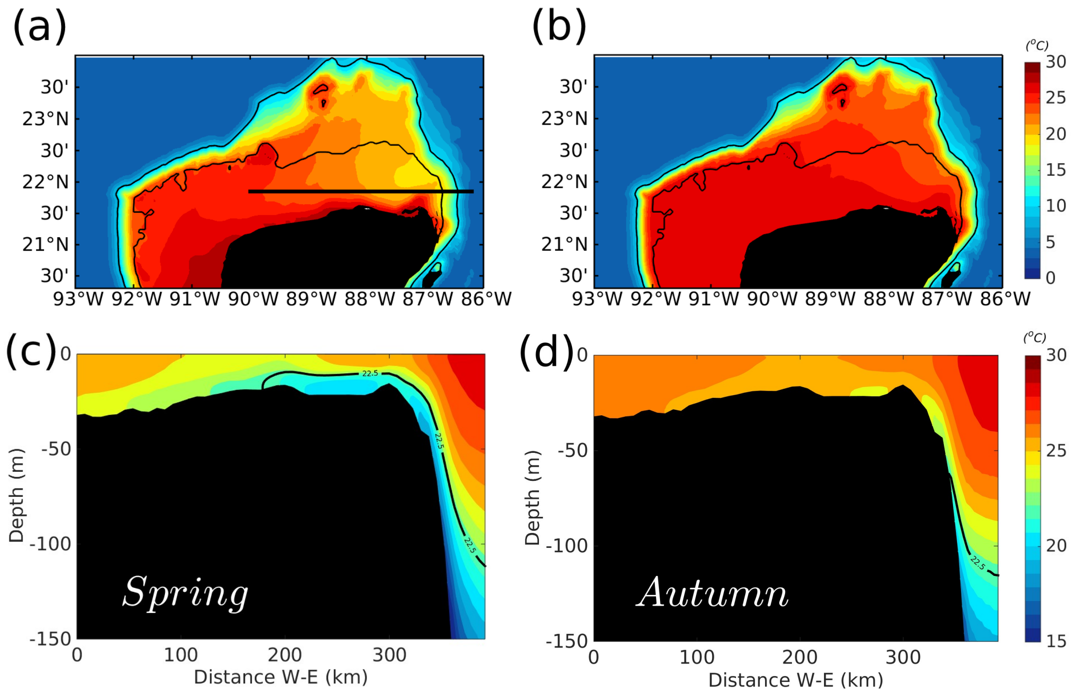

Figure 3. Seasonal climatology of bottom temperature (°C) for (a) Spring, and (b) Autumn, for the period between 2002 and 2010. The corresponding vertical sections, indicated by the zonal black line in (a), for (c) Spring and (d) Autumn. The contour in (a) and (b) denotes the isobaths of 50 and 250 m depth. The black contour in (c) and (d) shows the upwelling isotherm of 22.5°C.

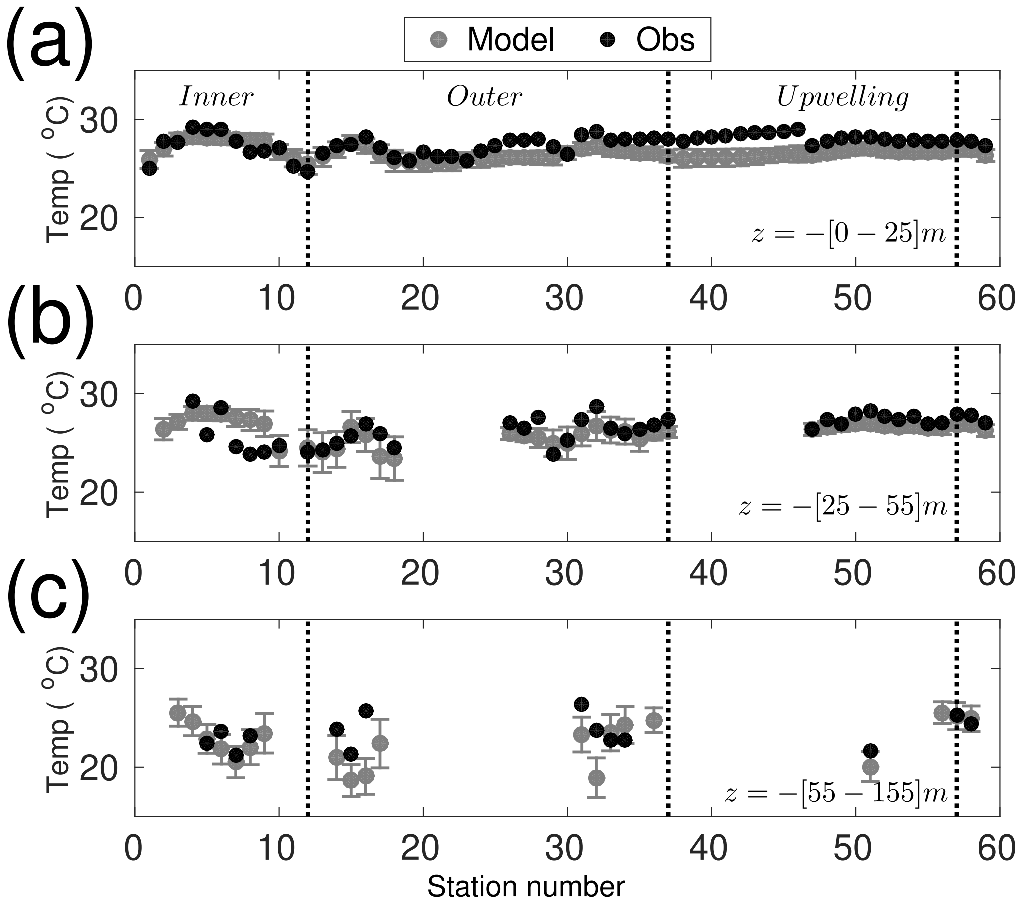

Figure 4. Comparison between ~~in situ~~ *in situ* data and simulated temperatures (~~T ^{o}~~°C). Temperatures values correspond to ~~a~~ each hydrographic station, averaged over three depths; (a) between surface and 25 m depth, (b) between 25 and 50 m depth, and (c) between 55 and the deepest measured concentration (z $\sim$ - 150 m). Black dots correspond to the observed values and open gray circles to the simulated variable. Vertical gray lines are the temporal standard deviation for the simulated values, as these are temporally averaged over all Novembers from 2002 to 2010. Vertical black lines delimit the group of stations for inner-shelf, outer-shelf and the upwelling area.

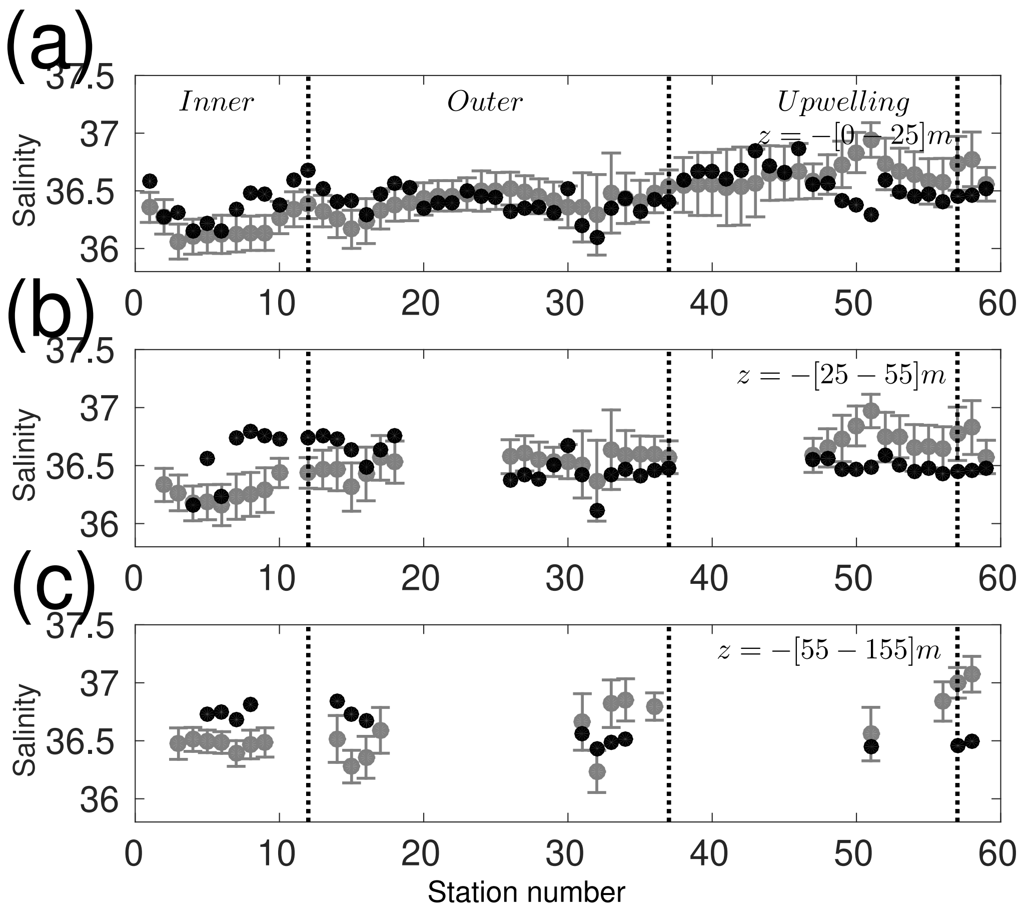

Figure 5. Same as Figure 4, but for salinity.

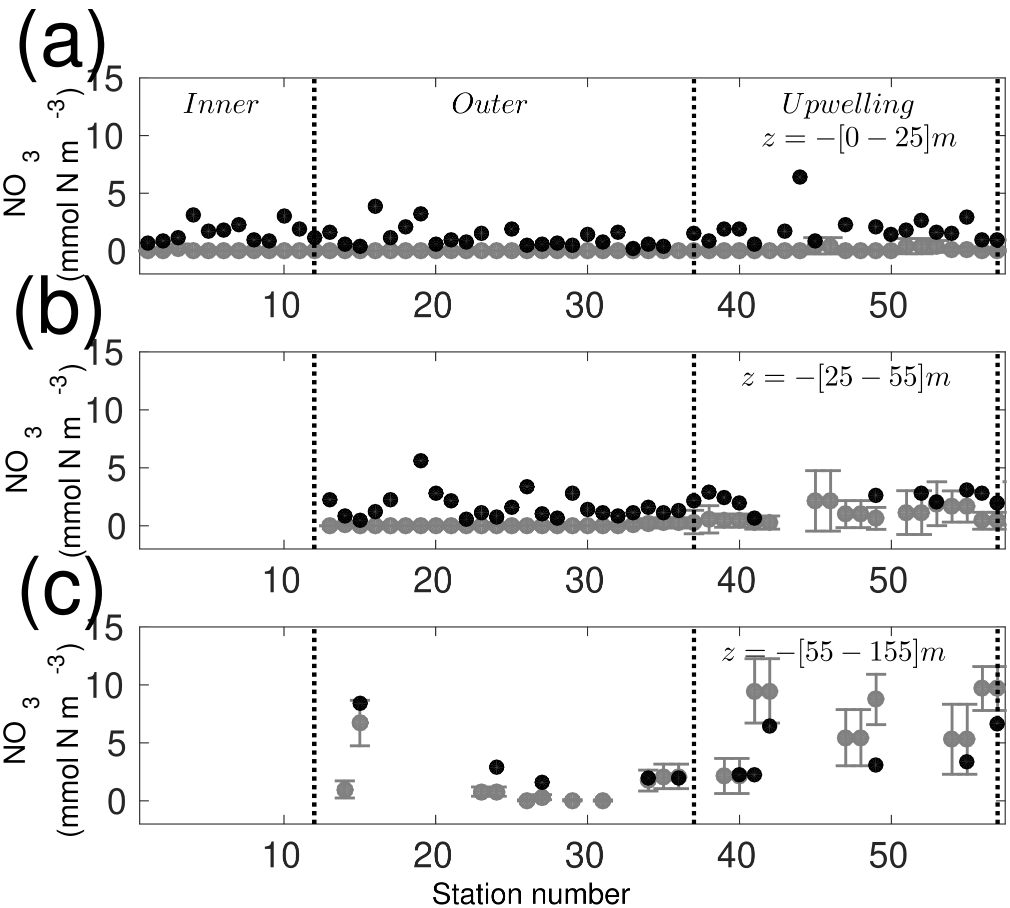

Figure 6. Same as Figure 4, but for nitrate concentrations ~~in mmol N~~ (mmolN m^{-3}).

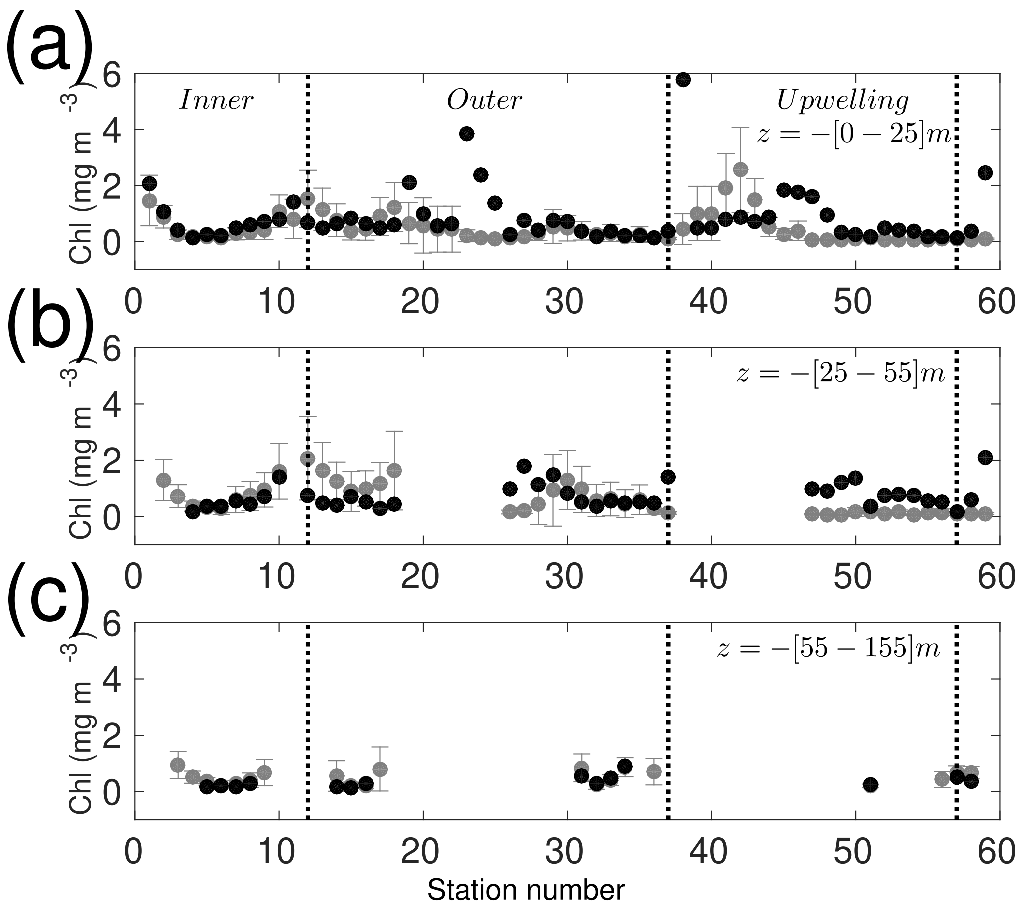

Figure 7. Same as Figure 4, but for chlorophyll concentrations ~~in mg Chl~~ (mgChl m^{-3}).

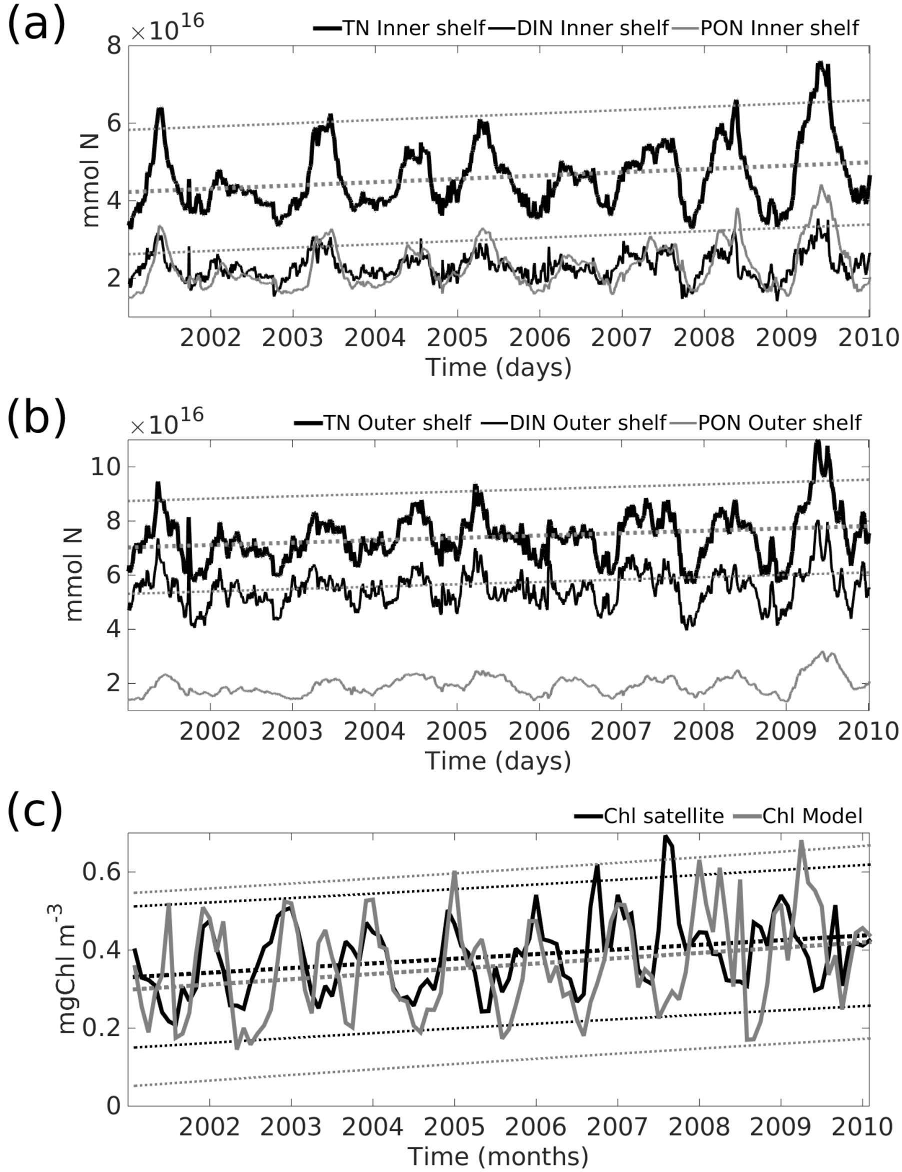

Figure 8. Temporal series of TN (thick black line), ~~PON~~ DIN (thin black line) and DIN (thin gray line) in mmolN, spatially integrated over~~the area of the inner shelf~~: (a) the inner shelf, and (b) ~~, and over the area of~~ the outer shelf. (c) ~~and (d). Temporal~~ are the temporal series ~~of~~ from monthly satellite chlorophyll ~~averaged over~~ (black, mgChl m^{-3}) and from the ~~YS area~~ model outputs (~~e~~gray) averaged over the whole Yucatan shelf. Dashed thick lines are the trend indicated by the linear fit for the TN or chlorophyll time series, where ~~gray vertical bars indicate standard deviation~~thiner dashed lines are the respective 95% confidence intervals. ~~The equation~~ Equations of each linear fit ~~is shown at the top of~~ are: TN (~~a~~Inner shelf) = 2.33 $\times 10^{12}$ days + 4.2 $\times 10^{16}$, TN (~~c) and (e~~Outer shelf) ~~, their respective p-values are 2.12~~= 2.40 $\times 10^{\cancel{-54}, \cancel{5.47} 12}$ days + 7.0 $\times 10^{\cancel{-51} 16}$, *Chl* (satellite) = 0.0010 months + 0.28, and ~~3.78×10^{-11}~~ *Chl* (model) = 0.0010 months + 0.30. Notice that the trend is positive for all the temporal series.

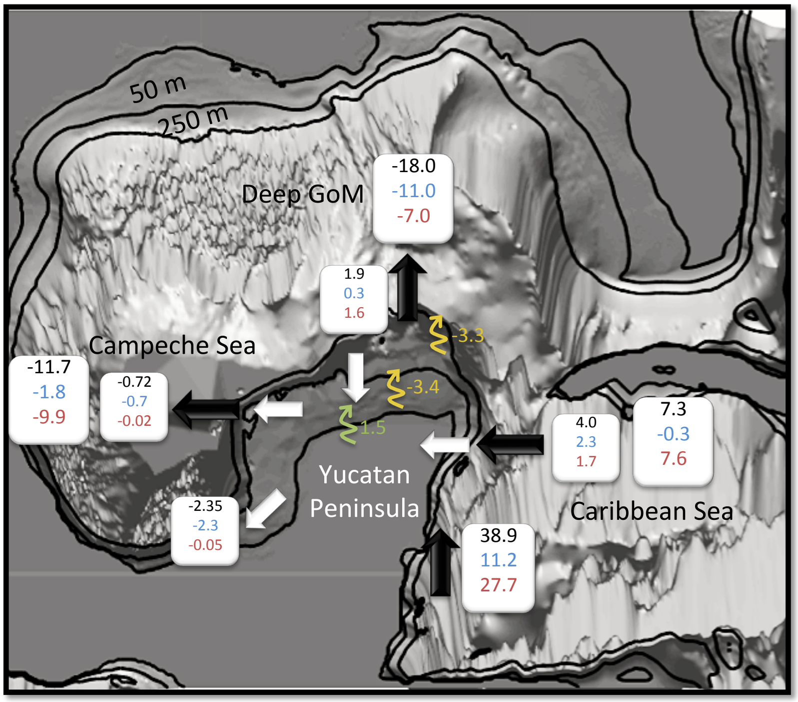

Figure 9. Scheme of the ~~Total Nitrogen (~~TN ~~)~~ budget for the Yucatan shelf. Black ~~arrows~~ and ~~contour~~ gray arrows denote cross-shelf direction flux ~~and the 250 m isobath delimiting~~ for the outer ~~shelf. Gray arrows~~ and ~~contour are analogous to the black but for the~~ inner shelf~~delimited by the 50 m isobath~~, respectively. In blue are the ~~Dissolved Inorganic Nitrogen (DIN)~~PON; in red the ~~Particulate Organic Nitrogen (PON)~~DIN; freshwater DIN sources (Rivers) are in green and sinks of TN due denitrification (DNF) are in yellow. The values are expressed in ~~mmolN s~~molN yr^{-1} $\times 10^{\cancel{13}10}$. Negative values indicate sink, whereas positive indicates source of TN. The isobaths that delimit the inner (50 m depth) and outer (250 m depth) shelves are also highlighted.

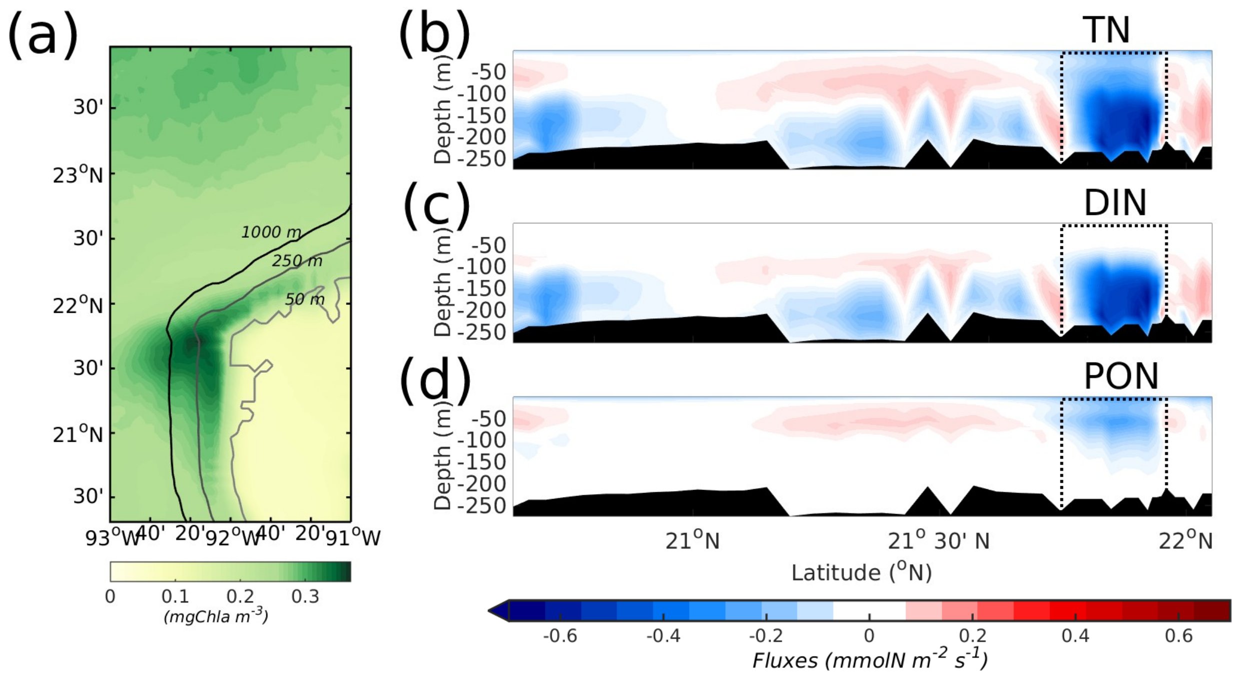

Figure 10. (a) Map of surface chlorophyll ~~in mgChla~~ (mgChl m^{-3}), averaged over the nine simulated years. The three characteristic ~~isobtahs~~ isobaths are denoted. ~~Flux vertical sections~~ Nine years averaged cross-shelf fluxes along the 250 m isobath at the western boundary of (b) ~~Total nitrogen~~TN, (c) DIN and (d) PON ~~in~~ (mmolN m^{-2} s^{-1}). Negative values indicate westward flux, i.e., TN flux from the shelf to the Campeche sea. The area delimited by dashed lines ~~show~~ shows the location of the filament depicted in (a), at the NW of the YS.~~Notice that vertical sections are plotted against the model vertical coordinate system. The depths in m are indicated as horizontal gray lines.~~

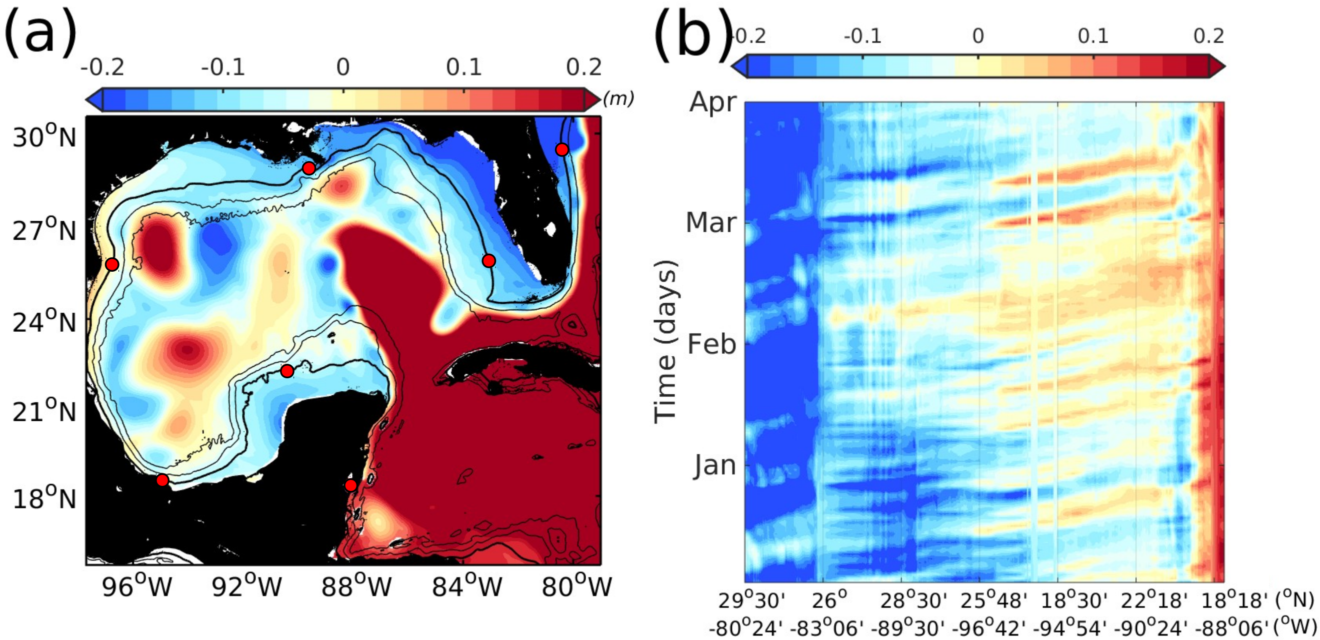

Figure 11. (a) Snapshot of sea level anomaly (η, m) for the simulated year 2005. (b) ~~Hovmoller~~ Hovmöller diagram of η along the 50 m isobath from January to April of the 2005 year. Red dots in (a) denote the latitude and longitude shown at the bottom of (b), from Florida to Yucatan peninsula.

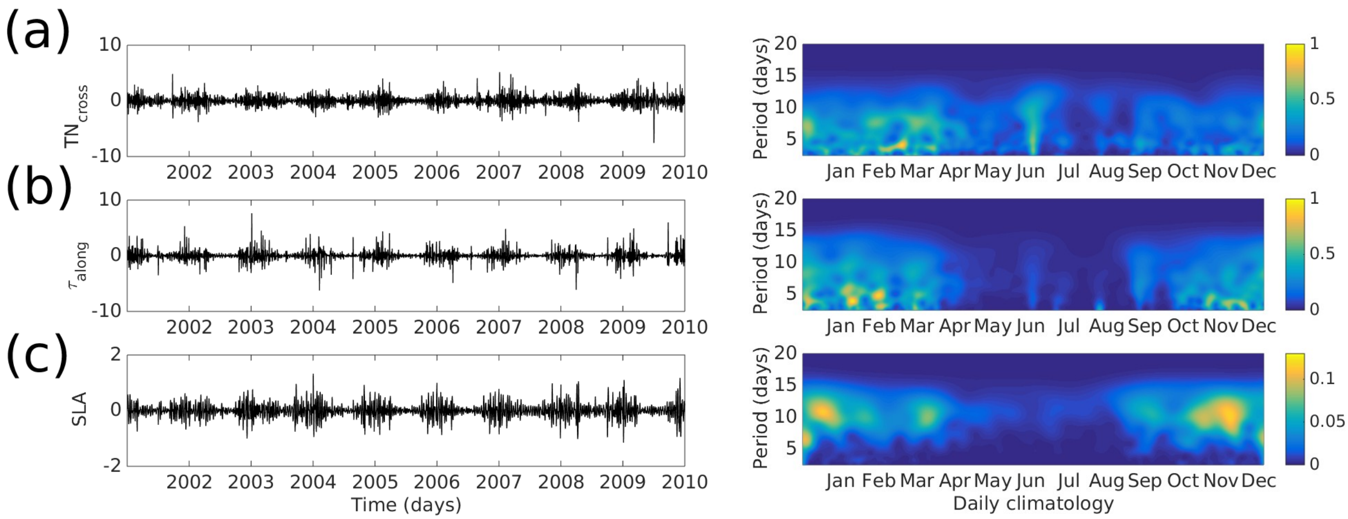

Figure 12. ~~Multi-taper spectrum (black line) on~~ Temporal series averaged over the ~~left hand side figures for time-series of west~~ western 50 m isobath of: (a) cross-shelf ~~velocity current;~~ total nitrogen flux vertically integrated (TN, mmolN m^{-1} s^{-1}), (b) ~~sea level anomaly~~ Along shelf wind stress (~~SLA~~ τ_{along}, N m^{-2}), and (c) ~~wind-stress~~Sea level anomaly (SLA, m). The temporal series are ~~previously~~ detrended, normalized, and filtered ~~with~~ by a ~~lanczos~~ lanksos high-pass filter with a cut-off of 15 days~~in order to remove low frequency process. The multi-taper spectra are built with 30 tapers or windows. The significance levels relative to the estimated noise background of 99% is shown as a gray line and is based on the spectral analysis of 1000 simulations of red noise, using the Monte-Carlo algorithm~~. In the ~~right hand~~ right-hand side figures, the wavelet power spectrum is shown for each of the time series~~(a), (b) and (c). The averaged period and standard deviation is shown at the left corner of each wavelet power spectrum. The characteristic periods obtained through the wavelet analysis by connecting maximums of power spectrum per day are shown in (d)~~.

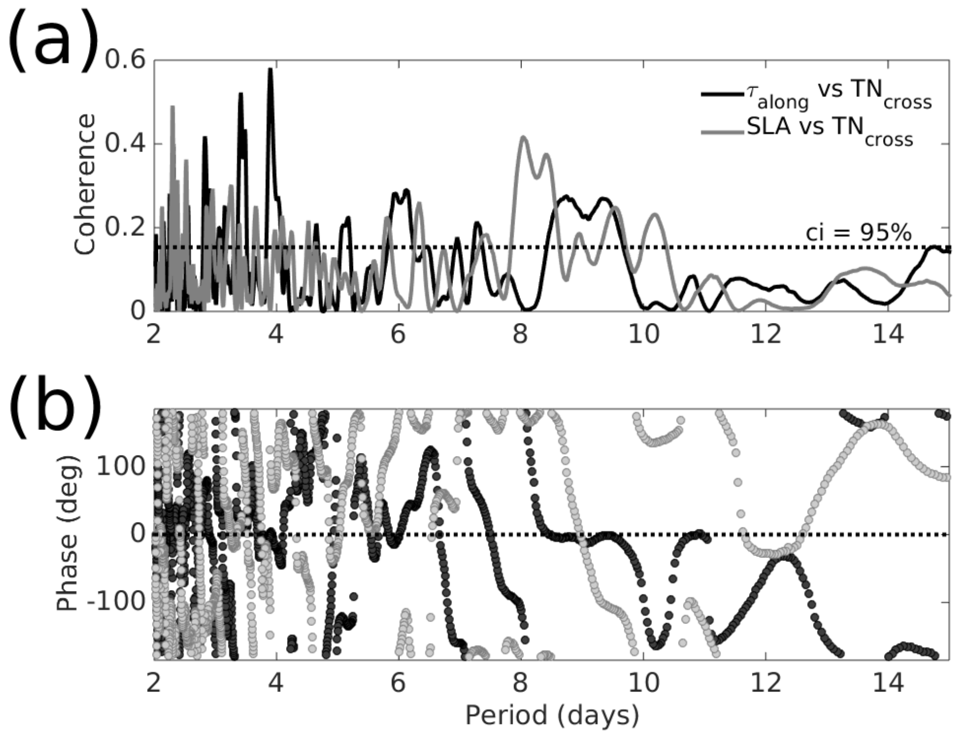

Figure 13. (a) Cross-correlation spectral analysis of the time series shown in Figure 12a, b, and c, indicating coherence between τ_{along} and TN, and between SLA and TN. The black horizontal line indicates the 95% confidence interval. (b) Phase in degrees for both coherence analysis.

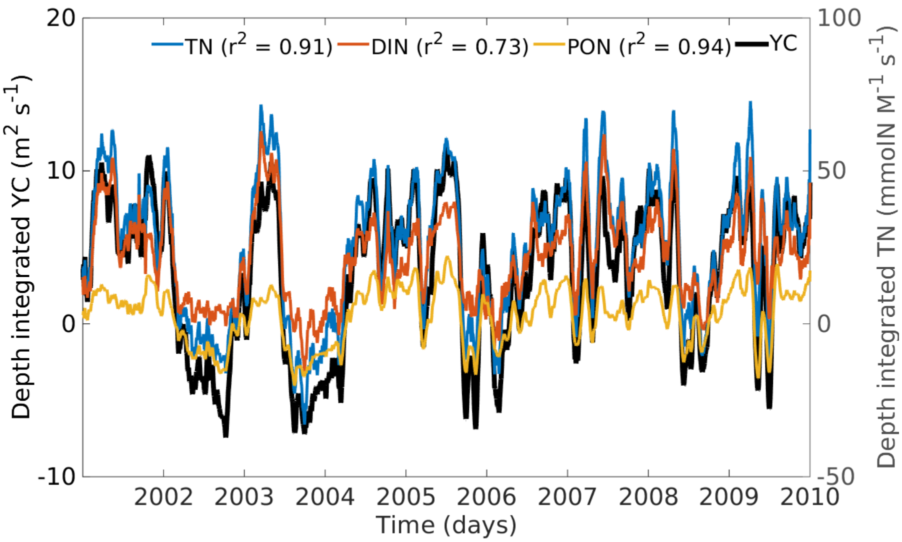

Figure 14. ~~(a) Map of the annual mean surface velocity current for the year 2003. Vectors represent the direction of the flux and the two 50 m and 250 m isobath are shown. Correlation of the annual mean surface velocity current, averaged in the black box denoted in (a), with the annual mean of the integrated nitrogen fluxes at the East outer shelf margin~~ Temporal series for the ~~10~~ nine simulated years of cross-shelf Yucatan Current component (~~b~~YC)~~the~~, Total Nitrogen (TN), ~~(c) the~~ Dissolved Inorganic Nitrogen (DIN) and~~(d) the~~, Particulate Organic Nitrogen (PON), vertically integrated and averaged over the isobath 250 m of the eastern boundary. The square of the correlation ~~values~~ coefficients (r^2), between YC and the biogeochemical variables are shown ~~at the right upper corner~~on top. The temporal series are filtered by a moving average of 30 days to remove daily variability.

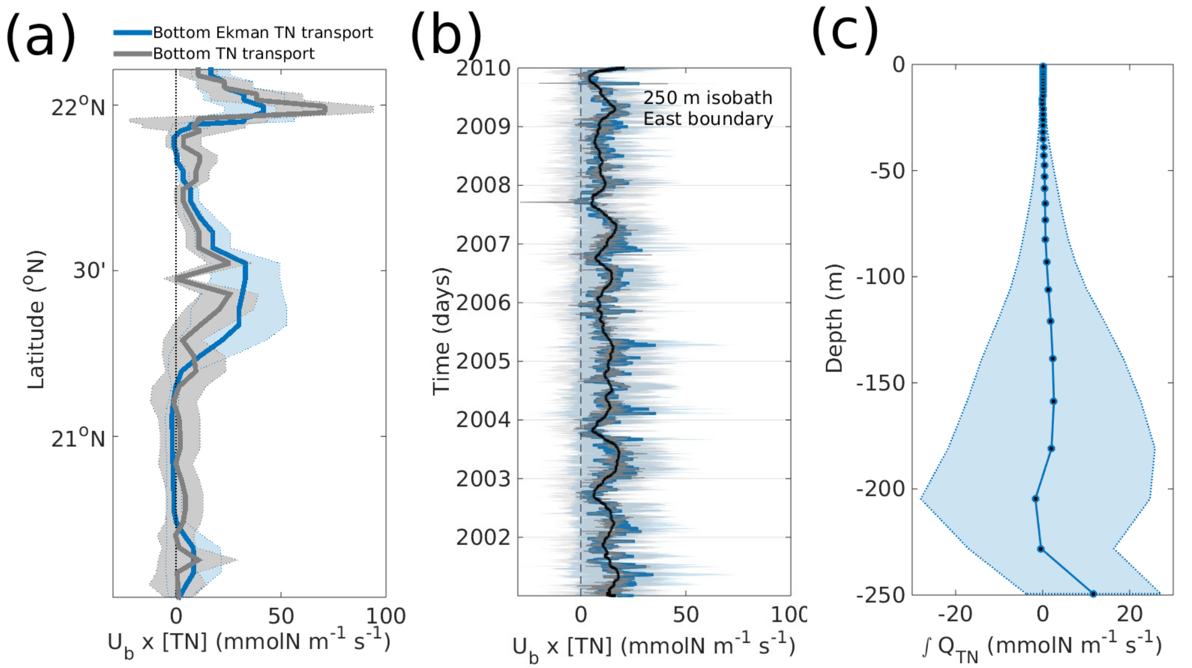

Figure 15. Flux of total nitrogen (~~TN~~Q_{TN}) computed by the Bottom Ekman transport (U_{bE}, m^2 s^{-1}) for the nine simulated years (blue) compared with the bottom-most layer TN flux (gray, mmolN m^{-1} s^{-1}) over the Ekman bottom layer for: (a) temporal averages, and (b) spatial averages over the 250 m isobath~~. Shaded areas denote the standard deviation of~~, where superimposed black line is the ~~averages~~bottom Ekman transport filtered with a 90 day moving average. (c) ~~Doubled spatial~~ Vertically integrated TN flux along the eastern 250 m isobath, averaged over latitude and over ~~s-layers. The TN flux is first averaged over~~ the nine simulated years in mmolN m^{-1} s^{-1}. Shaded areas denote the standard deviation of the averages.

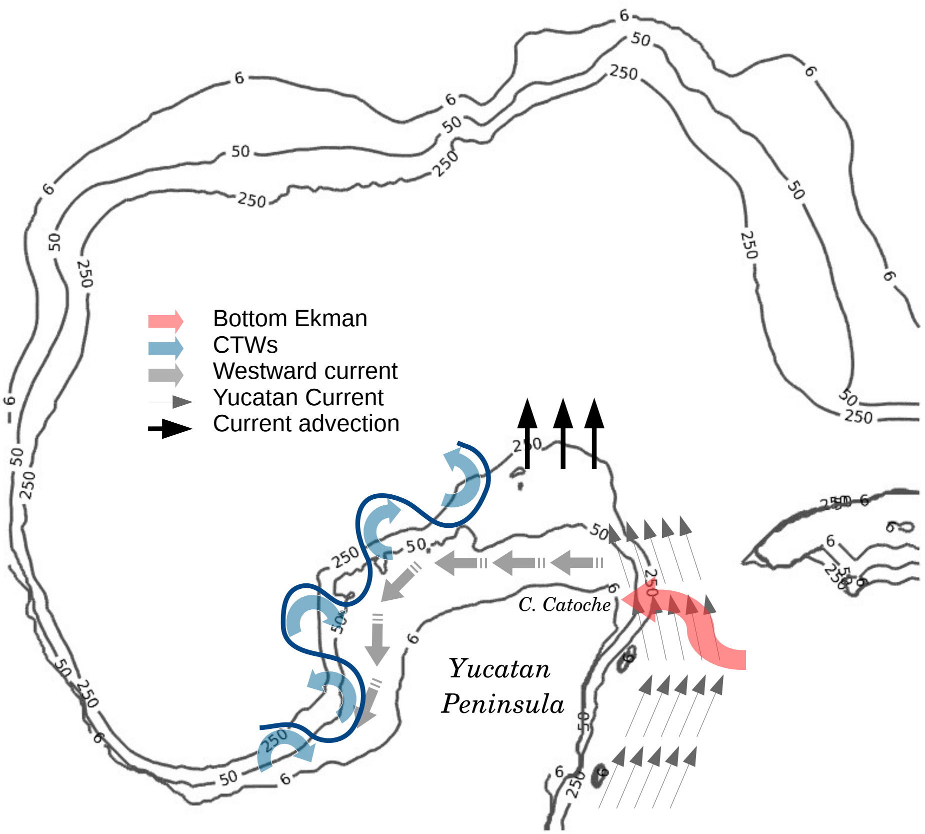

Figure 16. Schematic view of the main physical processes that modulate the cross-shelf transport of TN in the Yucatan shelf.

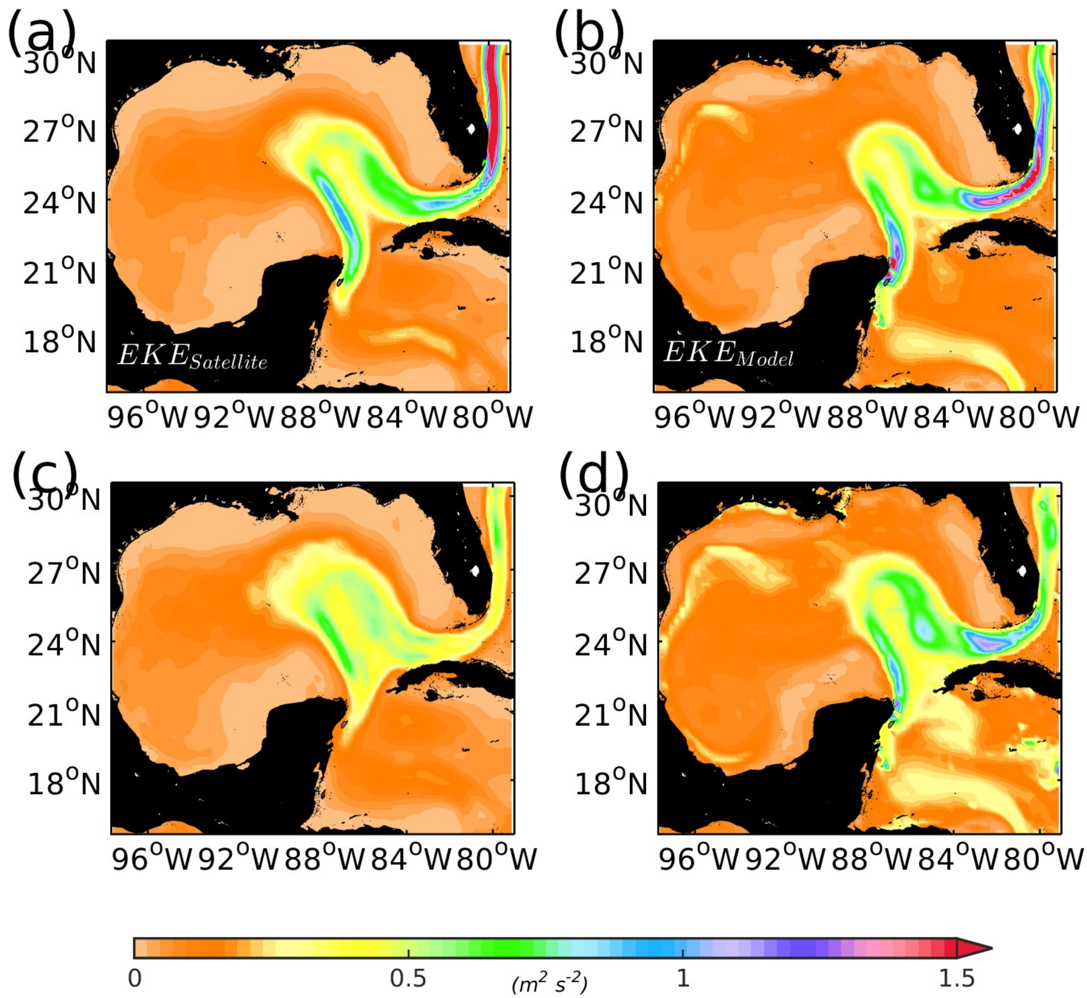

Figure A1. Comparison of 17 yr (1995-2012) averaged Eddy Kinetic Energy (EKE, m^2 s^{-2}) calculated in base on (a) AVISO SSH product and (b) ROMS model simulated SSH. (c) and (d) are the standard deviation for altimeter and model EKE, respectively.

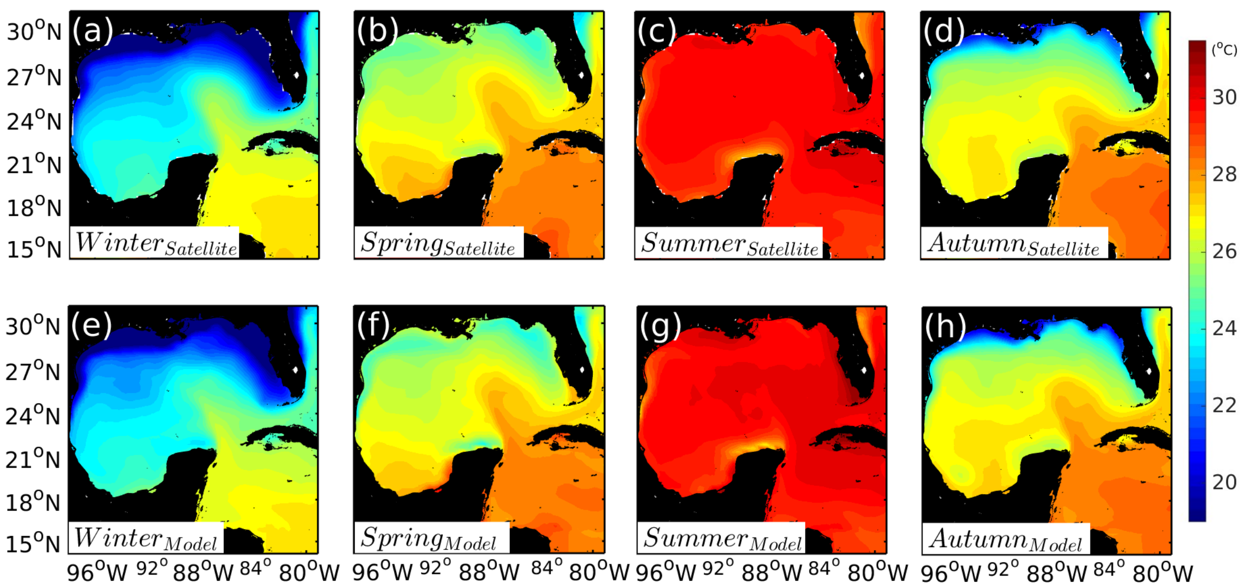

Figure A2. Seasonal climatologies of SST (~~ºC~~°C) for the GoM (2005 to 2012). Comparison between (a-d) satellital SST product and (e-h) model SST.

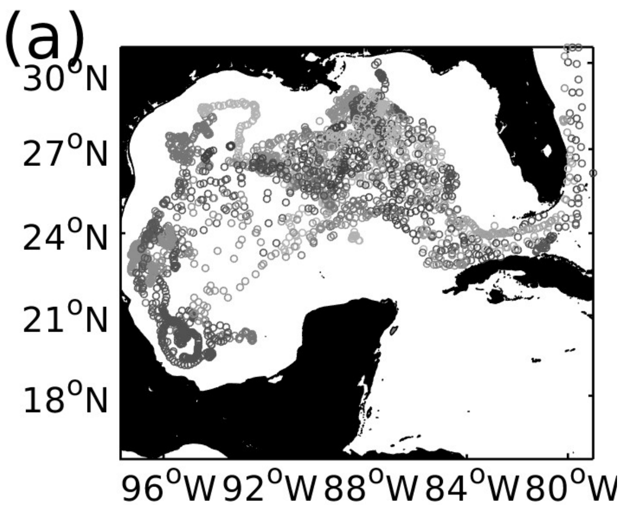

Figure A3. (a) Location of the 2629 ARGO profiles used ~~for~~ to compute the mixed layer depth (h_ρ, m). (b) Climatology comparison of mixed layer depths for ARGO profile floats (black boxes) and ~~for~~ the model (gray boxes). Vertical lines in the boxes denote standard deviation.

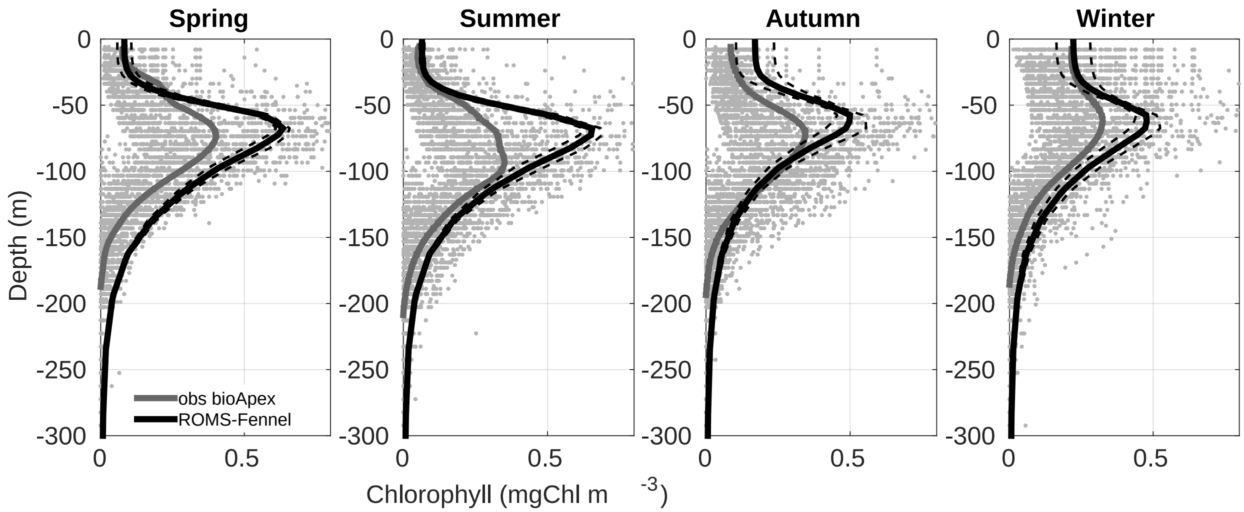

Figure A4. Seasonal comparison of chlorophyll profiles in mgChl m^{-3}, taking all the available Apex floats (Pasqueron de Fommervault et al., 2015), in order to evaluate the Deep Chlorophyll Maximum (DCM). Grey dots are the data observed from Apex floats; the average profile is shown in grey. In black is the averaged profile of the model data with its respective standard deviation in dashed black lines.

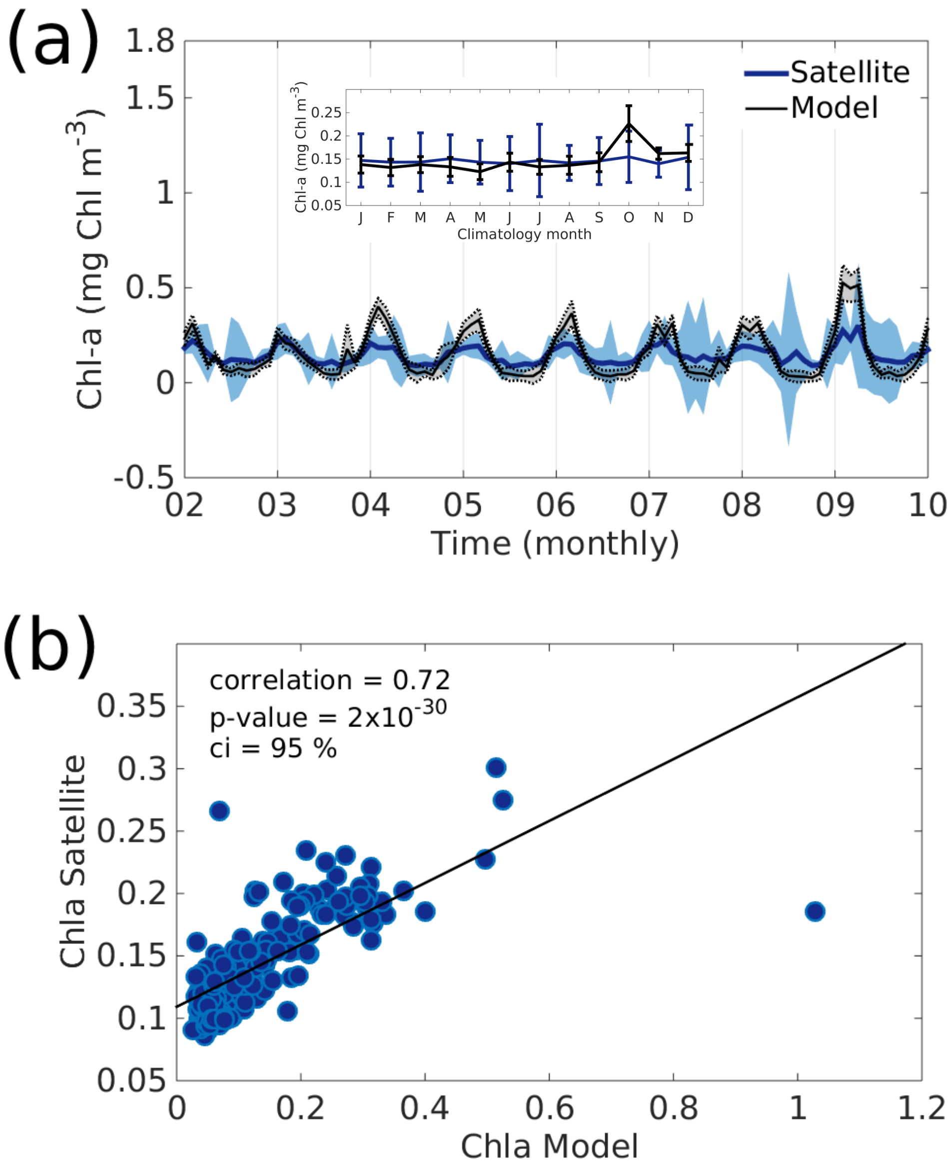

Figure A5. (a) Temporal series of surface chlorophyll in mgChl m^{-3} from satellite and model for the whole deep GoM. Standard deviations from the spatial averages are shown in shadow blue areas for satellite and dashed black lines for the model. The monthly climatology of the temporal series is shown at the upper part of the figure, where vertical bars indicate standard deviation from the temporal mean. In (b) are represented the correlation coefficient of both monthly temporal series and their respective linear fit in black line. The slope of the linear fit is 0.25.

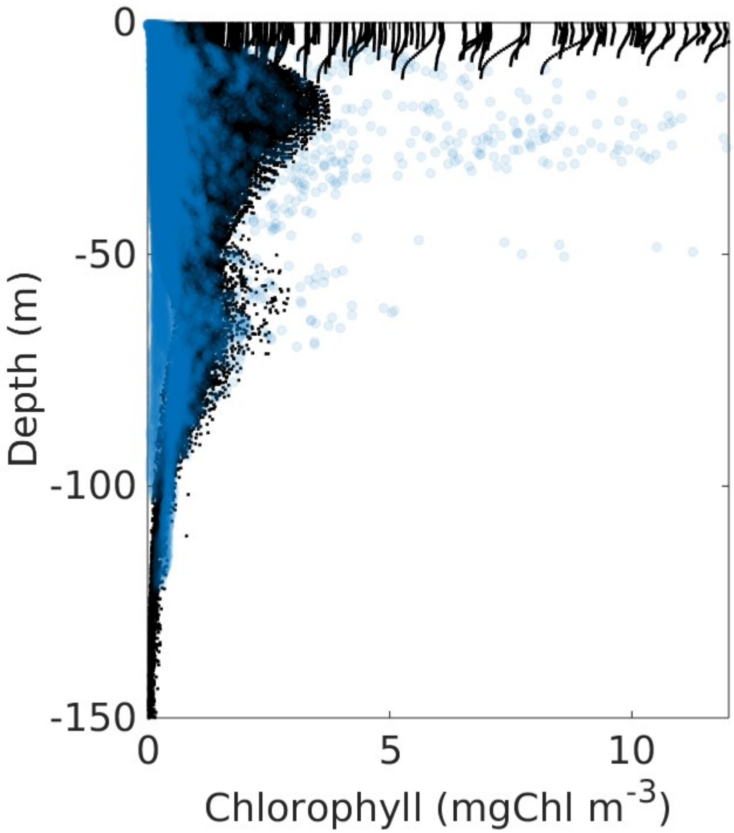

Figure A6. Profiles of chlorophyll (mg Chl m^{-3}). In black are the model profiles temporally averaged for all the July, August and November months of the nine simulated years. Superimposed in blue are the observed profiles of the three GOMEX cruises carried out during November 2015, August 2016 and July 2018.

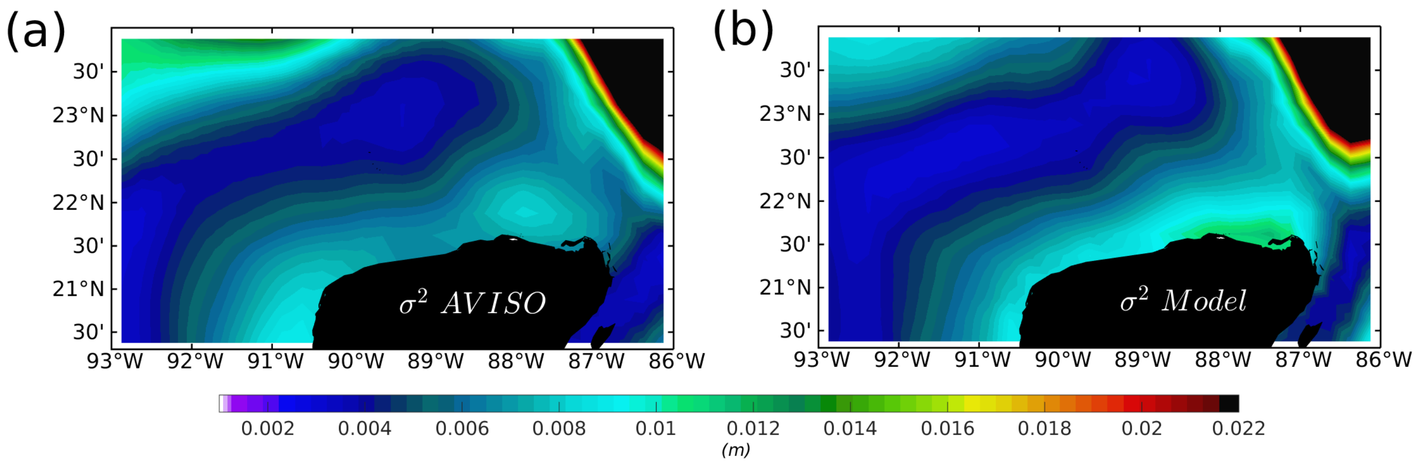

Figure A7. Variance (σ^2, m) for the range of years 2002-2010 of: (a) Absolute dynamic topography (ADT) extracted from the AVISO altimeter product, and (b) Mean sea level (η) from the ROMS outputs.

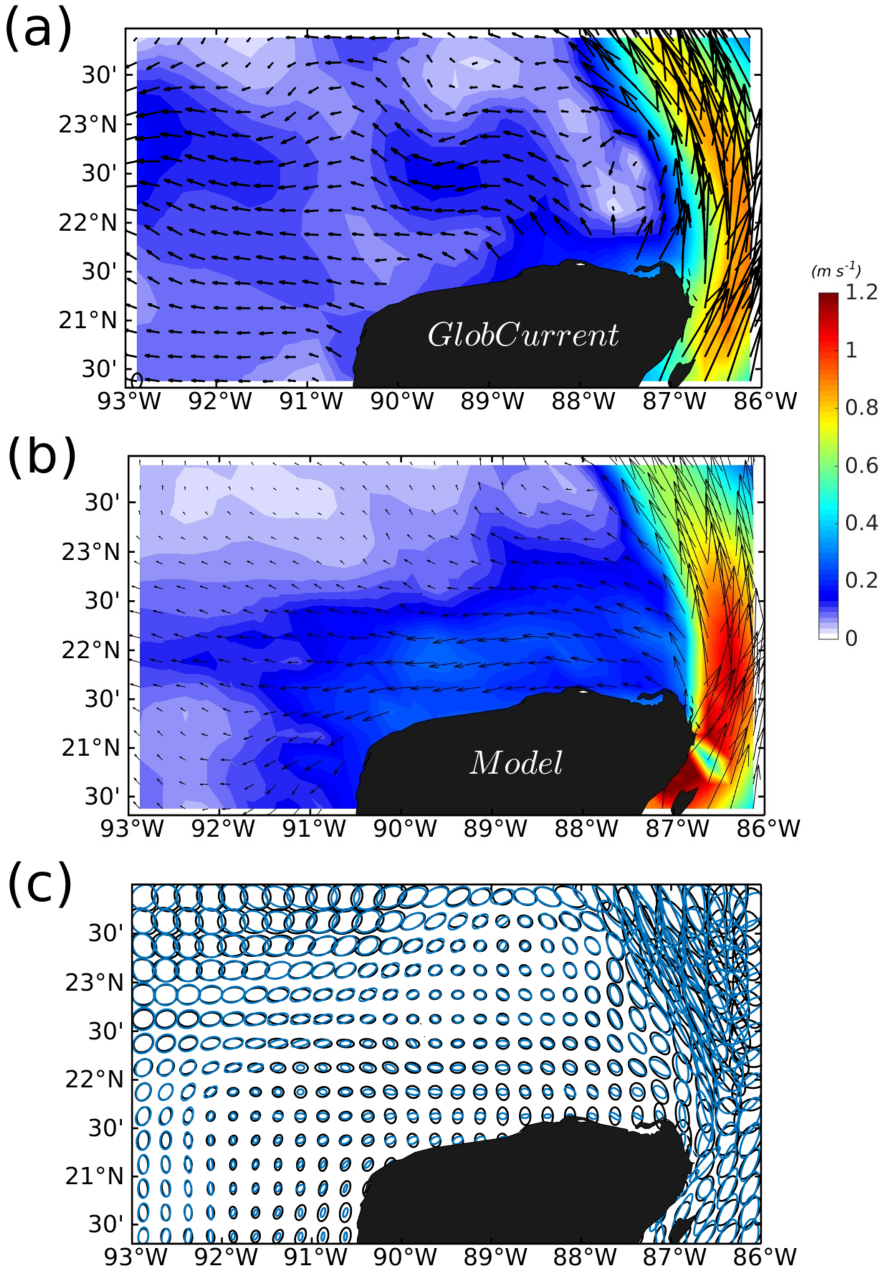

Figure A8. The current magnitude and their mean direction vectors averaged for the years 2002 to 2010 in m s^{-1}. (a) Mean geostrophic plus Ekman currents from GlobCurrent product; (b) Mean total current from the model outputs; (c) Ellipses of current field variability of the GlobCurrent product (black) and model outputs (blue).

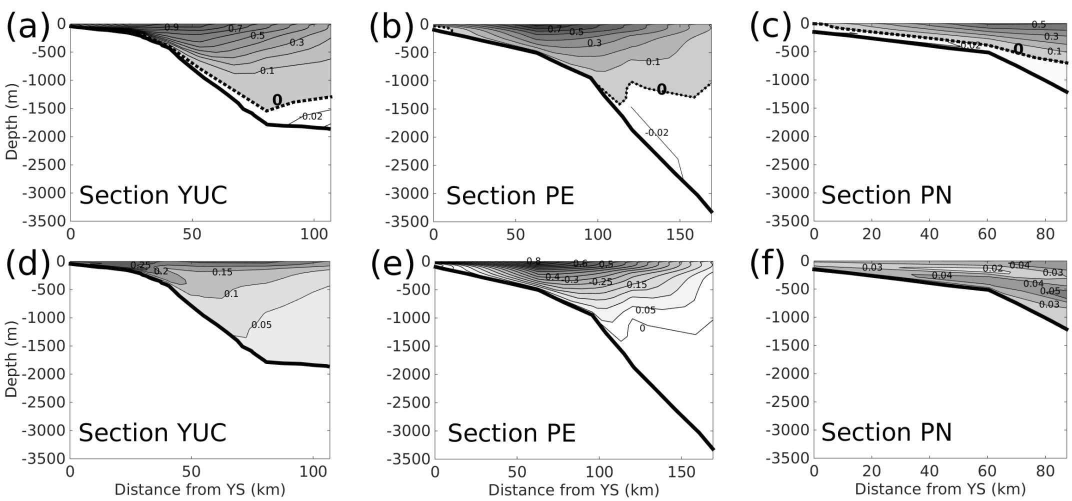

Figure A9. Mean model velocity (m s^{-1}) normal to the three sections: (a) YUC; (b) PE; and (c) PN, depicted in Figure 1a, for the years 2009 to 2011. To be compared with Sheinbaum et al. (2016), positive velocities are in gray (contours every 0.1 m s^{-1}) and negative velocities in white (contours every 0.03 m s^{-1}); dashed black contour shows zero velocity. (d), (e) and (f) shows the standard deviations for each transect (contours every 0.05 m s^{-1} for d and e, and every 0.01 m s^{-1} for f).

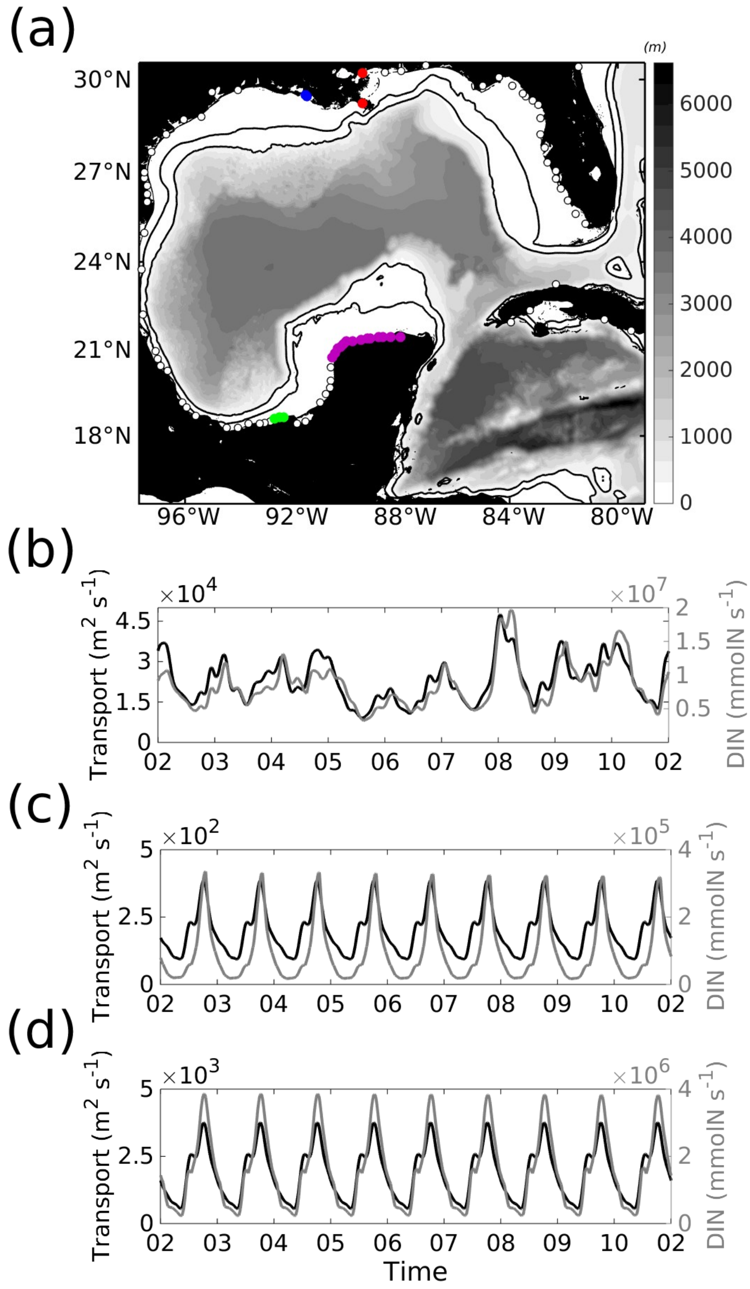

Figure A10. (a) Model bathymetry with the location of the input freshwater sources (white points). In red and blue points are the Mississippi and Atchafalaya riverine system, in green is the Usumacinta and Grijalva riverine system and in violet are the freshwater system of the YS. The panels below show the temporal series of water transport (m^3 s) and the DIN (NO_3 + NH_4) fluxes (mmolN s^{-1}) for the systems: (b) Mississippi-Atchafalaya; (c) Usumacinta-Grijalva; and (d) Yucatan shelf freshwater.